UNIVERSITAT POLITÈCNICA DE VALÈNCIA

PhD in Biotechnology

UNDERSTANDING AND DRUGGING THE BCL-2 TRANSMEMBRANE INTERACTOME FOR TUMOR TREATMENT

PhD. THESIS

Submitted by

Estefanía Lucendo Gutiérrez

Valencia, August 2020

PhD. Supervisor:

Dra. Mar Orzáez Calatayud

PRINCIPE FELIPE
CENTRO DE INVESTIGACION

PRINCIPE FELIPE
CENTRO DE INVESTIGACION

UNIVERSITAT POLITÈCNICA DE VALÈNCIA

MAR ORZÁEZ CALATAYUD, PhD in Biology and Head of the Peptide and Protein Chemistry group at the Centro de Investigación Príncipe Felipe, CERTIFY that the work

"UNDERSTANDING AND DRUGGING THE BCL-2 TRANSMEMBRANE INTERACTOME FOR TUMOR TREATMENT"

has been developed by Estefanía Lucendo Gutiérrez under her supervision in the Centro de Investigación Príncipe Felipe, as a Thesis Project to obtain a PhD degree in Biotechnology from the Universitat Politècnica de València.

Valencia, August 2020

Dra. Mar Orzáez Calatayud

Acknowledgments

The student has been granted with a PhD fellowship and a short-term fellowship from the Generalitat Valenciana (*Subvenciones para la contratación de personal investigador de carácter predoctoral*, 2016-2019, and *Grant for predoctoral stays out of the Comunitat Valenciana*, 2019). This work has been supported by the Spanish Ministry of Economy and Competitiveness (projects SAF2014-52614-R and SAF2017-84689-R).

Resumen

La familia de proteínas Bcl-2 regula la apoptosis a través de una compleja red de interacciones. Las células tumorales suelen presentar mutaciones que afectan a la expresión o las interacciones de las proteínas Bcl-2 para mejorar la progresión tumoral. Además, alteraciones en su regulación también promueven la migración de células cancerígenas, la invasión y la metástasis. Para llevar a cabo sus funciones, las proteínas Bcl-2 interaccionan entre sí tanto en el citoplasma como en las membranas intracelulares. Los equilibrios de interacción de los dominios Bcl externos a la membrana han sido ampliamente investigados y recientemente, se han propuesto como dianas terapéuticas. Sin embargo, el interactoma de los dominios transmembrana (TMD, *del inglés transmembrane domains*) sigue siendo poco conocido. En esta situación, es necesario un conocimiento profundo de la biología de las proteínas Bcl-2 para explotar eficientemente sus superficies de unión en el tratamiento del cáncer. Para llevar a cabo este objetivo, nuestra investigación se centra en tres áreas:

1. La comprensión detallada de la contribución del TMD al interactoma en membrana de Mcl-1 y a la funcionalidad de la proteína.
2. El descubrimiento de nuevos inhibidores de Mcl-1 que actúen sobre el segmento transmembrana que permitan el desarrollo de una clase de drogas anticancerígenas aún por explorar.

3. La caracterización molecular de mutaciones relacionadas con el cáncer descritas en los TMD de Bcl-2 y Bcl-xLy sus implicaciones en la supervivencia de las células tumorales.

La proteína antiapoptótica Mcl-1 inhibe a los miembros proapoptóticos Bak, Bax, Bok y Noxa, entre otros. Aunque se ha estudiado en detalle su actividad promoviendo la supervivencia celular, el mecanismo molecular por el cuál previene la apoptosis mediada por Bok aún no está claro. Además, el conocimiento de las actividades de Mcl-1, descritas hasta ahora, se basa exclusivamente en las estructuras resueltas de las regiones solubles en agua y en estudios centrados en los dominios externos a la membrana. Por primera vez, hemos demostrado la relevancia del TMD de Mcl-1 en su equilibrio de interacción. En este trabajo describimos su capacidad específica para homo- y hetero-oligomerizar con el TMD de Bok. También ponemos de manifiesto la influencia de estas interacciones en la modulación de apoptosis y resaltamos la relevancia clínica de los mutantes del TMD de Mcl-1 identificados en pacientes con cáncer.

Muchos tumores hematológicos y sólidos sobre-expresan Mcl-1 como un mecanismo para adquirir quimiorresistencia. Se han desarrollado miméticos de BH3 específicos para modular su actividad antiapoptótica en células cancerosas. Sin embargo, aún no disponemos de datos científicos que informen sobre su toxicidad en humanos y su eficacia. En este trabajo, proponemos la novedosa interacción de los TMDs de Mcl-1 y Bok como un nuevo sitio de actuación de fármacos en el desarrollo de quimioterapias. Hemos identificado tres inhibidores de esta interacción con prometedoras características que los hacen buenos candidatos para el desarrollo

farmacéutico, así como herramientas de investigación para el estudio molecular de la interacción de los TMDs de Mcl-1 y Bok.

Para beneficiarse de la modulación de la apoptosis, las células tumorales también presentan versiones mutadas de las proteínas antiapoptóticas Bcl-2 y Bcl-xL. En nuestro conocimiento, este es el primer estudio que analiza mutaciones derivadas de pacientes que afectan a los TMDs de Bcl-2 y Bcl-xL. Nuestro trabajo demuestra cómo estas mutaciones alteran el equilibrio en membrana de las proteínas. Además, nuestros resultados explican la influencia que algunos mutantes somáticos ejercen en la regulación de la apoptosis.

En general, los resultados científicos que aparecen en esta tesis resaltan el papel de los Bcl TMDs en el interactoma de las proteínas Bcl-2. Estos hallazgos corroboran que las interacciones laterales entre los TMDs son específicas de la secuencia y contribuyen activamente a la funcionalidad de la proteína. Por lo tanto, comprender los segmentos transmembrana Bcl puede proporcionar nuevos conocimientos sobre la biología de las proteínas Bcl-2 para su modulación farmacéutica en la terapia antitumoral.

Abstract

The family of the Bcl-2 proteins modulates the apoptotic pathway by a complex network of interactions. Tumor cells frequently present mutations that affect Bcl-2 proteins expression or interactions to enhance cancer progression. Dysregulation of these proteins also promotes cancer cell migration, invasion, and metastasis. To execute their functions, Bcl-2 proteins interact in both the cytosol and intracellular membranes. Binding equilibria of Bcl extramembrane domains has been largely investigated and recently proposed as chemotherapeutic targets. However, the interactome of transmembrane domains (TMDs) remains poorly understood. In this scenario, a deep knowledge of the biology of Bcl-2 proteins is needed to exploit efficiently their binding surfaces for cancer treatment. To address this aim, our research focuses on three areas:

1. The detailed comprehension of the TMD contribution to both the Mcl-1 membrane interactome and protein functionality.
2. The discovery of new Mcl-1 inhibitors that target the transmembrane surface to develop a class of anticancer drugs currently unexplored.
3. The molecular characterization of cancer-related mutations within the Bcl-2 and Bcl-xL TMDs and their implications for the survival of cancer cells.

Antiapoptotic Mcl-1 protein inhibits the proapoptotic members Bak, Bax, Bok, and Noxa, among others. Although its prosurvival activity has been

well studied, the molecular mechanism to prevent Bok-mediated apoptosis remains unclear. Furthermore, understanding of Mcl-1 activities described to date is only based on water-soluble structures and studies focused on extramembrane domains. For the first time, we uncover the relevance of the Mcl-1 TMD in the interaction equilibria of the protein. In the present work, we describe its specific capacity to self-associate and hetero-oligomerize with the Bok TMD. We also explain the influence of these interactions in the apoptotic pathway and highlight the clinical relevance of Mcl-1 TMD mutants identified in tumor patients.

Many hematological and solid malignancies overexpress Mcl-1 as an acquired chemoresistance mechanism. To modulate its antiapoptotic activity in cancer cells, specific BH3 mimetics have been developed; however, there is no scientific data yet regarding human toxicity and efficacy. In this work, we propose the novel Mcl-1 and Bok TMDs interaction interface as a drugging site in the development of chemotherapeutics. We identify three potential inhibitors of such molecular interface with promising features to become both drug candidates for pharmaceutical development and research toosl for the molecular study of the Mcl-1 and Bok TMDs interaction.

To take advantage of apoptosis modulation, tumor cells also present mutated versions of the antiapoptotic members Bcl-2 and Bcl-xL. To our knowledge, this is the first study that analyzes patient-derived mutations within Bcl-2 and Bcl-xL TMDs and demonstrates how said mutations alter the membrane equilibria of these proteins. The results presented here also

explain the functional influence of some somatic mutants in apoptosis regulation.

Overall, the scientific results exhibited in this Thesis highlight the role of Bcl TMDs in the interactome of Bcl-2 proteins. These findings corroborate that lateral interactions between TMDs are sequence-specific and actively contribute to protein functionality. Therefore, understanding of Bcl transmembrane segments may provide new insights into the biology of Bcl-2 proteins for their pharmaceutical modulation in antitumoral therapy.

Resum

La família de proteïnes Bcl-2 regula l'apoptosi a través d'una complexa xarxa d'interaccions. Les cèl·lules tumorals solen presentar mutacions que afecten l'expressió o les interaccions de les proteïnes Bcl-2 per a millorar la progressió tumoral. A més, alteracions en la seua regulació també promouen la migració de cèl·lules cancerígenes, la invasió i la metàstasi. Per a dur a terme les seues funcions, les proteïnes Bcl-2 interaccionen entre si tant en el citoplasma com en les membranes intracel·lulars. Els equilibris d'interacció dels dominis Bcl externs a la membrana han sigut àmpliament investigats i recentment, s'han proposat com a dianes terapèutiques. No obstant això, l'interactoma dels dominis transmembrana (TMD, de l'anglés *transmembrane domains*) continua sent poc conegut. En aquesta situació, és necessari un coneixement profund de la biologia de les proteïnes Bcl-2 per a explotar eficientment les seues superfícies d'unió en el tractament del càncer. Per a dur a terme aquest objectiu, la nostra investigació se centra en tres àrees:

1. La comprensió detallada de la contribució del TMD a l'interactoma en membrana de Mcl-1 i a la funcionalitat de la proteïna.
2. El descobriment de nous inhibidors de Mcl-1 que actuen sobre el segment transmembrana que permeten el desenvolupament d'una classe de drogues anticanceroses encara per explorar.
3. La caracterització molecular de mutacions relacionades amb el càncer descrites en els TMD de Bcl-2 i Bcl-xL i les seues implicacions en la supervivència de les cèl·lules tumorals.

La proteïna anti apoptòtica Mcl-1 inhibeix als membres pro apoptòtics Bak, Bax, Bok i Noxa, entre altres. Encara que s'ha estudiat detalladament la seua activitat promovent la supervivència cel·lular, el mecanisme molecular pel qual prevé l'apoptosi mediada per Bok encara no és clar. A més, el coneixement de les activitats de Mcl-1, descrites fins ara, es basa exclusivament en les estructures resoltes solubles en aigua i en estudis centrats en els dominis externs a la membrana. Per primera vegada, hem demostrat la rellevància del TMD de Mcl-1 el seu equilibri d'interacció. En aquest treball descrivim la seua capacitat específica per a unir-se amb si mateix i per a hetero-oligomeritzar amb el TMD de Bok. També expliquem la influència d'aquestes interaccions en l'apoptosi i ressaltem la rellevància clínica dels mutants del TMD de Mcl-1 identificats en pacients amb càncer.

Molts tumors hematològics i sòlids sobre-expressen Mcl-1 com un mecanisme per a adquirir quimioresistència. S'han desenvolupat mimètics de BH3 específics per a modular la seua activitat anti apoptòtica en cèl·lules canceroses. No obstant això, encara no disposem de dades científiques que informen sobre la seua toxicitat en humans i la seua eficàcia. Per això, proposem la nova interacció dels TMDs de Mcl-1 i Bok com un lloc d'actuació de fàrmacs en el desenvolupament de quimioteràpies. Hem identificat tres inhibidors d'aquesta interacció amb prometedores característiques que els fan bons candidats per al desenvolupament farmacèutic, així com eines d'investigació per a l'estudi molecular de la interacció dels TMDs de Mcl-1 i Bok.

Per a beneficiar-se de la modulació de l'apoptosi, les cèl·lules tumorals també presenten versions mutades de les proteïnes anti apoptòtiques Bcl-2 i

Bcl-xL. En el nostre coneixement, aquest és el primer estudi que analitza mutacions derivades de pacients que afecten els TMDs de Bcl-2 i Bcl-xL. El nostre treball demostra com aquestes mutacions alteren l'equilibri en membrana de les proteïnes. A més, els nostres resultats expliquen la influència que alguns mutants somàtics exerceixen en la regulació de l'apoptosi.

En general, els resultats científics que apareixen en aquesta tesi ressalten el paper dels Bcl TMDs en l'interactoma de les proteïnes Bcl-2. Aquestes troballes corroboren que les interaccions laterals entre els TMDs són específiques de la seqüència i contribueixen activament a la funcionalitat de la proteïna. Per tant, comprendre els segments transmembrana Bcl pot proporcionar nous coneixements sobre la biologia de les proteïnes Bcl-2 per a la seua modulació farmacèutica en la teràpia antitumoral.

Publications

The results of this PhD Thesis and other contributions have resulted in the following scientific publications:

- Andreu-Fernández V, Sancho M, Genovés A, **Lucendo E**, Todt F, Lauterwasser J, Funk K, Jahreis G, Pérez-Payá E, Mingarro I, Edlich F, Orzáez M. Bax transmembrane domain interacts with prosurvival Bcl-2 proteins in biological membranes. Proc Natl Acad Sci U S A **2017**;114(2):310-315.

- **Lucendo E**, Sancho M, Lolicato F, Javanainen M, Kulig W, Andreu-Fernández V, Mingarro I, Orzáez M. Mcl-1 and Bok transmembrane domains: unexpected players in the modulation of apoptosis. **2020**. (*Under review PNAS*).

Acronyms

AA	All-atom
ACD	Accidental cell death
Ac-DEVD-AFC	N-Acetyl-Asp-Glu-Val-Asp-7-amido-4-trifluoromethylcoumarin
AIF	Apoptosis-inducing factor
ANOVA	Analysis of variance
APAF	Apoptotic protease-activating factor 1
ATCC	American type culture collection
Bad	Bcl-2 antagonist of cell death
Bak	Bcl-2 associated killer protein
Bax	Bcl-2 associated X protein
BC groove	Bcl-2 family BH3 C-terminus-binding groove
BCA	Bicinchoninic acid
Bcl TMD	Bcl-2 proteins transmembrane domain
Bcl-2	B-cell lymphoma 2
Bcl-w	Bcl-2-like protein 2
Bcl-xAK	Bcl-x atipical killer
Bcl-xL	B-cell lymphoma-extra large
Bcl-xS	B-cell lymphoma-extra short

Becn1	Beclin 1
Bfl-1 (A1)	Bcl-2-related protein A1
BH	Bcl-2 homology
Bid	BH3-interacting domain death agonist
BiFC	Bimolecular fluorescent complementation
Bik	Bcl-2-interacting killer
Bim	Bcl-2-interacting mediator of cell death
BPTU	1-[2-(2-Tert-butylphenoxy)pyridin-3-yl]-3-[4-(trifluoromethoxy)phenyl]urea
Bmf	Bcl-2-modifying factor
Bok	Bcl-2-related ovarian killer
BokΔTMD	Bcl-2-related ovarian killer delta transmembrane domain
CARD	Caspase-recruitment domains
c-FLIP	FLICE (FADD-like IL-1β-converting enzyme)-inhibitory protein
CG	Coarse-grained
CLL	Chronic lymphocytic leukemia
COSMIC	Catalog of somatic mutations in cancer
DAPI	4′,6-diamidino-2-phenylindole
DED	Death effector domains

DISC	Death-inducing signaling complex
DIVA	Bcl-2-like protein 10
DMEM	Dulbecco's modified Eagle's medium
DMSO	Dimethyl sulfoxide
DNA	Deoxyribonucleic acid
DTT	Dithiothreitol
EBV	Epstein-Barr virus
ECL	Enhanced chemiluminescence
EDTA	Ethylenediaminetetraacetic acid
EGTA	Ethyleneglycoltetraacetic acid
EndoG	Endonuclease G
EPO	Erythropoietin
EPOR	Erythropoietin Receptor
ER	Endoplasmic reticulum
FADD	Fas-associated protein with death domain
FAS	Fas cell surface death receptor
FBS	Fetal bovine serum
FCCP	Carbonilcyanide p- triflouromethoxyphenylhydrazon
FDA	Food and drug administration
FLICE	FADD-like IL-1β-converting enzyme)-inhibitory

	protein (c-FLIP)
HCT116	Human colorectal carcinoma
HEPES	4-(2-hydroxyethyl)-1-piperazineethanesulfonic acid
HER2	Human epidermal growth factor receptor 2
hGLPR-1	Human glucagon-like peptide-1 receptor
Hrk	Activator of apoptosis Harakiri
HTRA2/OMI	High-temperature requirement protein A2
HTS	High-throughput screening
IP3R1	Inositol 1,4,5-triphosphate receptor
JAK	Janus kinase
LDH	Lactate dehydrogenase
LMP-1	Latent membrane protein-1
MAMs	Mitochondria-associated membranes
Mcl-1	Myeloid cell leukemia-1
Mcl-1$_{ES}$	Myeloid cell leukemia-1 extra short
MD	Molecular dynamics
MEFs	Mouse embryonic fibroblasts
MFI	Mean fluorescence intensity
mGluR2	Metabotropic glutamate receptor 2
MOM	Mitochondrial outer membrane

MOMP	Mitochondrial outer membrane permeabilization
m-MPEP	2-methyl-6-(phenylethynyl)pyridine
mPPIs	Membrane protein-protein interactions
MPTP	Mitochondrial permeability transition pore
NAD^+/NADH	Nicotinamide adenine dinucleotide
Noxa	Phorbol-12-myristate-13-acetate-induced protein
p75NTR	p75 neurotrophin receptor
PAGE	Polyacrylamide gel electrophoresis
PAR-1	Protease-activated receptor-1
PBS	Phosphate buffered saline
PCD	Programmed cell death
PDGF	Platelet-derived growth factor
PDGFR	Platelet-derived growth factor receptor
PFA	Paraformaldehyde
PLA	Proximity ligation assay
PMID	PubMed identifier
POPC	1-palmitoyl-2-oleoyl-glycero-3-phosphocholine
PPI	Protein-protein interaction
PS	Phosphatidylserine
Puma	p53 up-regulated modulator of apoptosis
Rambo	Bcl-2 like 13

RCD	Regulated cell death
ROS	Reactive oxygen species
SDS	Sodium dodecyl sulfate
SEM	Standard error of the mean
siRNA	Small interfering ribonucleic acid
SMAC/DIABLO	Second mitochondrial activator of caspases/ Direct IAP binding protein with low Pi
tBid	Truncate form of Bid
TMD	Transmembrane domain
TMRE	Tetramethylrhodamine ethyl ester
TNFR1	Tumor necrosis factor receptor 1
TNFRSF	Tumor necrosis factor receptor superfamily
TNFRSF1A	Tumor necrosis factor receptor superfamily member 1A
Tom20	Transporter outer membrane 20
ToxR	Cholera toxin transcriptional activator
TRAIL	TNF-related apoptosis-inducing ligand
TRAIL R1 and R2	TNF-related apoptosis-inducing ligand receptor 1 and 2
VC	Venus C-terminal fragment
VDAC1 and 2	Voltage-dependent anion channel 1 and 2

VN	Venus N-terminal fragment
WT	Wild-type
XIAP	X-linked inhibitor of apoptosis

Common abbreviations and symbols

Abs	Absorbance
Ca^{2+}	Calcium
Ctrl	Control
Cyt-*c*	Cytochrome-*c*
FL	Full-length
IP	Immunoprecipitation
Rand	Random
siRNA	Small interfering ribonucleic acid
STS	Staurosporine
α-tub	α-tubulin
$\Delta\psi m$	Mitochondrial transmembrane potential
λ	Wavelength

INDEX

GENERAL INTRODUCTION

1.1. CELL DEATH.

Every day, cells from multicellular organisms have to decide to live or die when they are exposed to homeostasis perturbations. This decision is crucial, not only for the individual cell itself but also for the tissues, organs, and organism. The Nomenclature Committee on Cell Death recommends referring to dead as '*only cells that either exhibit irreversible plasma membrane permeabilization or have undergone complete fragmentation*'[1]. More than 13 types of cell death are classified into two main categories: 'accidental' and 'regulated'. Accidental cell death (ACD) is the instantaneous and catastrophic demise of cells exposed to extreme physicochemical or mechanical stimuli. In contrast, regulated cell death (RCD) is initiated by a genetically encoded machinery and it can be activated in two opposed scenarios: as part of physiological programs for development and tissue turnover, or when adaptive responses to perturbations fail in the attempt to restore cellular homeostasis. Another difference is that RCD can be pharmacologically or genetically modulated, while ACD does not.

The term programmed cell death (PCD) refers to the completely physiologic forms of RCD related to development programs or tissue homeostasis, meaning it does not occur in pathological situations[1,2]. Since this concept was used for the first time in 1965 by Lockshin and Williams[3], the number of PCD modalities has increased and led to a classification based on specific morphological features, and quantifiable biochemical and molecular parameters. The current classification includes several types of

cell death such as autophagy, necroptosis, pyroptosis, or apoptosis[2], being the last one the best-studied RCD as described in the next section.

1.1.1. Apoptosis.

Ther term‘apoptosis’ (from the ancient Greek *άπόπτωσιζ*, meaning ‘falling off’) was originally coined by John F Kerr and colleagues, in 1972. It refers to a form of cellular demise characterized by morphological changes such as cytoplasmic shrinkage, plasma membrane blebbing, irreversible condensation of chromatin in the nucleus (pyknosis) followed by nuclear fragmentation (karyorrhexis) and culminating in the formation of discrete membrane-insulated corpses or apoptotic bodies[4,5]. A key step at the end of the apoptosis routine is the clearance of the apoptotic bodies performed by both professional and non-professional “neighboring” phagocytes. The first group includes macrophages and dendritic cells, while epithelial cells, endothelial cells, and fibroblasts form the second one. Overall, phagocytes recognize the “eat-me” signals exposed by the dying cells such as phosphatidylserine (PS) and calreticulin and engulf them into the phagosome, generally (but not always) avoiding the activation of inflammation[6].

The molecular features that describe apoptosis are mitochondrial outer membrane permeabilization (MOMP), mitochondrial depolarization, alteration of intracellular calcium (Ca^{2+}) levels, and release of apoptogenic factors from the mitochondrial intermembrane space to the cytosol[7,8]. In the

course of these events, the activation of the caspase cascade plays a key role being involved in the initiation, amplification, and execution of apoptosis[9,10].

Caspases are a family of cysteine aspartic acid-specific proteases that are related to apoptosis, inflammation, necroptosis and also, tissue differentiation[10]. The caspases involved in the apoptotic program are subdivided into the initiators (caspase-2, -8, -9, and -10) and the effectors or executioner (caspase-3, -6 and -7), based on their capability of auto-activation. Initiator caspases have specific protein interaction domains, such as death effector domains (DED) and caspase-recruitment domains (CARD) toward the N-terminus pro-domain, which facilitate their activation. Executioner caspases lack such interaction domains requiring external activation by initiators proteolytic cleavage[10,11]. Different stimuli can activate distinct caspase cascades, but in the end, they all converge into the activation of executioner caspases, which cleave specific cellular substrates to dismantle the cell, and are responsible for many of the morphological features of apoptosis[2].

1.1.2. Main apoptotic pathways.

Two main apoptotic pathways have evolved independently; however, they ultimately converge at mitochondria and the so-called mitochondrial outer membrane permeabilization (MOMP) process, leading to the activation of the same molecular effectors (Figure 1). They can be initiated by intracellular or extracellular stimuli, which classify them into the *intrinsic* and the *extrinsic* apoptotic pathway, respectively[12].

1.1.2.1. Extrinsic apoptotic pathway.

The extrinsic apoptotic pathway initiates when plasma membrane receptors detect perturbations of the extracellular microenvironment. These receptors are divided into two categories: death receptors (activated by the specific ligand(s)) and dependence receptors (activated when the levels of their cognate ligands fall below a specific threshold)[13-15].

The main receptors of the extrinsic pathway are Fas cell surface death receptor (FAS) and tumor necrosis factor receptor superfamily (TNFRSF) members, such as TNFRSF member 1A (TNFRSF1A) and TNF-related apoptosis-inducing ligand receptor 1 and 2 (TRAIL R1 and R2[16]). The molecular platforms activated by these receptors are formed by different protein complexes, but in general, all pathways recruit and activate caspase-8[17] (or caspase-10, in some circumstances) and FLICE (FADD-like IL-1β-converting enzyme)-inhibitory protein (c-FLIP). In the case of FAS, and TRAIL R1 and R2, preformed homo-trimers are stabilized by their ligands (FAS ligand and TRAIL, respectively), allowing the association with Fas-associated protein with death domain (FADD) and driving the assembly of the death-inducing signaling complex (DISC) and caspase-8 recruitment (Figure 1). For TNFR1, signaling activation with TNFRSF1A involves the formation of two multiprotein complexes (complex I and complex II) that also induces apoptosis by regulation of caspase-8 activity[16].

Under physiological conditions, specific ligands of dependence receptors are present at normal levels promoting cell survival, proliferation, and differentiation. But when ligand availability drops below a specific

threshold level lethal signaling cascades are activated (not completely elucidated), usually affecting caspase activity[18]. Some members of the dependence receptor family are p75 neurotrophin receptor (p75NTR), tyrosine kinase receptors, insulin receptor (IR), Semaphorin-3E receptor, and some integrins, among others[19].

Independently of the activation mechanism, the extrinsic apoptotic pathway is propagated by caspase-8 and accelerated by executioner caspases, mainly caspase-3.

1.1.2.2. Intrinsic apoptotic pathway.

In contrast to the extrinsic apoptotic pathway, the intrinsic or mitochondrial apoptotic pathway is initiated by a variety of exogenous and endogenous stimuli including excessive DNA damage, endoplasmic reticulum (ER) stress, aberrant Ca^{2+} fluxes, reactive oxygen species (ROS) overload, lack of survival signaling, viral infections, tumor suppressor gene expression, replication stress, chemical compounds and many other. These perturbations induce intracellular signals that directly act on targets within the cell, promoting alterations in the mitochondrial structure and function. The critical event or 'point of no return' for intrinsic apoptosis is the permeabilization of the mitochondrial outer membrane (MOMP), which is regulated by members of the Bcl-2 protein family[7,20]. The Bcl-2 pore forming proteins Bax and Bak oligomerize on the OMM, which results in MOMP and thus, the release of apoptogenic factors from the mitochondrial intermembrane space to the cytosol. These include cytochrome-*c* (Cyt-*c*), second mitochondrial activator of caspases/ direct IAP binding protein with

low Pi (SMAC/DIABLO) and the serine protease HTRA2/OMI[21]. These proteins promote caspase activation in two different ways. On one hand, SMAC and HTRA2/OMI block X-linked inhibitor of apoptosis (XIAP)-mediated inhibition of caspase-3 and -7, and release them for activation. On the second hand, Cyt-*c* binds to apoptotic protease-activating factor 1 (APAF1), inducing its oligomerization and further recruitment and activation of procaspase-9, leading to the formation of the apoptosome platform[20,22,23]. The caspase activation wave is propagated by the initiator caspase-9, which cleaves and activates procaspase-3 and -7, leading an efficient cell demolition (Figure 1).

During the late events of apoptosis (when the cell is committed to die), other proteins are also released from the mitochondria: endonuclease G (EndoG) and apoptosis-inducing factor (AIF). Both proteins normally reside in the mitochondria, but translocate to the nucleus after apoptosis induction, inducing chromatin condensation and DNA fragmentation in a caspase-independent manner[24,25].

Besides content leakage, mitochondria of apoptotic cells experience a decreased oxidative phosphorylation, lipid redistribution and peroxidation and eventually, the dissipation of the mitochondrial transmembrane potential ($\Delta\psi m$) and cristae remodeling[26,27].

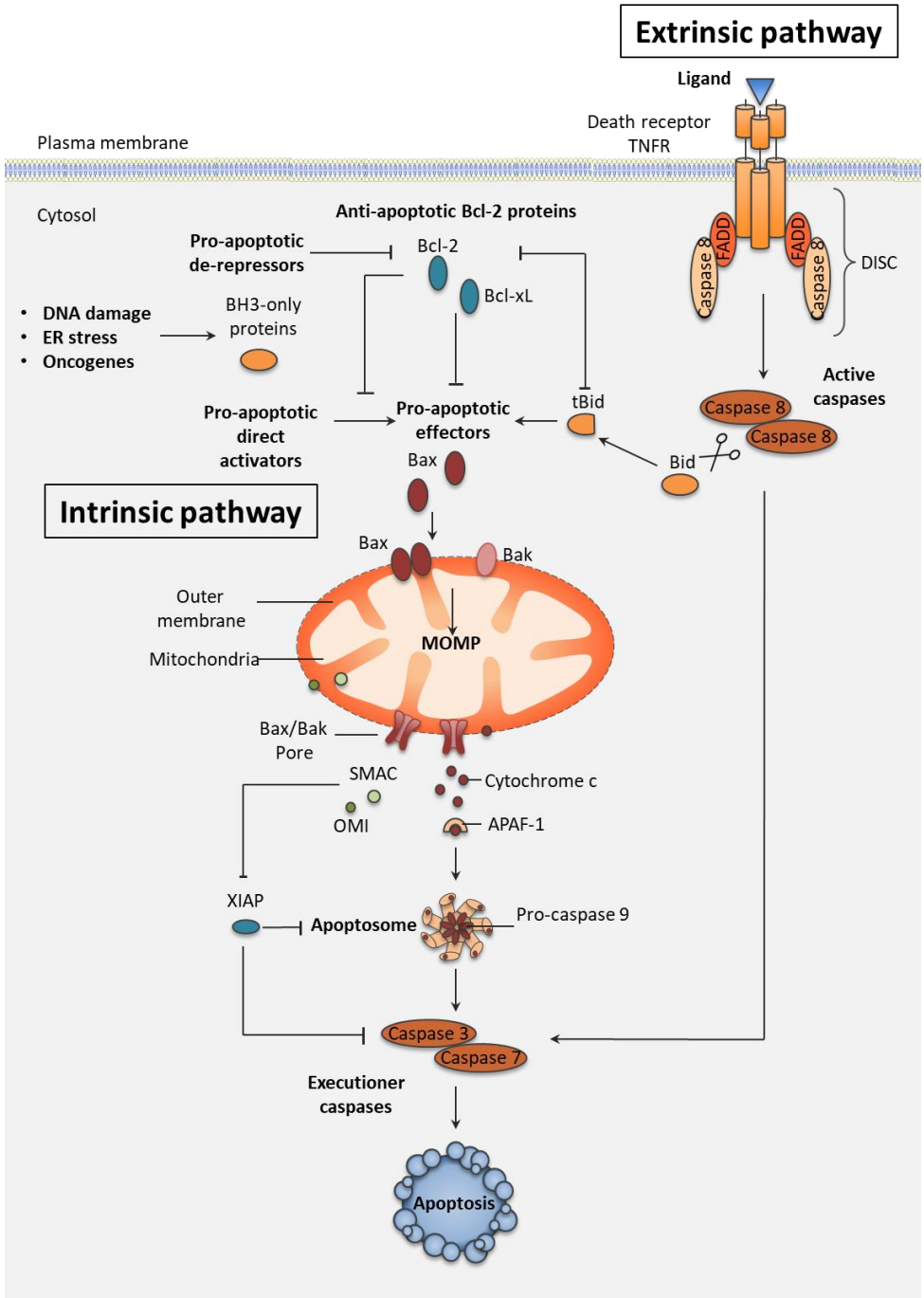
Extrinsic pathway
Ligand
Death receptor
TNFR
Plasma membrane
Cytosol
Anti-apoptotic Bcl-2 proteins
Pro-apoptotic
de-repressors
Bcl-2
Bcl-xL
DNA damage
ER stress
Oncogenes
BH3-only
proteins
Caspase 8
FADD
FADD
Caspase 8
DISC
Active
caspases
Caspase 8
Caspase 8
Pro-apoptotic
direct
activators
Pro-apoptotic
effectors
tBid
Bid
Bax
Intrinsic pathway
Bax
Bak
Outer
membrane
Mitochondria
MOMP
Bax/Bak
Pore
SMAC
OMI
Cytochrome c
APAF-1
XIAP
Apoptosome
Pro-caspase 9
Caspase 3
Caspase 7
Executioner
caspases
Apoptosis

Figure 1. Extrinsic and intrinsic apoptotic pathways. In the extrinsic pathway, ligand binding to the corresponding death receptor triggers DISC assembly (here formed by FADD and procaspase-8) that activates caspase-8 and promotes subsequent activation of executioner caspases (caspase-3 and 7). Besides, caspase-8 cleaves the BH3-only protein Bid into tBid, which connects the extrinsic pathway with the intrinsic or mitochondrial apoptotic pathway. In the last one, the MOMP results in the release of apoptogenic factors (e.g. cytochrome c) from the mitochondria to the cytosol. All these proteins allow the formation of the apoptosome where caspase-9 is activated. All the proteins from the Bcl-2 family regulate the MOMP, either leading its execution (multidomain or BH3-only proapoptotic proteins) or blocking the process (antiapoptotic members, such as Bcl-2 and Bcl-xL).

As mentioned before, MOMP is a common event shared in both the intrinsic and the death receptor extrinsic pathway. The crosstalk between them is mediated by Bid[28-30]. This protein is a member of the Bcl-2 protein family that is cleaved and activated by caspase-8 into its truncated form tBid[31]. It directly activates Bax and Bak[32], thus leading to the formation of Bax/Bak pores in the OMM.

1.2. THE BCL-2 PROTEIN FAMILY.

The Bcl-2 protein family plays a central role in the regulation of apoptosis, mainly but not restricted to the modulation of MOMP. Interestingly, they also regulate processes related to normal cell physiology such as metabolism at the inner mitochondrial membrane, mitochondrial morphology, Ca^{2+} homeostasis, unfolded protein response, glucose and lipid metabolism, macroautophagy, mitophagy and DNA damage response, among others[33,34].

The name of the family is derived from the first identified member Bcl-2 (B-cell lymphoma 2), which was constitutively expressed due to a t(14:18) chromosomal translocation, placing the *bcl-2* gene under the immunoglobulin heavy chain gene locus[35]. Since then, more than 20 Bcl-2 members have been identified in mammals, sharing conserved sequences in one to four regions so-called Bcl-2 homology (BH) domains, which are BH1, 2, 3, and 4[36]. Most of them also have a highly hydrophobic and helical C-terminal region that targets and/or anchors them to the intracellular membranes[37]. Based on the number of BH motifs and their functional activity, they are subdivided into three categories[38,39] (Figure 2):

1. Multidomain proteins:
    a) Antiapoptotic or prosurvival: Bcl-2, Bcl-xL, Bcl-w, Mcl-1, Bfl-1/A1 and Bcl-B that impede MOMP by inhibiting the proapoptotic members.
    b) Proapoptotic or cell death executioners: Bax, Bak, and Bok that oligomerize in and permeabilize the MOM.

2. BH3-only, proapoptotic proteins that activate the executioners or engage the prosurvival members rendering them ineffective:
    a) Direct activators: Bid and Bim.
    b) Sensitizers/direct activators: Noxa, Puma, Bmf.
    c) Sensitizers: Hrk, Bik, Bad, Bmf, Bnip3.

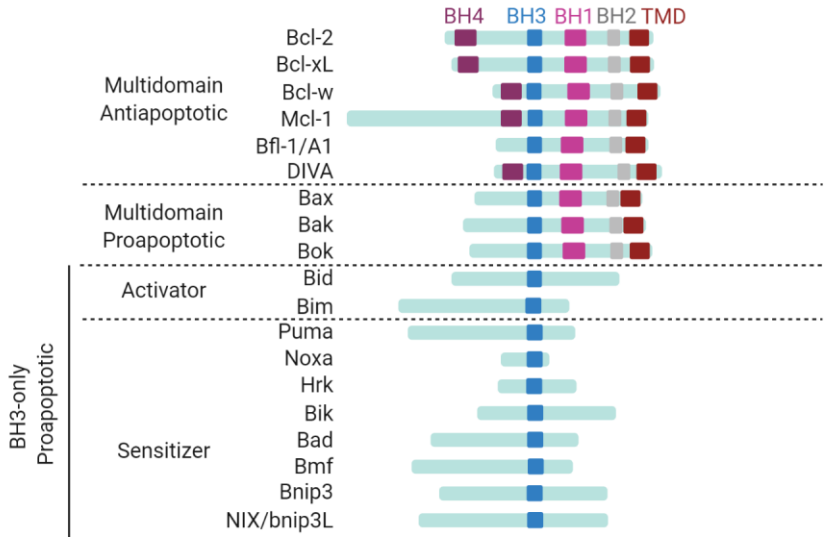

Figure 2. Classification of Bcl-2 family members. The Bcl-2 family proteins are grouped into two subgroups, by their ability to inhibit (antiapoptotic proteins) or activate (proapoptotic proteins) apoptosis. The proapoptotic group is further subdivided structurally and functionally into those that are multidomain proteins and show pore-forming activity, inducing MOMP, or those that contain only the BH3 domain and promote apoptosis through either inhibiting the antiapoptotic proteins or activating Bax and Bak. Bcl-2 homology (BH) motifs and transmembrane domains (TMD) are depicted. Adapted from[40].

1.2.1. Structure of Bcl-2 proteins.

Bcl-2 members are structurally categorized as globular proteins. The multidomain antiapoptotic and effector proteins share a conserved 'Bcl-2 core', comprised of eight amphipathic alpha (α) helices that hide and bury a central hydrophobic helix α5. The protein surface presents a central hydrophobic cleft delimited by the BH1 (α4–α5) and BH2 (α7–α8) motifs

on one side, and the BH3 motif (α2) and α3 on the other side, with the BH4 (α1–α6) motif stabilizing the BH1-BH3 regions[36].

The hydrophobic cleft is also known as 'Bcl-2 family BH3 and C-terminus-binding (BC) groove'. As the 'BC groove' term indicates, the C-terminal helix of some members, such as Bcl-w, Bcl-xL, Bax, and Mcl-1 binds and blocks their BC groove[41-44]. The BC groove of multidomain proteins is also involved in their canonical interactions, by binding BH3 regions of proapoptotic members and forming homo-oligomeric or hetero-dimeric complexes[45] (Figure 3). The structural similarities and differences within the BC grooves determine their interaction with BH3 ligands and are related to the biological functions of the Bcl-2 family proteins[46-48].

The structure of multidomain members is similar to the membrane translocation and pore-forming domain of bacterial toxins such as the colicins and diphtheria toxin. Indeed, Bcl-xL and Bcl-2 have been shown to form pores in artificial membranes[48].

Opposite to the multidomain Bcl-2 proteins, BH3-only proteins (except Bid) lack a globular fold and are intrinsically disordered[45].

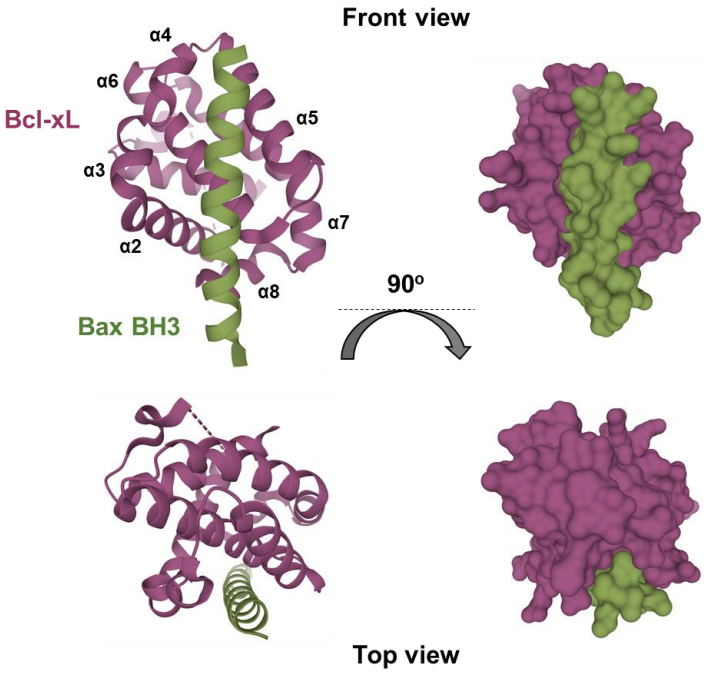

Figure 3. Crystal structure for Bcl-xL in complex with the Bax BH3 domain. Bcl-xL (purple) binds the Bax BH3 domain (green) into the BC groove (PDB 3PL7). The left panel depicts α-helices of Bcl-xL and the right panel represents its globular structure. The image was created using the crystal structure published in[49] with Mol* (D. Sehnal, A.S. Rose, J. Kovca, S.K. Burley, S. Velankar (2018) Mol*: Towards a common library and tools for web molecular graphics MolVA/EuroVis Proceedings. doi:10.2312/molva.20181103); provided by RCSB PDB (https://www.rcsb.org/).

1.2.2. Molecular mechanisms of Bcl-2 family regulation.

Various competing but not exclusive models describe the interactions among the Bcl-2 family proteins in the regulation of MOMP. In all models, the BH3 region has a key role in the primary apoptotic function of Bcl-2

family members and their interactions at the intracellular membranes[34] (Figure 4).

Direct activation model: this model categorizes the BH3-only proteins in 'activators' and 'sensitizers', based on their affinity for binding and activating Bax and Bak or for binding and inhibiting antiapoptotic proteins, respectively[50]. MOMP is promoted by Bax and Bak, which are activated by direct interaction with BH3 activators, while antiapoptotic proteins inhibit MOMP specifically sequestering the activator BH3 proteins. Another interaction included in this model is the binding of sensitizer BH3 proteins with antiapoptotic members, inducing the release of the 'activators' and thus, favoring the activation and oligomerization of Bax and Bak and promoting MOMP[51].

Indirect activation or de-repression model: this model assumes that Bax and Bak are constitutively and structurally active in healthy cells, but the interaction with antiapoptotic proteins inhibit their activity. Here, BH3 proteins are divided based on their affinities for binding antiapoptotic proteins (they are not considered as direct Bax and Bak activators)[47].

Embedded together model: the major aspects of the previous models are combined in this one. All binding interactions of Bcl-2 family proteins are reversible, and equilibria are governed by local affinities and relative protein concentrations. Interactions on, at or within the MOM, change their affinities, and therefore, they have an active role in the functions of the proteins[52,53]. Binding of the activator BH3 proteins to membranes increases their affinity for the proapoptotic executioners, which are active to

oligomerize and promote MOMP. The antiapoptotic proteins inhibit both the proapoptotic executioners and BH3-only proteins by mutual sequestration in the membranes or by preventing their binding to the membranes. The sensitizer BH3 proteins bind to and inhibit the antiapoptotic members by mutual sequestration too. Finally, the local concentrations of Bcl-2 proteins at intracellular membranes are different, affecting their binding to the membrane and the equilibria between each family member[34,54].

Unified model: it distinguishes two antiapoptotic mechanisms. The sequestration of BH3-only activators by antiapoptotic members as mode 1, and the sequestration of the pore-forming proteins Bax and Bak, as mode 2. Specifically, it predicts that mode 2 repression is more efficient inhibiting MOMP than mode 1 since activated Bax/Bak can activate other Bax/Bak proteins[55]. This model also links MOMP with mitochondrial dynamics, since Bax and Bak have been involved in mitochondrial fission and fusion[54].

As mentioned before, the interactions with the MOM change the affinities of Bcl-2 proteins due to the lipid composition of the MOM. The 'Lipid central model' has been recently proposed and supports that mitochondrial lipids are not only structural elements of the MOM but also display a functional role regulating apoptosis. Lipids can alter the physical properties of the MOM and/or directly interact with some mitochondrial proteins in a specific manner. In this way, they modulate the activation and function of Bcl-2 family proteins[56,57].

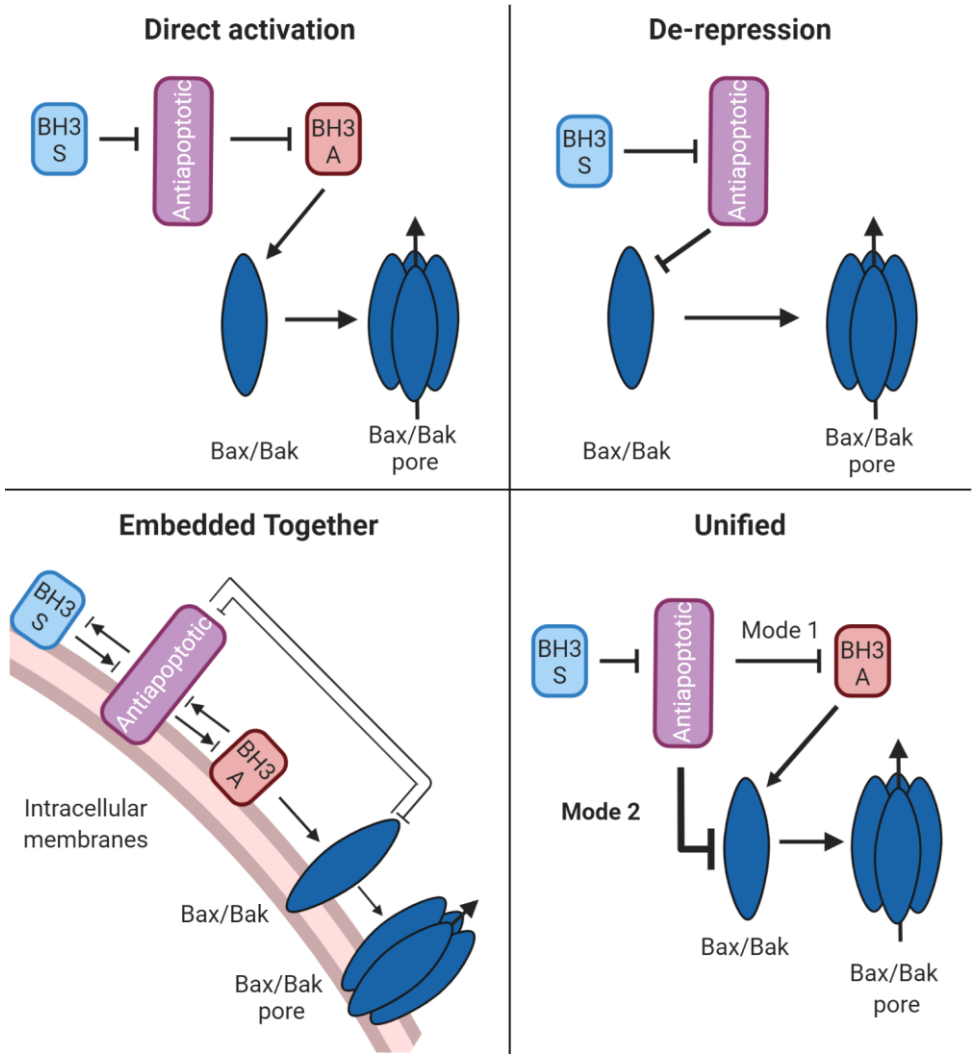

Figure 4. Proposed models for the regulation of MOMP by Bcl-2 proteins. (→) Activation; (⊤) inhibition; (→|) mutual recruitment/sequestration. BH3 S and BH3 A indicate sensitizers and activators BH3-only proteins, respectively. Sensitizers bind and inhibit prosurvival proteins, while activators activate Bax and Bak pore-forming proteins.

In general, all the accepted models to date are based on the BH3 binding into groove interactions. However, non-canonical interactions of Bcl-2 proteins are currently gaining attention in the field. Some of them are the previously described lipid:protein binding or the interaction of Bcl-2 transmembrane domains (TMDs)[58]. In contrast to the well-characterized BH3:groove interface that has been mainly described in aqueous solutions, these non-canonical interaction surfaces have been identified using membrane environments. Considering that most of the interactions that modulate apoptosis occur when they are inserted into the MOM, it is necessary to identify the interactions that govern their equilibria by using intracellular membrane models.

1.3. SUBCELLULAR DISTRIBUTION OF BCL-2 FAMILY PROTEINS.

Proper subcellular distribution and targeting are critical for the function of intracellular proteins. As MOMP regulators, Bcl-2 members mainly localize at the mitochondrial membrane. However, they can also regulate MOMP in a remote fashion and participate in additional non-apoptotic functions targeting other organelles including the ER, the Golgi apparatus, the nuclear outer membrane, and the nucleus itself or reside in the cytoplasm[59]. Their specific subcellular localization (Figure 5) is determined by their different affinities for various intracellular membranes and binding partners at each location[34].

The antiapoptotic Bcl-2 protein resides on the ER membrane, the nuclear envelope, and the MOM under normal conditions[37,60,61]. Bcl-xL is mainly present in the MOM and the cytosol[37,62], being translocated to the MOM during apoptosis[63], although it also appears as an ER resident. A similar distribution is described for Bcl-w (mainly cytosolic in healthy cells), which translocates and inserts into the MOM under apoptotic conditions, triggered by BH3-only protein binding to its hydrophobic groove[64]. The most promiscuous distribution is presented by Mcl-1 that localizes at the mitochondria (it appears into the MOM, the mitochondrial inner membrane and the mitochondrial matrix), the nucleus, the cytosol, and the ER, being accumulated into the MOM after apoptosis induction[65-69].

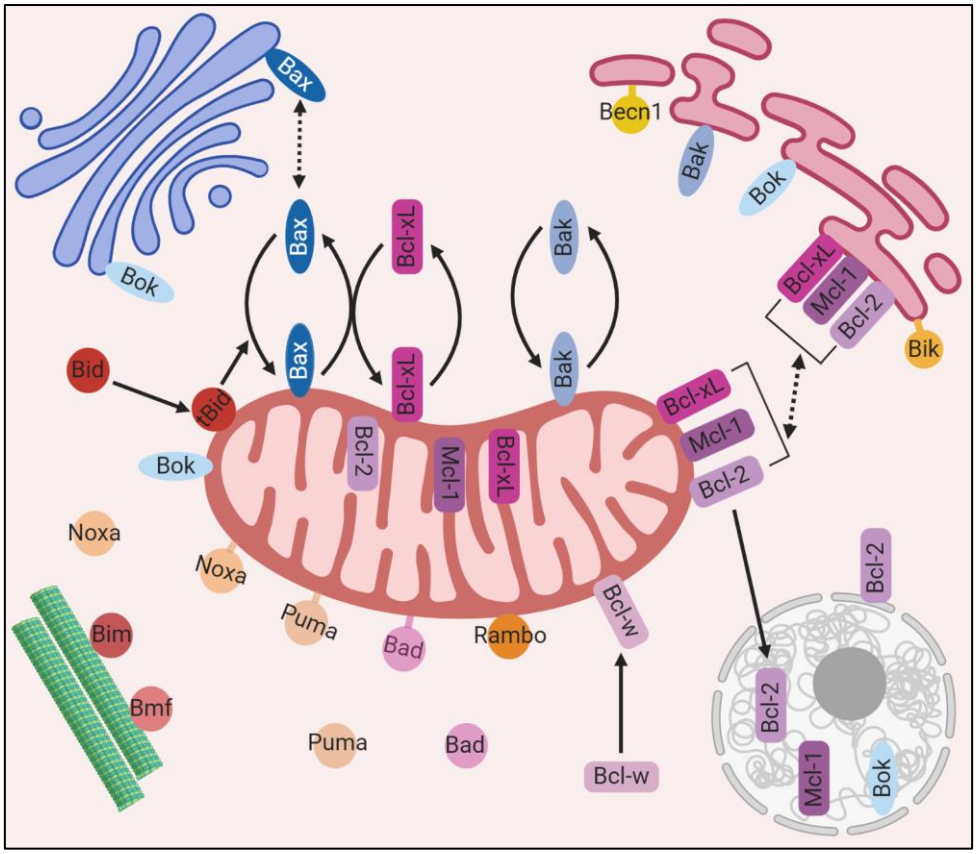

Figure 5. Subcellular distribution and dynamics of the Bcl-2 family of proteins. Continuous and bold lines represent protein translocation in normal and stress conditions. Dashed lines represent possible subcellular translocation. Adapted from[59].

The proapoptotic protein Bax is mostly cytosolic in healthy conditions and translocates to the MOM upon apoptotic stimuli[43,70,71], while Bak is constitutively inserted into the MOM and to a lesser extent into the ER membrane[72,73]. The third pore-forming member Bok targets the MOM, the nucleus, and the membranes of the ER and the Golgi apparatus[74-76].

After activation, BH3-only proteins target mitochondrial and ER membranes. However, in normal conditions, they appear in different intracellular locations. Bim and Bmf are bound to the cytoskeleton[77-79]; Rambo localizes at the MOM[80]; Puma, Noxa, and Bad are both soluble in the cytosol and bound to the MOM[81-86]; Bid is located in the cytosol[87] while Bik and Beclin 1 target the ER[88,89].

Once activated, multidomain Bcl-2 proteins and BH3-only proteins migrate to and insert into the mitochondrial membrane by different mechanisms: 1) direct post-translational anchorage into the MOM by tail-anchor sequences[37,85,90]; 2) interaction with other Bcl-2 family proteins[91,92]; 3) interaction with non–Bcl-2 family proteins, such as TOM/TIM complexes and enzymes that produce post-translational modifications[93]; and 4) interacting with mitochondrial lipids, such as cardiolipin or cholesterol[94,95].

As mentioned before, almost all the multidomain Bcl-2 proteins and some BH3-only members target and insert into the intracellular membranes by their tail-anchor sequence or TMD. The transmembrane domains are highly hydrophobic and helical C-terminal segments, of 15 to 22 amino acids, flanked by charged amino acids. The hydrophobicity of the TMD and the basicity of the flanking sequences have a relevant role for the membrane specific targeting of the proteins[37,96,97]. Well-defined TMDs are present in Bak, Bcl-2, Bcl-xL, Bcl-w, and Mcl-1, while C-terminal segments of Bax, Bfl-1, or some BH3-only proteins do not show general criteria of canonical TMD sequences but still translocate these proteinsfrom the cytosol to the

membrane upon apoptosis stimulation[97]. Bok also has an unconventional TMD sequence although it exclusively resides in membranes[74,76].

1.3.1. Bcl-2 transmembrane domains in the context of full-length proteins: membrane targeting and functional role.

Bcl-xL has a well-defined TMD. Its preferential mitochondrial targeting is favored by the presence of two basic amino acids at both ends of the C-terminal segment[37]. The Bcl-xL TMD is not only involved in the intracellular anchoring but also the homo-dimer formation and interaction with Bax[58,98]. Indeed, the Bcl-xL TMD mediates Bax retrotranslocation from the mitochondria into the cytosol by direct binding with Bax[91], modulating Bax accumulation on the mitochondria and thus, the formation of Bax oligomers and its proapoptotic activity. The C-terminus of Bcl-xL also influences the Bcl-xL shuttling off the mitochondria[91].

Table 1. Transmembrane domains of the Bcl-2 family.

Protein	Predicted sequence	Target
Bcl-2	$_{212}$FSWLSLKTLLSLALVGACITLGAYLGHK$_{239}$	ER, MOM, Nucleus
Bcl-xL	$_{203}$SRKGQERFNRWFLTGMTVAGVVLLGSLFSRK$_{233}$	MOM, ER
Bcl-w	$_{163}$REGNWASVRTVLTGAVALGALVTVGAFFASK$_{193}$	MOM
Mcl-1	$_{328}$IRNVLLAFAGVAGVGAGLAYLIR$_{350}$	MOM, ER, Nucleus
Bfl-1	$_{151}$KSGWMTFLEVTGKICEMLSLLKQYC$_{175}$	MOM, ER, Nucleus
Bax	$_{169}$TWQTVTIFVAGVLTASLTIWKKMG$_{192}$	MOM, ER, Golgi
Bak	$_{188}$ILNVLVVLGVVLLGQFVVRRFFKS$_{211}$	MOM, ER
Bok	$_{186}$RSHWLVAALCSFGRFLKAAFFVLLPER$_{212}$	ER, Golgi, MOM

Underlined residues represent the flanking regions of the TMD, which are influence the subcellular targeting. Intracellular targeting extracted from[34].

In addition to the role in the interaction equilibrium, the Bcl-xL TMD is related to mitochondrial morphology (increased proportion of mitochondria with an expanded matrix) and confers moderated cell death resistance in response to staurosporine[99]. Pécot and colleagues[100] have also pointed out the implication of the Bcl-xL TMD in the chemotherapeutic resistance to the BH3 mimetic and Bcl-xL inhibitor WEHI-539. It has been proposed that upon WEHI-539 treatment, the BH3-only protein Puma is released from the Bcl-xL sequestration and thus, activates Bax oligomerization. However, in cellular systems, BH3 mimetics might not fully inhibit intracellular Bcl-xL[101]. This is due to membrane-anchored Bcl-xL has an enhanced antiapoptotic activity than the soluble forms used in drug design studies. Hence, mutations within the C-terminal end alter

Bcl-xL intracellular localization, which has an impact on its BH3 binding properties and the cellular response to BH3 mimetics[100].

There are three Bcl-x isoforms described: Bcl-xL, Bcl-xS, and Bcl-xAK. Both Bcl-xS and Bcl-xAK isoforms contain the TMD and are proapoptotic proteins[102-105]. The Bcl-xS includes the BH3 and BH4 domains together with the loop and the transmembrane segment[106,107]. It has been proposed that Bcl-xS requires the TMD to localize in mitochondria and exerts its cell-killing effect[107]. In the case of Bcl-xAK isoform, it encloses BH2, BH4, and the TMD, and executes cell death in a Bax/Bak and caspase-dependent manner[108].

In contrast to the mainly mitochondrial localization of Bcl-xL, **Bcl-2** also targets the ER and the nuclear envelope. The different distribution of these two proteins is explained by TMD differences. The Bcl-2 TMD is more hydrophobic in its N-terminal half and fewer basic residues surround it, which causes a decrease in Bcl-2 MOM-specificity, leading to a greater localization on the ER membrane and nuclear envelope[37]. Despite their differences, Bcl-2 and Bcl-xL TMDs can form homo-oligomers and hetero-oligomerize with the Bax TMD. In a previous work[58], we demonstrated that Bcl-2:Bax and Bcl-xL:Bax TMDs hetero-oligomers regulates Bax pore-forming activity by direct competition, decreasing Bax oligomerization and MOMP.

Bfl-1 does not contain a well-defined TMD, although its C-terminal helix anchors Bfl-1 to the mitochondrial membrane. Interestingly, the

amphipathic character of the C-terminal domain is required for protein anchorage to mitochondria and regulates its prosurvival function[109].

The **Mcl-1** TMD is essential for protein localization and mitochondrial membrane insertion[110], as well as the nuclear and the ER membranes[111]. It has been described that cleaved Mcl-1 fragments and a splice variant, which contain the C-terminal segment, exert proapoptotic functions. More in detail, the cleavage at Aspartate 127 results in the Mcl-$1^{128\text{-}350}$ product that induces cell death in several cell lines and primary malignant B-cells[112-115]. On the other hand, the extra short (Mcl-1_{ES}) splice variant induces mitochondrial apoptosis in a Bax/Bak independent manner[116]. Both, the Mcl-$1^{128\text{-}350}$ fragment and Mcl-1_{ES} isoform retain BH1 to BH3 domains and the TMD, therefore the specific role of the TMD in cell death induction is not clear. However, it has been recently described a possible role for the Mcl-1 TMD in the antiapoptotic function of Mcl-1 under Bok-induced apoptosis[117].

The C-terminal segment of **Bcl-w** is folded back into the hydrophobic pocket in healthy cells. In response to an apoptotic stimulus, Bcl-w undergoes a conformational change, during which the C-terminus is displaced from the pocket and Bcl-w inserts into the MOM. The C-terminal truncated version can sequester BH3-only proteins such as Bim, although its antiapoptotic activity is impaired[41,118].

In the inactive and cytosolic **Bax**, the C-terminal segment (α9) is folded back into the hydrophobic groove. After apoptosis induction, the C-terminal region is released, directing Bax to the mitochondrial membrane and allowing the binding of BH3 domains of other Bcl-2 proteins[43]. There are a

few amino acids identified as key elements for mitochondrial targeting or apoptotic activity: P168, G179, T182, and S184[58,70,119,120].

Different groups have investigated the role of P168 in Bax localization and apoptosis execution, getting contradictory results. Shinzel et al.[119] concluded that the P168A mutation abrogates Bax mitochondrial targeting in both normal and apoptotic conditions. However, other data have shown the opposite effects of P168 mutants. In a yeast system, the P168A mutant exhibited an increased capacity to insert into the MOM and to promote the release of Cyt-*c* [121]. In agreement with this, Simonyan et al.[122] showed that Bax P168A has a greater ability to bind to membranes, oligomerize and thus, release Cyt-*c* from mitochondria.

In the case of the residue 179, a Glycine to Proline mutation impairs large oligomers formation[70] and Bax C-terminal dimerization, as demonstrated in our previous work[58]. However, Newmeyer's group and we have gotten contradictory results regarding Bax G179P mitochondrial localization. They showed a cytoplasmic distribution of Bax G179P full-length (FL) protein in $Bax^{-/-}Bak^{-/-}$ mouse embryonic fibroblasts (MEFs), with and without the apoptosis inducer staurosporine; while we demonstrated that the Bax G179P TMD associated with mitochondria in Bax/Bak proficient HCT116 cells. A possible explanation for these contradictory results is that, in our system, the presence of the endogenous Bax WT protein may allow a marginal interaction with the overexpressed Bax G179P TMD. This seems to be sufficient for the membrane targeting of the Bax G179P TMD and suggests that Bax TMD:Bax TMD

dimerization may be involved in the mitochondrial localization of the protein. Newmeyer's group has also described that Bax G179P impairs Bax function, showing a devoid apoptotic activity after staurosporine stimulation[70]. In addition to these observations, Bax G179E mutation also affects Bax proapoptotic activity. This mutation has been identified in ABT-199–resistant human lymphoma cells, where it blocks ABT-199–induced apoptosis and led partial cross-resistance to other chemotherapeutic drugs[123].

The other mentioned important TMD residue is S184. The S184V mutation constitutively associates Bax with mitochondria[43,120] because of its slow retrotranslocation. This process is also reduced in the Bax T182I mutant promoting a predominantly mitochondrial localization. The T182 mutation makes Bax less efficient in oligomer formation and liposome membrane permeabilization[70].

The Bax helix 9 is not only involved in protein targeting but also dimerization contacts of Bax oligomers[124,125]. The α9:α9 dimerization enlarges Bax pores allowing the release of large proteins from the mitochondria[125].

In a study with yeast mitochondria, Arokium et al.[126] demonstrated that Bax C-terminus is involved in Bax/Bcl-xL interaction since mutations of this segment impaired the inhibitory effect of Bcl-xL over Bax insertion. In agreement with this, we have also demonstrated that the Bax TMD oligomerizes with the Bcl-xL TMD in the mitochondrial membrane[58]. Indeed, we showed that Bax TMD-induced apoptosis was partially protected

under Bcl-xL TMD overexpression, suggesting that the interaction of both TMDs can modulate cell fate in apoptotic cells.

Biophysical studies have revealed that the **Bak** TMD (α9) inserts itself into membranes, adopting an α-helical structure and perturbing the physical properties of the membrane[127]. Complementary data from Iyer and colleagues[128] have demonstrated that after Bak activation, α9 helices come into proximity before BH3:groove dimerization. They identified an α9:α9 interface in the Bak apoptotic pore, although no dimerization motif was evidenced and the Bak α9 TMD did not directly contribute to the pore structure. However, α9:α9 binding can link BH3:groove dimers to higher-order oligomers. The Bak C-terminal segment shows another functional role, as its hydrophobicity determines the shuttling rate of Bak from the mitochondria to the cytosol, influencing its apoptotic activity[129]. The residency of Bak in mitochondria is also regulated by voltage-dependent anion channel 2 (VDAC2) sequestration and mediated by direct interaction with the Bak TMD. This complex maintains Bak in an inactive conformation, thereby raising the stimulation threshold necessary for MOMP[130].

The **Bok** TMD is necessary for ER and Golgi apparatus targeting since BokΔTMD is diffusely distributed in the cytosol and the nucleus[74]. It has also been proposed that the Bok TMD may directly interact with Mcl-1 during the inhibition of apoptosis induced by Bok overexpression[117].

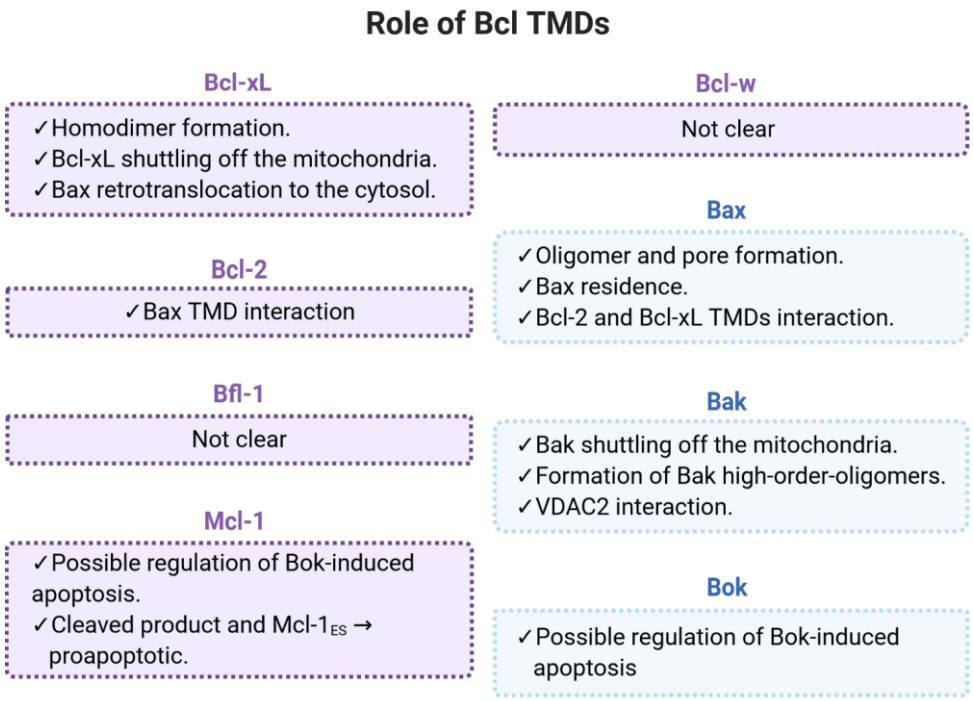

Figure 6. Transmembrane domains from the Bcl-2 family of proteins act as membrane anchors but they also play crucial roles in apoptosis orchestration.

1.4. BCL-2 PROTEIN FAMILY IN DISEASE

1.4.1. Targeting Bcl-2 proteins in cancer therapy.

One of the cancer traits or hallmarks is the capability to evade programmed cell death[131]; for example, by altering of Bcl-2 proteins expression or disturbing their interaction equilibria. Several tumors have shown alterations in Bcl-2 proteins, such as follicular lymphoma[132], hepatocellular carcinoma[133], prostate cancer[134], breast cancer[135-137], or

small-cell lung carcinoma[138]. Cancer cells evade apoptosis through different mechanisms:

1. Insufficient activator BH3-only proteins.
2. Inactive or low levels of proapoptotic proteins Bax and Bak.
3. Overexpression of antiapoptotic members Bcl-2, Bcl-xL, and Mcl-1.
4. Mutations that disturb the interaction equilibria between pro and antiapoptotic members, in both the cytosol and the membrane.

Bcl-2 proteins not only act as oncogenic drivers but also, they contribute to acquiring chemotherapy resistance[139,140]. Moreover, recent studies have demonstrated that Bcl-2 proteins play additional non-apoptotic roles related to cancer cell survival and tumor development. Some of them include regulation of mitochondrial physiology (morphology, permeability transition, electron transport chain, metabolism), ER physiology (Ca^{2+} homeostasis, unfolded protein response), autophagy, nuclear processes (cell cycle, DNA damage response), and glucose and lipids metabolism[141].

Studies at the cellular level, using mouse models or analyzing patient samples evidence the role of this family of proteins in promoting cell migration, invasion, and cancer metastasis[142]. To mention a few examples, Bcl-xL up-regulation correlates with invasion (vascular or stromal invasion) and metastasis (lymph node or distal metastasis) in retinoblastoma patient samples[143]. In triple-negative breast cancer cells, the Bcl-xL mitochondrion-localized isoform interacts with VDAC1 to regulate the transference of Ca^{2+} from the ER to mitochondria in a BH3-dependent manner, promoting cell migration[144]. Lastly, Bcl-w up-regulation is

significantly associated with infiltrative types of gastric cancer[145] and enhances the invasiveness of glioblastoma cells[146].

The involvement of Bcl-2 proteins in these cellular processes supports their pharmacological targeting for anticancer therapy, not only to kill tumor cells but also to avoid metastasis dissemination. Based on structural and protein interaction features, the so-called BH3 mimetics have been developed to mimic the action of certain BH3-only proteins and inhibit the prosurvival members[147,148]. The BH3 mimetics bind to the hydrophobic cleft of antiapoptotic proteins, releasing proapoptotic BH3-only proteins, who in turn activate Bax and Bak, and commits cells to mitochondrial apoptosis. The first generated BH3 mimetics were ABT-737, which inhibits Bcl-xL, Bcl-2, and Bcl-w[149], and its orally bioavailable analog ABT-263 (navitoclax)[150], both developed by Abbott Laboratories. Navitoclax showed efficacy as monotherapy in clinical trials for hematological malignancies[151] and small cell lung cancer[152]. Furthermore, ongoing clinical trials also evaluate its combination with other chemotherapeutic drugs[153-155]. However, the use of navitoclax in the clinic is impaired by dose-dependent Bcl-xL–mediated thrombocytopenia due to platelet apoptosis[156,157].

For this reason, a more potent and selective Bcl-2 inhibitor, ABT-199 (venetoclax), was developed and became the first BH3 mimetic to be FDA-approved for the treatment of relapsed/refractory chronic lymphocytic leukemia (CLL). In a monotherapy trial of this disease, venetoclax treatment showed a manageable safety profile, with a partial response observed in 79% of patients and a complete response in 20% of them[158]. Many studies have

also assessed its efficacy in combination therapies to improve its clinical activity[159-161].

However, despite the good clinical results obtained with venetoclax, resistances have already been observed, because of overexpression of other antiapoptotic proteins or by mutation of the BH3 binding groove. Therefore, complementary treatments to overcome these resistances are urgently needed.

1.4.2. Druggability of transmembrane domains.

About fifty percent of all therapeutics target membrane proteins[162], mainly binding solvated regions outside the membrane. Traditionally, drug discovery has looked 'for drug targets where looking is easiest'. However, membrane protein interactions have been considered 'undruggable' targets by standard methodologies[163] due to the general lack of structural information and the special physicochemical characteristics of membrane proteins[162].

Membrane proteins establish protein-protein interactions (mPPIs), as well as protein-lipid and protein-nucleic acid interactions. It is estimated that there are about 130,000 to 650,000 types of mPPIs in the human interactome[164,165]. However, pharmaceutical targeting of mPPIs for therapeutic intervention is challenging because their interface is generally large and flat (lacking binding pockets), often exposed to solvent, dominated by hydrophobic characteristics[166-168], and governed by energetic rules still not completely understood. These features difficult that small molecules

effectively interrupt mPPIs. Nevertheless, for the last years, mPPIs have emerged as viable drug targets, especially those interfaces exposed outside the membrane. This is because it has been traditionally considered that no specific interactions occur within the membrane and that TMDs are simply passive membrane-spanning anchors. Despite this assumption, TMDs play active roles in oligomerization and specifically drive protein functional activities within membranes[163]. This is the case of integrin TMDs that make switchable hetero-dimeric interactions stabilizing their inactive conformation[169,170]. In the same line, a recent study highlights the role of human epidermal growth factor receptor 2 (HER2) TMD in oncogenesis[171]. HER2 is a member of the receptor tyrosine kinase family ErbB and a major target for cancer therapy, due to its potential role as oncogene[172]. Recurrent mutations within the HER2 TMD identified in cancer patients improve the dimer interface and stabilize an active conformation of the receptor[171]. Other examples are viral peptides that interact with the TMDs of growth factors or cytokine receptors to cause cellular transformation[173,174] (Figure 7).

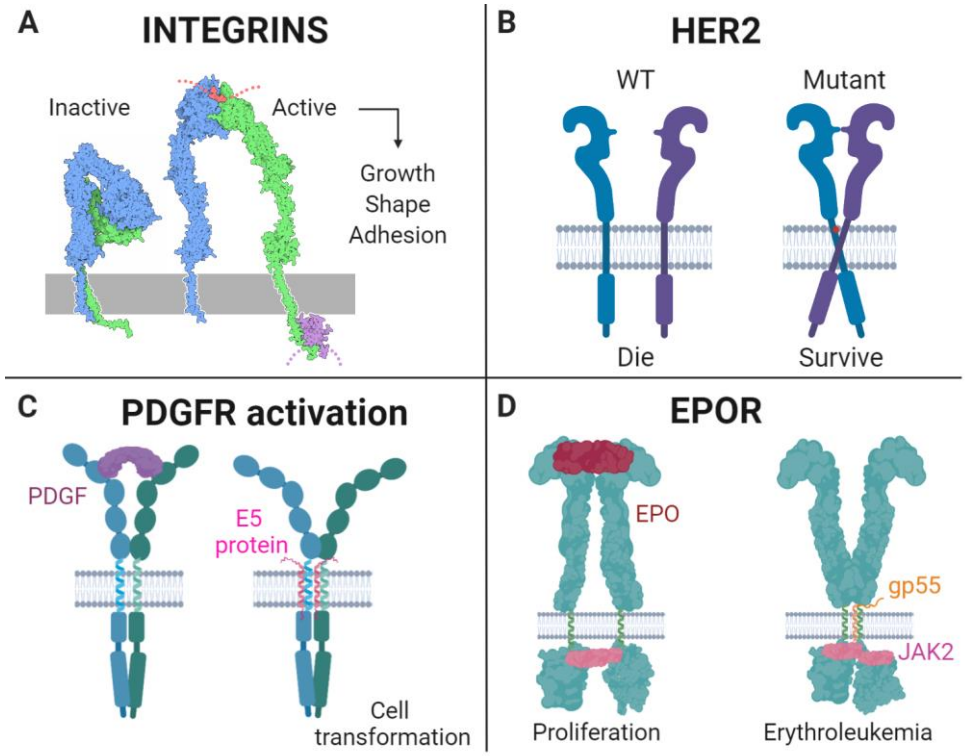

Figure 7. Functional significance of TMD interactions. A) Integrin activation model, where dimer formation through TMD interaction maintains an inactive state. **B)** The human epidermal growth factor receptor 2 (HER2) is an oncogenic driver and a major anticancer therapy target. TMD-activating mutations promote HER2 homodimerization and lead to allosteric activation of the kinase domain. **C)** Platelet-derived growth factor (PDGF) receptors (PDGFR) are necessary for the growth of several cell types. Upon ligand-dependent activation, they form homo and heterodimers and the mitogenic signal is transduced. The bovine papillomavirus E5 protein acts as an oncoprotein by direct binding with the PDGFR-TMD and inducing ligand-independent activation. **D)** Erythropoietin (EPO) activates the EPO receptor (EPOR) that ultimately results in the proliferation and differentiation of red blood cell precursors. The Friend Erythroleukemia Virus expresses gp55 protein, which binds the murine EPOR-TMD, activating EPOR and inducing uncontrolled red blood cell proliferation and hence, erythroleukemia.

Druggability of TMD interaction surfaces is also challenging due to the presence of the highly hydrophobic and still poorly understood membrane environment. However, recent scientific advances have allowed the discovery of modulators of these transmembrane interactions. A selective inhibitor of latent membrane protein-1 (LMP-1), the NSC295242 compound, was identified by using a cell-based screening. The transmembrane domain 5 (TMD-5) of LMP-1 drives its homo-trimerization, leading to the constitutive oncogenic activation of the Epstein-Barr virus (EBV). NSC295242 prevents TMD-5 homo-trimerization and thus, inhibits the oncogenic signaling of LMP-1[175]. The protease-activated receptor-1 (PAR-1) is also pharmacologically modulated by the TMD ligand vorapaxar[176] to prevent platelet aggregation[177]. Molecular dynamics (MD) analysis described that possibly, vorapaxar binds and dissociates from PAR-1 through a tunnel formed by TMD6 and TMD7 into the lipid bilayer, interacting with the extracellular leaflet of the plasma membrane[176].

Altogether, these examples pave the way for exploring TMDs as new points for pharmacological intervention, a still-emergent but promising field. Advances in structural biology (especially the development of cryoelectron microscopy[178,179]), and biological systems (such as the BiFC[180] and the ToxR systems[181,182]) facilitate the identification of new specific TMD PPIs in native environments. Therefore, improving the knowledge of TMDs structural-function relationship will help to modulate more feasibly TMD PPIs.

In this scenario, our studies of Bcl TMDs interactions not only give a new vision of the Bcl-2 proteins equilibria in the membrane but also highlight the role of these TMDs as druggable targets.

OBJECTIVES

Apoptosis is the best-characterized form of programmed cell death and its alteration in cancer cells provides them an advantage for tumor progression. This cellular process is regulated by interactions of the Bcl-2 family of proteins. Bcl-2 interactions occur in both the cytosol and intracellular membranes where they anchor by their transmembrane segments. The interaction network of the Bcl-2 cytosolic domains has been largely studied; however, the membrane equilibria that govern the mitochondrial apoptotic pathway is poorly understood. Given the relevance of this family of proteins in apoptosis regulation and the implication of antiapoptotic proteins in cancer progression, this thesis aims to understand the biological significance of Bcl TMDs interactions and exploit these binding interfaces as new chemotherapy targets.

The specific objectives referred to each chapter are:

- To analyze the contribution of the Mcl-1 TMD to both the oligomerization state of the protein and its antiapoptotic function.

- To identify inhibitors that specifically target Mcl-1 TMD-lateral hetero-interactions as novel anticancer drugs and TMD modulators.

- To evaluate the functional relevance of mutations described in the Bcl-2 and Bcl-xL TMDs that have been identified in cancer patients.

Chapter I

Mcl-1 and Bok Transmembrane Domains: Unexpected Players in the Modulation of Apoptosis

Graphical abstract

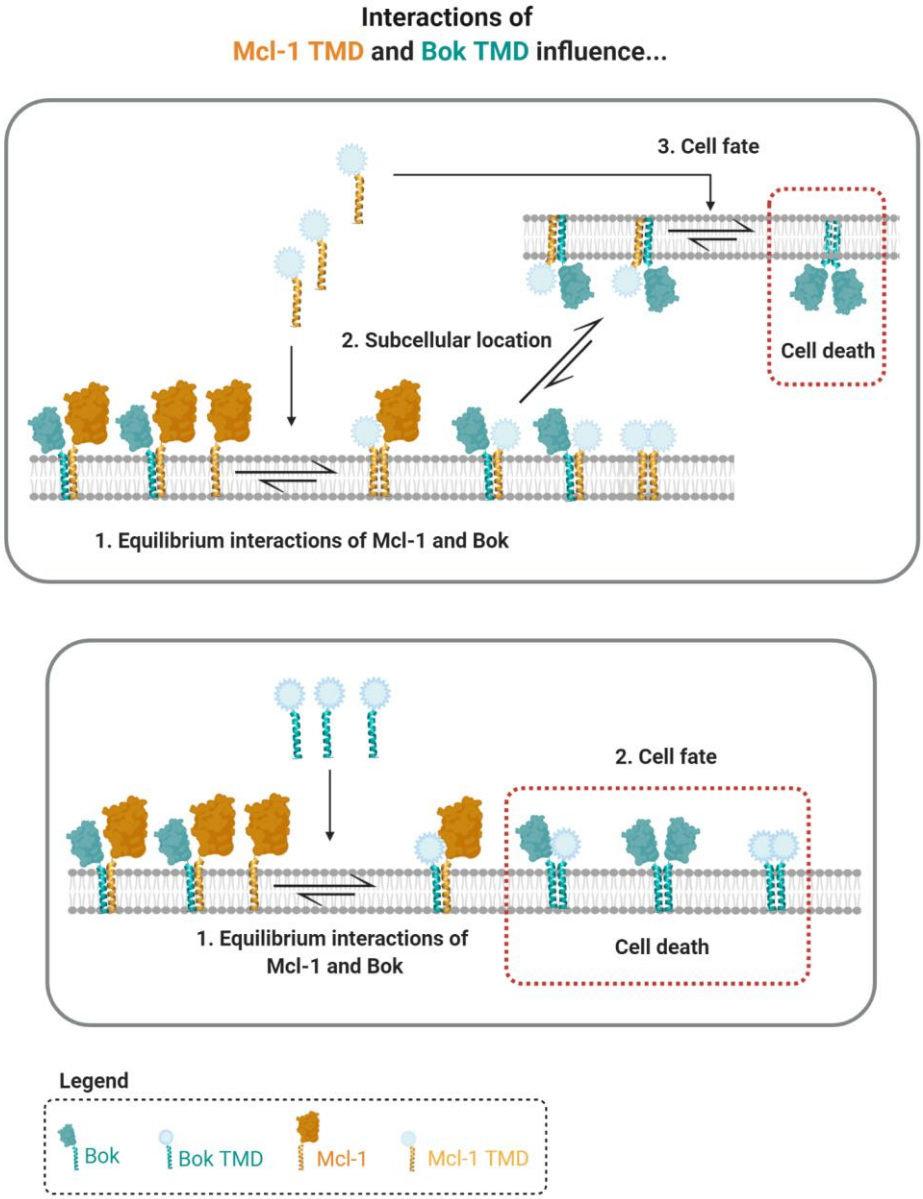

The experimental research presented within this Thesis Chapter has been carried out in collaboration with Dr. Matti Javanainen and Dr. Waldemar Kulig's groups, who have performed the molecular dynamics simulations. As a result of this collaboration, the publication *Mcl-1 and Bok Transmembrane Domains: Unexpected Players in the Modulation of Apoptosis* is under revision in the journal Proceedings of the National Academy of Sciences.

3.1. INTRODUCTION

Bcl-2 proteins are structurally characterized by the presence of at most four BH domains and a C-terminal transmembrane segment that in almost all members serves as a transmembrane domain. During the apoptotic process, most interactions between Bcl-2 proteins occur at intracellular membranes, where TMDs of Bcl-2 proteins (Bcl TMDs) have been traditionally described only as membrane anchor domains. However, mechanistic studies have demonstrated that Bcl TMDs fulfill many other crucial functions (as mentioned in the *General Introduction*). For example, in our previous work, we described the interaction of Bax TMD with Bcl-2 or Bcl-xL TMDs as a new level of apoptosis regulation[58].

Despite this evidence, the underlying network of Bcl TMD interactions and their functional contribution to apoptosis modulation remains poorly understood. To increase our knowledge of the modulatory events that take

place within the membrane and influence the apoptotic pathway, we focused the present work on the study of the Mcl-1 TMD.

The antiapoptotic protein Mcl-1 acts sequestering both BH3-only activators (Noxa, Bid, Bim, and Puma)[183] and the multidomain pore-forming proteins (Bax, Bak, and Bok)[184-186]. Mcl-1 is characterized by its wide intracellular distribution[67,187] and its short half-life[69,188]. Structurally, it differs from its antiapoptotic relatives due to the presence of an N-terminal sequence enriched in proline (P), glutamic acid (E), serine (S), and threonine (T) (PEST sequence)[189] that is responsible for proteasome-dependent Mcl-1 degradation.

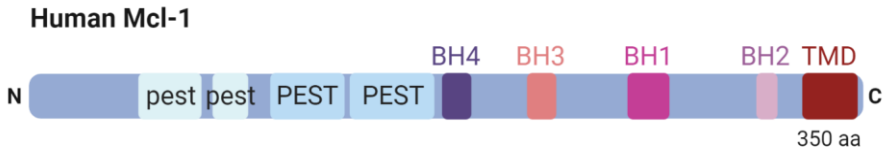

Figure 8. Schematic representation of the human Mcl-1 protein. Functional regions (BH1-4 domains and the TMD), and minor (lower case) and major (upper case) PEST sequences are depicted.

Overexpression of Mcl-1 has been observed in hematological malignancies, such as B- and T-lineage non-Hodgkin lymphomas[190] and several solid tumors, including hepatocellular carcinoma[191], esophageal squamous cell carcinoma[192], breast cancer[193], lung cancer[194], among others. Mcl-1 overexpression also associates with innate and acquired resistance to chemotherapy. Hence, Mcl-1 inhibitors have gained the attention of the pharmaceutical industry as anti-tumor agents[195]. Currently, neutralizing its

BC groove with BH3 mimetics is the main strategy to inhibit Mcl-1. Indeed, several clinical trials are undergoing evaluation of four Mcl-1–BH3 mimetics (NCT03218683, NCT02675452, NCT03797261, NCT03465540, NCT02979366, NCT02992483, and NCT03672695). However, there are still no conclusive data regarding whether their side effects will be manageable in humans.

Progression toward using Mcl-1 inhibitors depends on understanding its structure, interactome, and functions, but also its poorly explored TMD. Results from the computational analysis have had direct implications on the design of specific inhibitors of antiapoptotic proteins[196,197]; however, molecular dynamics (MD) simulations have focused on the binding mode between the Bcl-2 extramembrane domains and chemical modulators, neglecting Bcl TMD interactions. Methodological advancements in all-atom (AA) simulations have enabled to analyze the stability of TMD pre-formed dimers[198] and estimate the dimerization energetics of dimers with solved structures[199,200]. Recent coarse-grained (CG) models allow larger and longer simulations and are currently employed to predict dimer structures and dimerization energetics[201,202].

The combination of experimental analysis and atomistic simulations can provide a deep understanding of the molecular interaction and functional relevance of the Mcl-1 TMD, which may allow the identification of new points for Mcl-1 pharmacological intervention and the development of alternative therapeutic strategies to inhibit it. Thus, the aim of this work is to combine experimental studies and MD simulations to uncover the relevance of the Mcl-1 TMD in apoptosis modulation.

3.2.MATERIALS AND METHODS

3.2.1. Cell cultures.

The human colorectal carcinoma wild-type (WT) and $Bax^{-/-}Bak^{-/-}$ HCT116 cells were kindly provided by Prof. Richard Youle and by Prof. Bert Vogelstein, and grown in McCoy's 5A medium (Gibco, Thermo Scientific™) supplemented with 10% fetal bovine serum (FBS, Sigma-Aldrich). The human cervix adenocarcinoma HeLa cell line was obtained from the American Type Culture Collection (ATCC, Rockville, MD, USA) and HeLa mtDsRed cells were kindly provided by Prof. Juan V. Esplugues. Both HeLa cell lines were cultured in Dulbecco's Modified Eagle's Medium (DMEM, Sigma-Aldrich) supplemented with 10% FBS. All cell lines were maintained at 37 ºC in a humidified atmosphere with 5% CO_2.

3.2.2. Bcl transmembrane domains oligomerization assays.

Bimolecular fluorescence complementation (BiFC) assay was performed as previously described[58,203,204]. It represents a good imaging tool for direct visualization of PPIs in living cells. The basic principle of the BiFC system is the complementation of two non-fluorescent N- and C-terminal fragments from the enhanced yellow fluorescent protein Venus. These two fragments (VN 1-155 and VC 155-238) can be fused to a pair of proteins and reconstitute Venus fluorescence when the two proteins interact. Therefore, PPIs can be easily monitored by Venus fluorescence under a

microscope. In this work, we used a VN fragment with the point mutation I152L that specifically decreases the signal-to-noise ratio of the BiFC assay. In a previous thesis of our group[205] different Bcl TMDs were cloned at the C terminus of VN and VC fragments, according to their natural topology in full-length proteins.

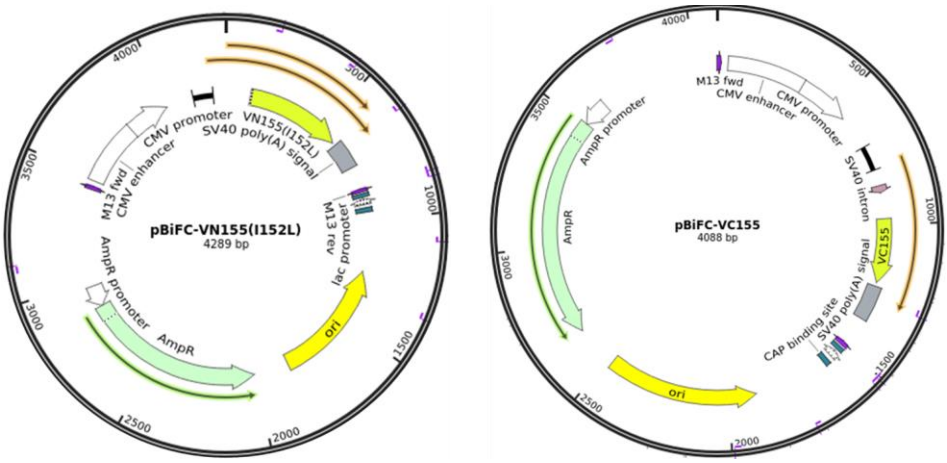

Figure 9. Plasmids encoding for N- and C-terminal Venus protein (https://www.addgene.org).

Analyses of the Mcl-1 TMD oligomerization capability were performed in HCT116 cells, seeded in 6-well plates (400,000 cells/well) and transfected with 0.5 µg VN and 0.5 µg VC Mcl-1 TMD plasmids, using 6 µl TurboFect (Thermo Scientific™) as transfection reagent. Twenty hours post-transfection, cells were harvested and centrifuged. The cellular pellet was resuspended in 150 µl phosphate buffered saline (PBS) and transferred

to a dark 96-well plate to measure Venus fluorescence emission in a Wallac 1420 Workstation at 535 nm (λexcitation 500 nm).

3.2.3. Immunoblotting.

For immunoblotting, unless otherwise indicated, whole-cell extracts were obtained by lysing cells in lysis buffer (25 mM Tris-HCl pH 7.4, 1 mM ethylenediaminetetraacetic acid (EDTA), 1 mM ethyleneglycoltetraacetic acid (EGTA) and 1% sodium dodecyl sulfate (SDS)) supplemented with protease and phosphatase inhibitor cocktails (Roche). The protein concentration was determined by the bicinchoninic acid (BCA) protein assay (Thermo Scientific™). Equal amounts of lysates were prepared with reducing Laemmli buffer, separated on 12% SDS-polyacrylamide gel electrophoresis (PAGE) gels, transferred to a nitrocellulose membrane (GE Healthcare Amersham™ Protran™ Premium NC Nitrocellulose Membranes) and blocked with 5% skimmed milk (Becton Dickinson) for 1 h. Then, membranes were incubated overnight with primary antibodies at 4 ºC (Table 2). Commercial secondary antibodies specific for mouse, rabbit, or rat IgG conjugated with peroxidase for enhanced chemiluminescence (ECL) detection (Amersham Pharmacia Biotech) were purchased from Sigma-Aldrich. Immunoblot signals were detected using GE Healthcare's ECL detection reagents and acquired in an ECL™ Detection System.

Table 2. Primary antibodies used for immunoblotting.

Primary antibody	Isotype	Purchased from	Dilution
Myc-Tag (9B11)	Monoclonal Mouse IgG2a	Cell signaling (#2276)	1:1000
HA-Tag (C29F4)	Monoclonal Rabbit IgG	Cell signaling (#3724S)	1:1000
Tubulin (YL1/2)	Monoclonal IgG2a	Abcam (ab6160)	1:10000
Tom20 (FL-145)	Polyclonal Rabbit IgG	Santa Cruz (11415)	1:1000
Mcl-1	Polyclonal Rabbit IgG	Cell signaling (#4572)	1:1000
Bcl-2 (50E3)	Monoclonal Rabbit	Cell signaling (#2870)	1:1000
Bcl-xL (54H6)	Rabbit IgG	Cell signaling (#2764)	1:1000
Bok (EPR15331)	Monoclonal Rabbit IgG	Abcam (ab186745)	1:1000

3.2.4. Subcellular fractionation.

To obtain heavy membranes and cytosolic fractions, a total of $1x10^7$ cells were seeded in 150-mm plates and transfected after 24 h with 6 µg VN and 6 µg VC Bcl TMD plasmids. Cells were harvested, washed in cold PBS and resuspended in cold SEM buffer (10 mM HEPES, 250 mM sucrose, pH 7.2) supplemented with protease inhibitor cocktail (Complete, Roche). Then, samples were mechanically lysed by passing them through a 23 G needle and centrifuged at 500 g, 4 min, 4 ºC to remove nuclei and cellular debris. The post-nuclear supernatant was centrifuged at 15,000 g, 30 min, 4 ºC, and cytosol (supernatant) and heavy membranes (pellet) fractions were

separated. The crude heavy membranes pellet was washed twice in cold SEM buffer and centrifuged at 13,000 g, 5 min, 4 ºC. The resulting pellets were solubilized in Laemmli buffer. The cytosolic fraction was ultracentrifuged at 100,000 g, 1 h, 4 ºC, and the supernatant was subjected to acetone precipitation for 1 h at -20 ºC. After centrifugation, cytosolic pellets were also solubilized in Laemmli buffer. Protein samples were separated on denaturing 12% SDS-PAGE gels and analyzed by western blotting. Proteins Tom20 and tubulin were used as mitochondrial and cytosolic markers, respectively.

3.2.5. Confocal live-cell imaging.

For BiFC visualization, HCT116 cells expressing VN and VC Bcl TMD plasmids were analyzed, while their subcellular distribution was observed in HeLa mtDsRed cells. In both cases, cells were transfected with VN and VC Bcl TMD plasmids as previously described, in a microscope cover glass (24 mm diameter), stained with Hoechst for nuclei detection and maintained in their corresponding medium at 37°C and 5% CO_2 for imaging. Venus (Bcl TMDs oligomerization) and mtDsRed (mitochondrial marker, MTS sequence of pre-ornithine transcarbamylase fused to the *Discosoma* sp. red fluorescent protein) fluorescence were taken using confocal microscopy. A Leica TCS SP8 confocal microscope equipped with solid-state diode-pumped lasers with excitation wavelengths of 405 nm (for blue emission), 488 nm (for green emission) and 552 nm (for red emission); and a Leica DMi8 motorized inverted microscope equipped with a precision motorized XY Stage were used for imaging. Images were acquired and

deconvolved through HyVolution Module, using Leica Plan-Apochromat 63x 1.4 NA objective and hybrid detectors. Co-localization was quantitatively assessed by drawing regions around individual cells and computing the Pearson's correlation coefficient by using the Leica Application Suite X software. Confocal experiments were performed at the Príncipe Felipe Research Center Confocal Microscopy Facility.

3.2.6. Determination of caspase 3/7 activity.

Caspase-3 and -7 are executioner caspases of the apoptotic pathway. Their activity was measure after Bcl TMDs transfection, to determine the apoptosis induction capability of these constructs, using a specific fluorescent substrate. To avoid Venus fluorescence emission and thus, signal interference with the caspase 3/7 substrate, we only transfected the VN Bcl TMDs. Cell extracts were prepared from $4x10^5$ cells seeded in 6-well plates and transfected the next day, as mentioned before. After 20 h VN Bcl TMDs expression, cells were scrapped, washed with PBS, and collected by centrifugation at 800 g, 5 min, at 4 ºC. The pellets were resuspended in lysis buffer (10.20 mM HEPES pH 7.4, 10 mM KCl, 1 mM EDTA, 1 mM EGTA, 1 mM DTT and 1.5 mM Mg_2Cl, supplemented with protease inhibitor mixture from Roche). After three times of frozen/thawed in liquid nitrogen, the cell lysates were centrifuged at 13,200 rpm for 7 min and supernatants were collected. Total protein concentration was quantified by the BCA method. For caspase 3/7 kinetic, a total of 50 µg protein was mixed with 200 µl caspase assay buffer (PBS, 10 % glycerol, and 2 mM DTT) containing 20 µM of the specific substrate Ac-DEVD-AFC

(Peptanova). Caspase activity was monitored by continuously measuring the release of the fluorescent AFC product using a Wallac 1420 Workstation (λexcitation 400 nm and λemission 508 nm). Caspase 3/7 activity was expressed as the increase of the arbitrary units (a.u.).

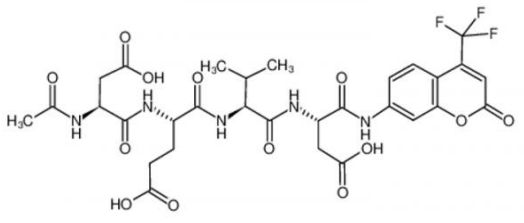

Figure 10. AC-DEVD-AFC Structure.

3.2.7. Mitochondrial depolarization assay.

Loss of ΔΨm is closely associated with Cyt-*c* release during apoptosis[206]. Therefore, mitochondrial depolarization is often associated with apoptosis induction. The ΔΨm can be analyzed by tetramethylrhodamine ethyl ester (TMRE, T669, Invitrogen) staining. TMRE is a cell-permeant, cationic dye that is readily sequestered by active mitochondria and can be detected by flow cytometry. Low TMRE staining is associated with loss of ΔΨm.

To measure the ΔΨm, cells transfected with 1 µg VN Mcl-1 TMDs in the above-described conditions were incubated with 50 nM TMRE at 37 ºC, 5 % CO_2, for 30 min. Then, samples were analyzed in a CytoFLEX flow cytometer (Beckman Coulter). Cells pretreated during 10 min with 20 µM carbonilcyanide p-triflouromethoxyphenylhydrazon (FCCP) were used as positive control for mitochondrial depolarization.

3.2.8. Lactate dehydrogenase release.

As a result of necrotic or late apoptotic cell death, the plasma membrane is permeabilized and the cytosolic glycolytic enzyme lactate dehydrogenase (LDH) is released to the medium[207]. To measure cell viability by LDH release, CytoTox-ONE™ Homogeneous Membrane Integrity Assay kit (Promega) was used according to the manufacturer's instructions. It is based on the enzymatic conversion of resazurin into resorufin fluorescent product, where the amount of resorufin is proportional to the number of dead cells. The release of LDH was calculated as follows:

$$LDH\ release\ (\%) = 100\ x\ \frac{Abs\ treated\ cells - Abs\ untreated\ cells}{Abs\ untreated\ lysed\ cells}$$

where the absorbance was measured at 490 nm and untreated cells were lysed with Triton 9%, which represented the maximum release of LDH

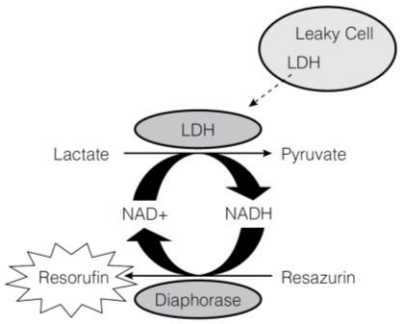

Figure 11. Release of LDH. The generation of the fluorescent resorufin product is proportional to the amount of LDH and therefore, to the amount of cell death (www.promega.com/protocols/).

3.2.9. Immunoprecipitation.

$1x10^7$ HCT116 cells were seeded in 150-mm plates and transfected on the following day with 12 µg VN Mcl-1 plasmid +/- 12 µg Bok full-length (FL) plasmid plus the transfection reagent TurboFect. Twenty hours post-transfection, immunoprecipitation was performed with a Pierce™ Classic IP Kit (Thermo Scientific™) following the manufacturer's instructions. Briefly, cells were harvested and lysed in 1.5 ml IP Lysis/Wash Buffer for 5 min on ice. Lysates were cleared by centrifugation and 500 µg of supernatants were precleared using 80 µl of the Control Agarose Resin slurry for 1 h at 4 ºC on a rotating wheel. Precleared lysates were added to columns containing 5 µg of immobilized anti-Myc-Tag 9B11 antibody, and the mixture was incubated overnight at 4 ºC on a rotating wheel. Samples were eluted by centrifugation and immunoprecipitates were analyzed by immunoblotting.

3.2.10. Bok silencing.

HCT116 cells were plated in 6-well plates at a concentration of 400,000 cells/well. Cells were transfected with the On-Target plus Human Bok small interfering RNA (siRNA) pool of 4 oligos (Dharmacon). Transfection solution (Opti-MEM Reduced Serum Media, Gibco, Thermo Scientific™) contained 2.5 µl Lipofectamine 2000 (Invitrogen) and 150 µM siRNA. Twenty-four hours post-siRNA–transfection, cells were transfected with 1 µg VN Mcl-1 TMD plasmid, and cell extracts were processed after 18 h, to measure caspase 3/7 activity, and analyze Bok and c-myc expression by western blotting.

3.2.11. Molecular dynamics simulations.

Molecular dynamics simulations were performed to predict homo- and hetero-dimers formation using Mcl-1, Bok, and Bax TMDs. First, α-helical TMD peptides were constructed in the atomistic resolution, exposed to a lipid bilayer of 128 1-palmitoyl-2-oleoyl-sn-glycero-3-phosphocholine (POPC) molecules until they equilibrated, and allowed their conformations to relax. Next, α-helical TMD peptide structures were transformed into coarse-grained resolution and 1,000 initial structures of the two peptides were generated[201]. Then, the TMD peptides were embedded in a lipid bilayer[208] and allow them to dimerize. To analyze the stability and structural details of the predicted homo- and hetero-dimers, the dimer structures were clustered allowing the identification of the two most populated clusters or binding modes. For each TMD homo- and hetero-dimer, their centroids were fine-grained, embedded in lipid bilayers of 150 POPC molecules using the CHARMM-GUI server[209] and simulated for 1 μs each. Finally, dimer stability and structural fetaures such as the crossing angles between the two TMDs and the amino acids of the binding interface were analyzed.

3.2.12. In situ proximity ligation assay.

To detect mitochondria-associated membranes (MAMs) we performed in situ proximity ligation assays (PLA), which allows the detection of endogenous protein-protein interactions[210]. Specifically, we used primary antibodies against VDAC1 (mitochondria) and IP3R (ER). To perform Duolink PLA (Sigma Aldrich), HeLa cells were plated on a microscope cover glass (200,000 cells/well) and transfected as indicated above, with

VN/VC Mock TMD or VN Mcl-1/VC Bok TMD constructs. Cells were washed with PBS, fixed with 4% paraformaldehyde (PFA) for 10 min, and permeabilized with 0.1% Triton X-100 for 10 min at room temperature. The blocking step was performed with Duolink blocking solution for 1 h at 37 °C, and cells were then incubated with VDAC1 (ab14734, Abcam) and IP3R (ab5804, Abcam) primary antibodies overnight at 4 °C. The plus and minus PLA probes were used for antibodies hybridization, followed by ligation and amplification reactions performed according to the manufacturer's protocol. Duolink in situ mounting medium with DAPI was added to the slides and pictures were acquired using a Leica TCS SP8 confocal microscope. Three experiments were performed and MAMs were quantified in a total of 20 transfected cells per condition. Data represent the number of MAMs per cell.

3.2.13. Mcl-1 somatic mutations.

Somatic mutations within the TMD of the antiapoptotic protein Mcl-1 were identified by searching the catalog of somatic mutations in cancer (COSMIC). All selected mutations had a high pathological score.

Mcl-1 somatic mutations were introduced in the BiFC system (VN and VC plasmids) to analyze the oligomeric state and subcellular localization of the mutants. The pcDNA3.1 vector containing Mcl-1 FL protein was also mutated to study the functional consequences of these somatic mutations.

The Mcl-1 TMD BiFC and Mcl-1 FL pcDNA3.1 point mutations were obtained using standard site-directed mutagenesis with the Stratagene Quickchange II kit (Agilent), according to the manufacturer’s instructions.

Primers were designed using the web-based QuikChange Primer Design Program available online at www.agilent.com/genomics/qcpd. All constructs were verified by sequencing in the Genomics and Translational Genetics Service, at the Príncipe Felipe Research Center.

Table 3. Primers for Mcl-1 TMD mutagenesis.

Protein	TMD Mutation	Forward (5' - 3')	Reverse (5' - 3')
Mcl-1	A339T	gcttttgcaggtgtta ctggagtaggagcta	tagctcctactccagt aacacctgcaaaagc
	L348V	gctattttggcatatg taataagatgagcgg	ccgctcatcttattac atatgccaaaatagc
	L348V (pcDNA3.1)	gctggtttggcatat gtaataagatagggc	tgccctatcttatta catatgccaaaccagc

3.2.14. Statistical analysis.

All the values represent the mean ± the standard error of the mean (SEM) of at least three independent experiments. Statistical significance was determined by one-way ANOVA, applying the Dunnet´s test, or two-way ANOVA, using Sidak's post-test. $P < 0.05$ was designated as statistically significant. Specific details of each experiment are indicated in the figure legends.

3.2.15. Software.

Bcl TMD-BiFC system was 'Created with Biorender.com' and using the PyMOL software. Confocal image analysis was performed using the Leica Application Suite X software. MAMs were quantified using FiJi software. The Graph Pad 8 software was used for statistical analysis.

3.3. RESULTS

3.3.1. The Mcl-1 TMD oligomerizes in intracellular membranes.

To analyze Mcl-1 TMD interactions, we first studied its self-association in living cells using the BiFC assay (Figure 12A), where the TMD is fused to the VN and VC fragments of the Venus fluorescent protein. We transfected both, VN and VC Mcl-1 TMD constructs into HCT116 cancer cells and Venus reconstitution was detected by fluorescence emission, at the same level that we previously described for Bcl-xL TMD[58] (Figure 12B). This indicates that the Mcl-1 TMD forms homo-oligomers in living cells. As a negative control for Venus complementation and therefore, for TMDs interaction, we employed the alpha 6 helix of Bid (Bid TMD)[211]. Detection of c-myc and HA tags by immunoblotting showed equivalent expression levels of VN and VC constructs, respectively (Figure 12B).

A

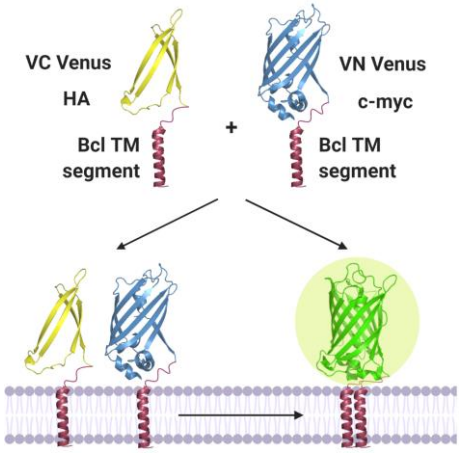

Mcl-1 TMD

$_{328}$IRNVLLAFAGVA**G**VGA**G**LAYLIR$_{350}$

B

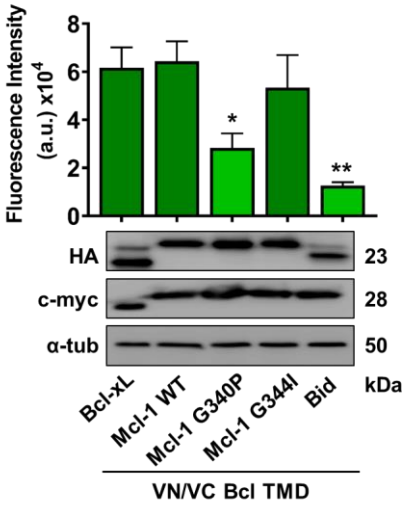

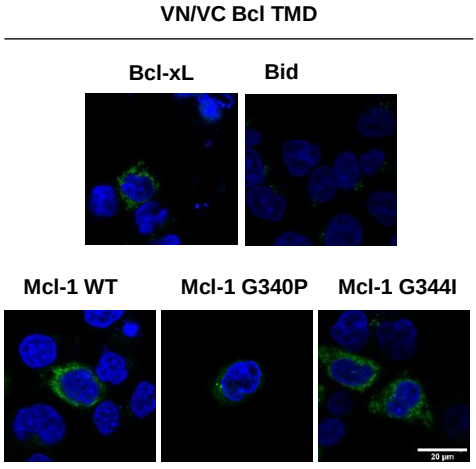

C

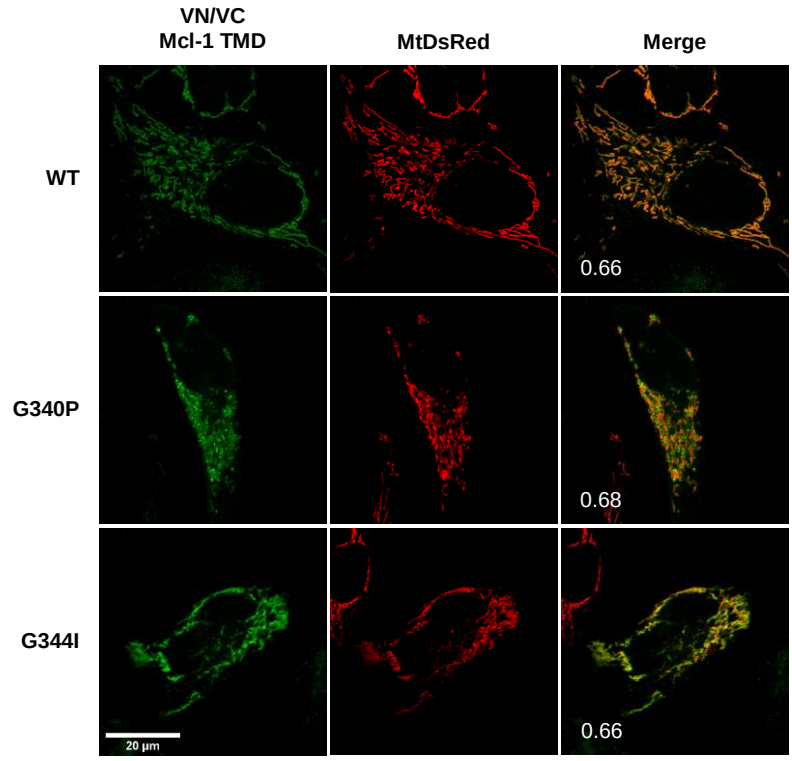
VN/VC
Mcl-1 TMD
MtDsRed
Merge
WT
G340P
G344I
0.66
0.68
0.66
20 µm

D

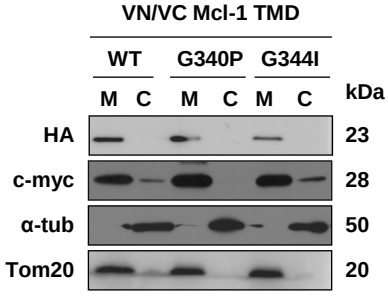
VN/VC Mcl-1 TMD
WT
G340P
G344I
M C M C M C
kDa
HA
c-myc
α-tub
Tom20
23
28
50
20

Figure 12. The Mcl-1 TMD homo-oligomerizes in the mitochondrial membrane. A) Schematic representation of the Bimolecular Fluorescent Complementation (BiFC) assay where Bcl TMD-driven oligomerization results in complementation of two non-fluorescent fragments (VN and VC) of the Venus fluorescent protein and its reconstitution. Rigth panel depicts the Mcl-1 TMD sequence, with central Glycine residues in bold. **B)** Self-interaction of wild-type and single amino acid mutants Mcl-1 TMDs measured by BiFC assay in HCT116 cells. Representative images of fluorescent signal in the confocal microscope are represented in the right panel (scale bar, 20 μm). The graph (left panel) shows the Venus fluorescent quantification. The Bcl-xL TMD homo-oligomerization and the Bid TMD served as positive and negative controls, respectively. Error bars represent the mean ± SEM, n = 6. Significant differences compared to the Mcl-1 WT TMD were analyzed using Dunnett's Multiple Comparison Test (*P < 0.05, **P < 0.01). Protein expression of VN (c-myc) and VC (HA) chimeric proteins appears in the bottom panel; α-tubulin was included as loading control. **C)** Representative confocal images of HeLa cells expressing a red mitochondrial matrix marker (MtDsRed) and transfected with three versions of the VN/VC Mcl-1 TMD: WT, G340P, and G344I. Homo-oligomers were detected in the green channel (scale bar, 20 μm). Merge images show co-localization with Pearson's correlation coefficient. **D)** Subcellular fractionation of HCT116 cells transfected with VN (c-myc) and VC (HA) Mcl-1 TMD constructs, where mitochondrial fraction (M) was controlled using Tom20 and cytosol fraction (C) with α-tubulin.

To corroborate packing specificity of Mcl-1 TMD oligomerization, we searched for relevant residues or 'hot spots' which mediate helix-helix interactions. Structural studies have revealed that Glycines in transmembrane regions, in contrast to soluble domains, predominantly face helix-helix interfaces and have a high occurrence at helix crossing points[212-214]. Specifically, there are several examples where GxxxG motifs are involved in TMD helices interaction[213]. The analysis of the Mcl-1 TMD amino acid sequence revealed central Glycine residues (Glycine 340 and

Glycine 344) as potential hot spots. To evaluate the relevance of these residues in the packing interface, we generated two point mutants using site-directed mutagenesis: the Mcl-1 G340P and the Mcl-1 G344I TMDs. Mutated proteins were expressed at similar levels as the wild type protein. However, the Mcl-1 G340P TMD mutant showed a decreased reconstitution of Venus fluorescent protein, which may be due to a disruption of Mcl-1 TMD oligomerization and demonstrates the specificity of this packing interaction. The Mcl-1 G344I TMD did not affect the oligomerization state, suggesting that this Glycine is not an interacting residue of the Mcl-1 TMD dimerization interface (Figure 12B).

Many of the proteins from the Bcl-2 family must be targeted to intracellular membranes to execute their functions[215]. Besides, MOMP regulation by Bcl-2 proteins requires protein interactions and oligomer formation in the membranes[216]. For that reason, we examined the intracellular distribution of Mcl-1 TMDs by microscopy studies. To address this, VN and VC Mcl-1 TMD segments were transfected in HeLa cells stably overexpressing a *Discosoma* sp. red fluorescent protein (DsRed) fused to the mitochondrial signaling sequence of pre-ornithine transcarbamylase (MtDsRed)[217]. Confocal microscopy studies showed that Mcl-1 WT, G340P, and G344I TMDs co-localize with mitochondria (Figure 12C). Their same pattern of distribution again confirms that a lower Venus fluorescence obtained with the G340P mutant is exclusively due to an impaired oligomeric capability.

The mitochondrial distribution of Mcl-1 TMDs was also corroborated by cellular fractionation studies, where VN and VC Mcl-1 TMD fragments

were detected in the same fraction as the Tom20 outer mitochondrial membrane protein (Figure 12D).

Altogether, these results demonstrate that the Mcl-1 TMD presents a sequence-specific packing interface and homo-oligomerizes in intracellular membranes of non-apoptotic cells.

3.3.2. The Mcl-1 TMD induces cell death by competition with the full-length Mcl-1 protein.

Accumulating data have recognized that the oligomerization between transmembrane segments can control the function of the whole protein[218,219]. Specifically, functional roles for Bcl TMDs have been previously described by our group and others[58,91,117,120], highlighting the notion that interactions of Bcl TMDs are relevant for apoptosis modulation. For this reason, we explored here the role of the Mcl-1 TMD oligomerization in apoptosis regulation. Cells undergoing cell death activate the executioner caspase-3[220], therefore we first tested its enzymatic activation in HCT116 cells transfected with VN Mcl-1 TMD fragments. Interestingly, those constructs that homo-oligomerized, such as Mcl-1 WT and G344I TMDs, induced caspase 3/7 activation; while the non-interacting mutant Mcl-1 G340P TMD showed a significant decrease in the cell death ability (Figure 13A). The caspase-3 activation is a common event in different types of cell death, like necrosis and apoptosis. To elucidate which mechanism of cell death the Mcl-1 TMD induces, we also measured the cytosolic lactate dehydrogenase (LDH) activity as a necrotic marker, due to during necrosis cells release LDH to the medium as a consequence of cell lysis. HCT116 cells overexpressing the

Mcl-1 WT TMD or the mutated versions did not release LDH to the extracellular media (Figure 13B), confirming that Mcl-1 TMDs did not induce necrosis.

The pore-forming proteins Bax, Bak, and Bok can generate pores in the MOM[221,222], destabilizing it, and causing the loss of Δψm. Due to Mcl-1 TMDs insert into the mitochondrial membrane, we evaluated whether they may disrupt the Δψm by tetramethylrhodamine ethyl ester (TMRE) staining. The TMRE is a cell-permeant, cationic, dye that is readily sequestered by active mitochondria. Therefore, low TMRE staining is associated with loss of Δψm. HCT116 cells were transfected with VN Mcl-1 TMD segments, stained with TMRE, and analyzed by flow cytometry. The uncoupler of mitochondrial oxidative phosphorylation FCCP was used as a positive control of mitochondrial membrane depolarization. As shown in figure 13C, the Mcl-1 WT TMD and its mutants induced a slight mitochondrial depolarization with a pattern similar to that of caspase 3/7 activity, where the non-oligomerizing Mcl-1 G340P TMD mutant provoked the lowest mitochondrial depolarization.

Our previous work described that Bax TMD-induced apoptosis is partially blocked by the overexpression of Bcl-xL FL protein, due to Bcl-xL and Bax TMDs interaction[58]. For that reason, we analyzed whether co-transfection of antiapoptotic full-length proteins (pcDNA3/Mcl-1, Bcl-xL or Bcl-2) and the Mcl-1 TMD interfered with its apoptosis activation capability. The proapoptotic effect of the VN Mcl-1 TMD was significantly reduced in the presence of Mcl-1 FL protein, but not when its relatives Bcl-xL or Bcl-2 FL were co-expressed (Figure 13D). These results suggest that

the Mcl-1 TMD can act as a molecular competitor of the endogenous Mcl-1 protein, displacing it from its antiapoptotic function in the cell, thereby inducing cell death.

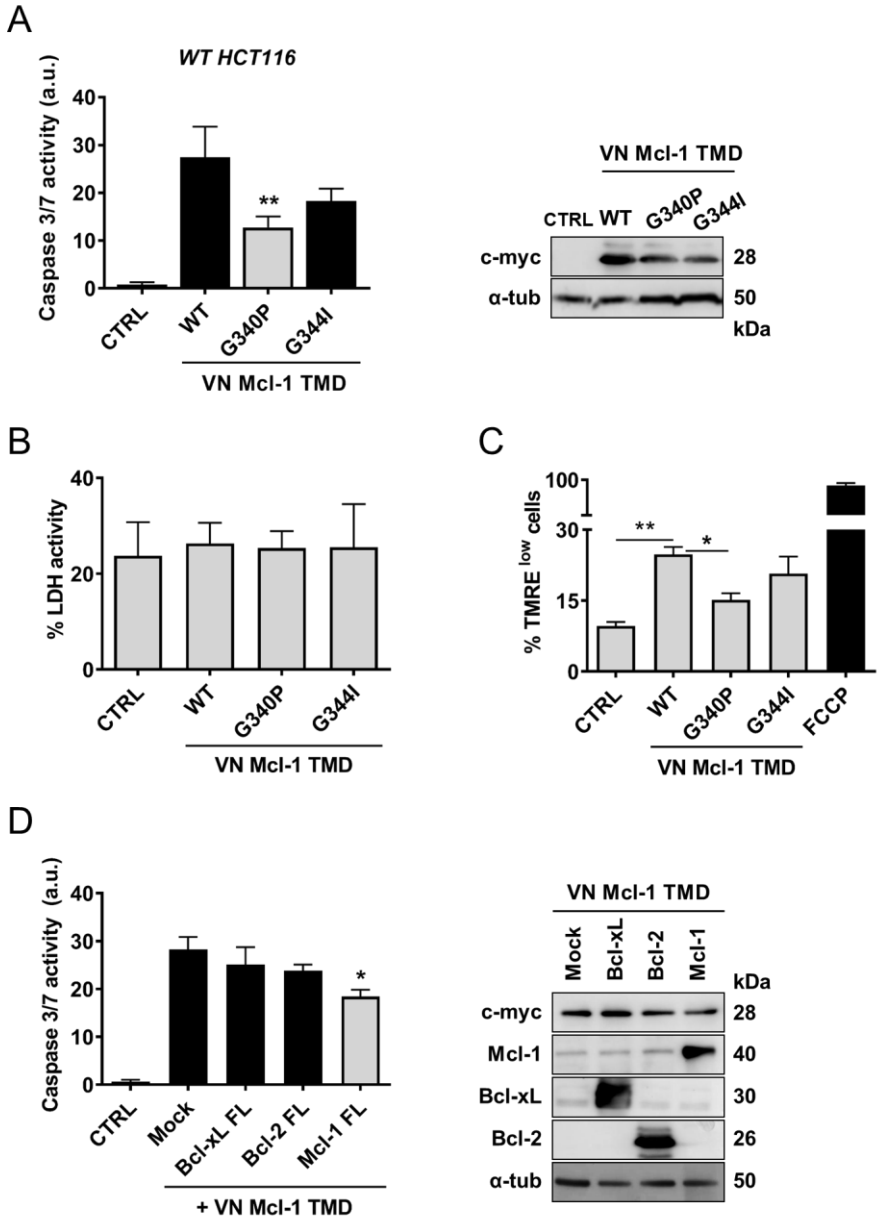

Figure 13. The Mcl-1 TMD induces cell death. A) Caspase 3/7 activity was analyzed in cytosolic extracts of HCT116 cells, 16 h after transfection of the VN Mcl-1 WT TMD, and its single amino acid mutants. Error bars represent the mean ± SEM, n = 3. Significant

differences were compared to the WT Mcl-1 TMD (*P*-value according to Dunnett's test is displayed. **P < 0.01. VN Mcl-1 TMDs expression (c-myc) was analyzed by western blotting, using α-tubulin as a loading control (right panel). Lactate dehydrogenase activity **(B)** and **(C)** mitochondrial polarization status were measured in the above-described conditions. **D)** HCT116 cells were transfected with Mcl-1, Bcl-xL or Bcl-2 full-length (FL) proteins. After 24 h, the VN Mcl-1 TMD was expressed for 16 h and caspase 3/7 activity measured in cytosolic extracts. Error bars represent the mean ± SEM, n = 5. Significant differences were compared to the VN Mcl-1 TMD/Mock sample.*P < 0.05. Chimeric protein expression of the VN Mcl-1 TMD (c-myc) and Mcl-1, Bcl-xL or Bcl-2 FL proteins is shown in the right panel using α-tubulin as a loading control.

3.3.3. The Mcl-1 TMD induces apoptosis in a Bax/Bak independent and Bok dependent manner.

Mcl-1 exerts its antiapoptotic function by sequestering multidomain proapoptotic effectors Bak and Bax, or BH3-only proteins such as Bid and Bim[183,223-225]. It has also been demonstrated that Mcl-1 interacts with the pore-forming protein Bok[76,186], although the regulation of Bok-induced apoptosis by Mcl-1 remains controversial[74,76,117].

To elucidate the relevance of the Mcl-1 TMD modulating the function of the multidomain proapoptotic proteins, we first examined the hetero-oligomerization capability of the Mcl-1 TMD with Bax, Bak, and Bok TMDs. BiFC experiments revealed that the Mcl-1 TMD strongly interacted with the Bok TMD and to a lesser extend with Bax and Bak TMDs (Figure 14A). These results are in agreement with a recent report, in which the lack of the Mcl-1 TMD does not impede the interaction with Bak[226] and

suggests that Mcl-1 FL utilizes a different molecular mechanism to modulate the activity of Bak and Bok.

As explained above, recent studies have revealed the functional implications of Bcl TMD interactions in the apoptotic scenario. For example, Bax TMD-mediated cell death is prevented by interaction with Bcl-xL and Bcl-2 TMDs[58]. Another example is the apoptosis induced by Bok, where transmembrane segments of both Bok and Mcl-1 are essential to inhibit cell death efficiently[117]. For that reason, we wondered whether hetero-oligomerization between TMDs of Mcl-1 and proapoptotic members could modulate their activity. As shown in figure 14B, Bax and Bok TMDs induced cell death measured by caspase 3/7 activation, while Bak TMD did not. Interestingly, the presence of the Mcl-1 TMD significantly reduced Bok TMD-induced apoptosis but it did not have any effect in the case of Bax TMD. These results confirm that the Mcl-1 TMD specifically interacts and modulates the apoptotic activity of the Bok TMD.

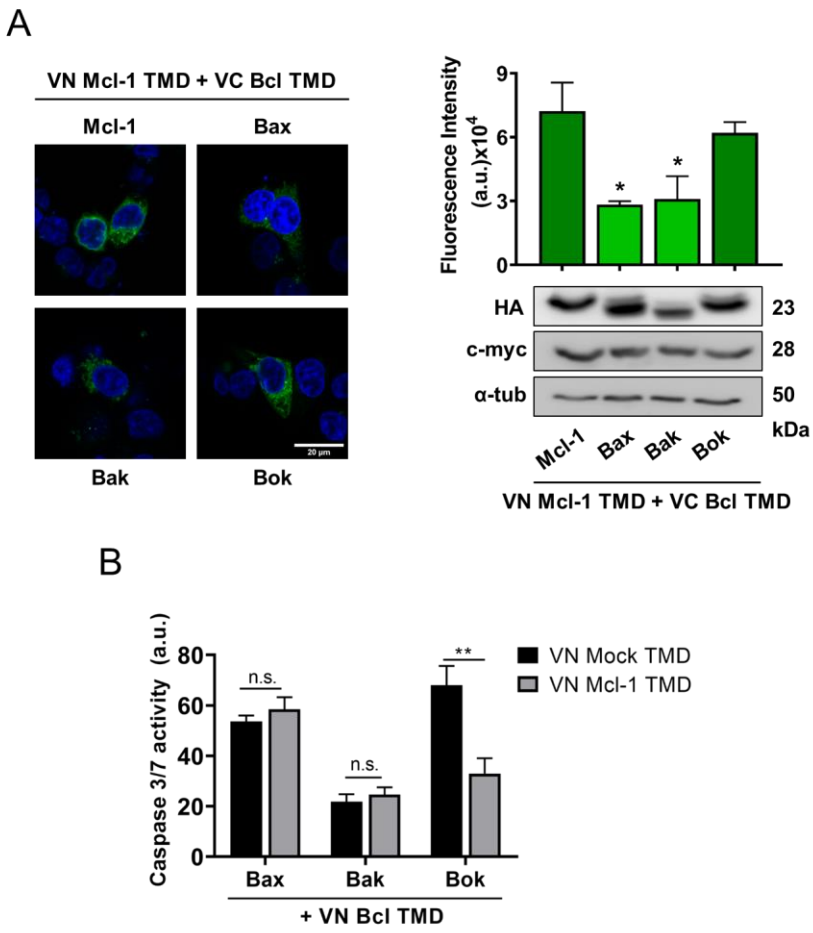

Figure 14. The Mcl-1 TMD interacts with the Bok TMD. A) Transmembrane domain interactions between the Mcl-1 TMD and TMDs from the proapoptotic proteins Bax, Bak, and Bok, analyzed by the BiFC system in HCT116 cells. Representative confocal images of the Bcl TMD oligomers (scale bar, 20 μm) (left panel). The graph represents the quantification of the Venus fluorescence. Error bars represent the mean ± SEM, n = 4. Significant differences were compared to the VN/VC Mcl-1 TMD. *P*-value according to Dunnett's test is displayed. *P < 0.05. The bottom section of the graph shows VN and VC Bcl TMDs protein expression. **B)** The Mcl-1 TMD partially inhibits the proapoptotic effect

of the Bok TMD, measured by caspase 3/7 activity, in HCT116 cells co-transfected with VN Bcl TMD constructs. Error bars represent the mean ± SEM, n = 3. **P < 0.01.

Based on these findings, we proposed that Mcl-1 TMD cell death activation was independent of Bax and Bak FL proteins. To investigate this, $Bax^{-/-}Bak^{-/-}$ HCT116 cells were transfected with the VN Mcl-1 WT TMD and the mutated versions G340P and G344I. Confirming our hypothesis, the cell death-mediating capacity of Mcl-1 TMDs was independent of Bax and Bak since caspase 3/7 activity showed comparable levels of induction than in WT HCT116 cells (Figure 15A).

We next analyzed whether Bok FL played a role in this process by silencing its expression in WT and $Bax^{-/-}Bak^{-/-}$ HCT116 cells. The downregulation of Bok significantly reduced the cell death effect of the Mcl-1 TMD in both cell lines, demonstrating the relevance of Bok in this process (Figure 15B and C).

These results strongly suggested the existence of PPIs between the Mcl-1 TMD and Bok. To address this question, we performed co-immunoprecipitation experiments of exogenously expressed Myc-tagged VN Mcl-1 TMD and Bok FL proteins. The VN Mcl-1 TMD was immunoprecipitated with anti-Myc antibody, validating its interaction with Bok FL protein (Figure 15D) and reinforcing the notion that the Mcl-1 TMD and Bok (TMD and FL) interact by a specific interface.

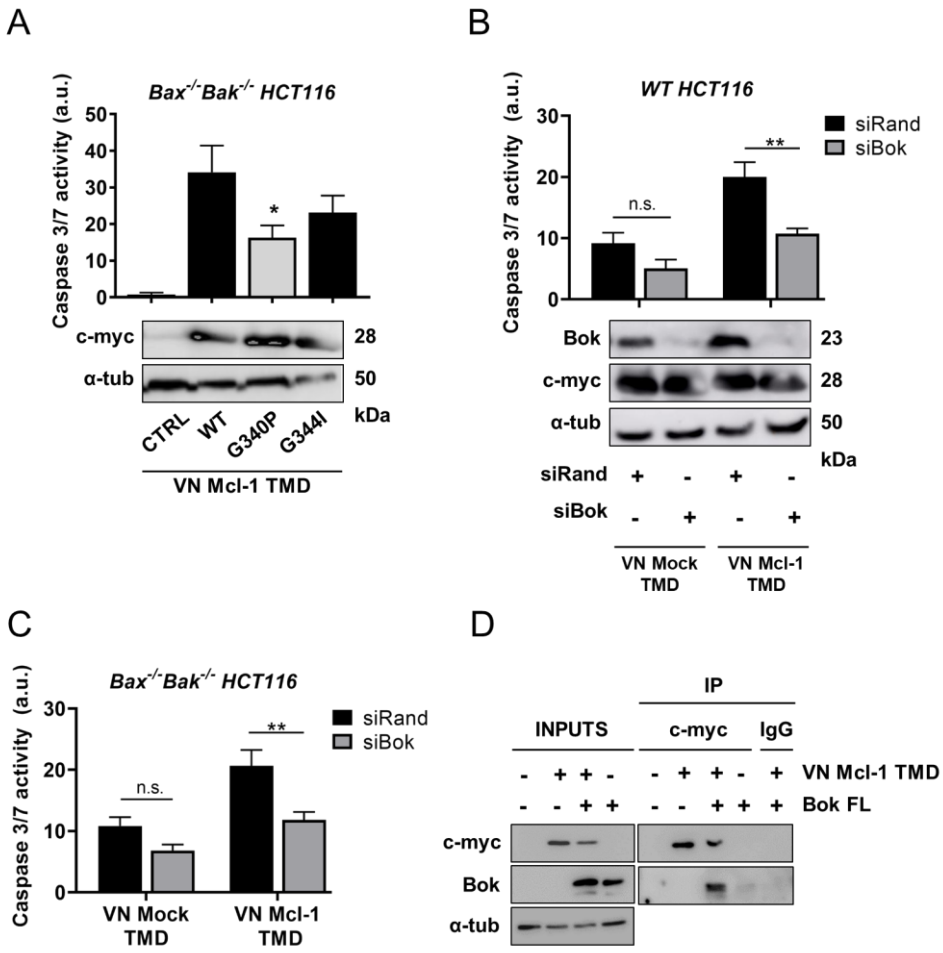

Figure 15. The Mcl-1 TMD apoptosis induction is Bok dependent. A) Caspase 3/7 activity was monitored in Bax$^{-/-}$Bak$^{-/-}$ HCT116 cells 16 h post-transfection of the VN Mcl-1 WT TMD and single amino acid variants. Error bars represent the mean ± SEM, n = 4. Significant differences were compared to the WT Mcl-1 TMD. *P*-value according to Dunnett's test is displayed. *P < 0.05. c-myc expression was analyzed for all constructs (bottom panel). α-tubulin was used as a loading control. Bok silencing was performed in WT **(B)** and Bax$^{-/-}$Bak$^{-/-}$ **(C)** HCT116 cells. After 24 h, they were transfected with the VN Mcl-1 and the VN Mock TMDs. Caspase 3/7 activation (graphs) and protein expression

(c-myc, Bok, and α-tubulin) were evaluated (siRNA Bok, siBok; siRNA Random, siRand). Error bars represent the mean ± SEM, n = 4. **P < 0.01. **D)** Immunoprecipitation of the VN Mcl-1 TMD (c-myc) from lysates of WT HCT116 cells co-transfected or not with the Bok FL construct.

3.3.4. Molecular simulation studies of Mcl-1 TMD membrane interactions.

To obtain a deeper understanding of the Mcl-1 TMD molecular interaction pattern, we performed multiscale MD simulations of both homo- and hetero-dimers, in collaboration with Dr. Matti Javanainen and Dr. Waldemar Kulig's groups. Since the Mcl-1 TMD have shown different hetero-oligomerizing behaviors with the Bax and Bok TMDs (Figure 14A), we analyzed homo- and hetero-dimer structures of Mcl-1, Bok, and Bax TMDs. Additionally, we reasoned that Bax TMD homo-dimer could serve as a positive control for dimer formation since its self-association has been experimentally demonstrated by us and others[58,124,125].

We identified two binding modes or clusters for each homo-dimer: Cluster1 and Cluster2 (Figure 16). The binding mode Cluster2 displayed more inter-peptide contacts and therefore, more stable dimers. Molecular dynamics simulations showed that during the simulation time (1 μs each) all tested TMDs (Mcl-1, Bok, and Bax TMDs) formed stable dimers (Figure 16). Representation of Cluster2 binding mode depicts the interacting residues of such dimers (Figure 17).

In the case of the hetero-dimers, the stable Mcl-1/Bok TMDs dimer formation was predicted for most of the simulations, with one exception

where the dimer dissociated (Figures 16 and 17). However, the majority of the Mcl-1/Bax TMDs hetero-dimers dissociated within 600 ns of the simulation (Figure 16). From most stable to least stable, Mcl-1 TMD dimers can be ordered as follows: Mcl-1 TMD homo-dimer > Mcl-1/Bok TMDs hetero-dimer >> Mcl-1/Bax TMDs hetero-dimer, in agreement with the oligomerization results obtained in the BiFC experimental assay (Figure 14A).

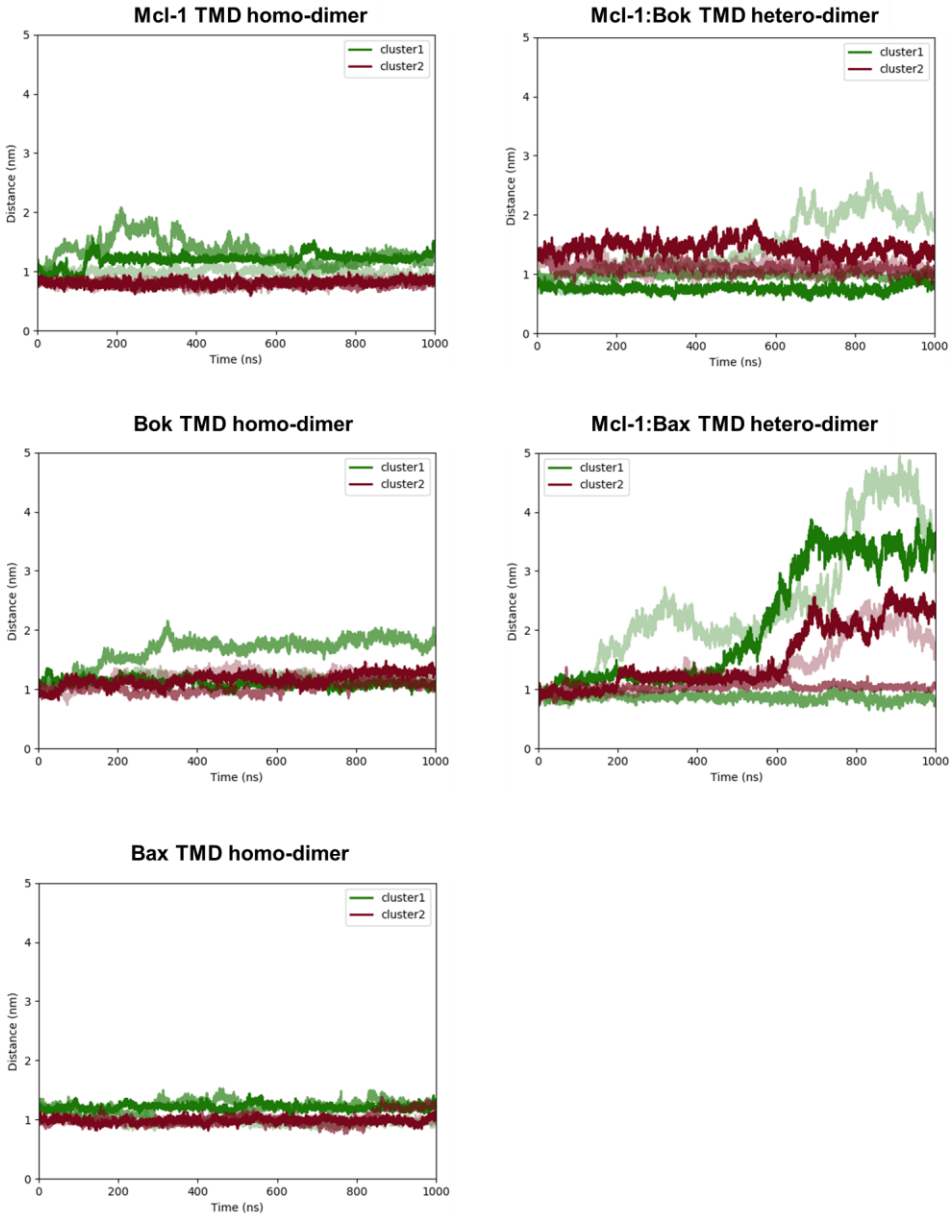

Figure 16. Time evolution of Mcl-1 TMD homo- and hetero-dimers simulations. Graphs represent the distance between the centers of mass of each monomer, including three repetitions per cluster (different shades of red and green).

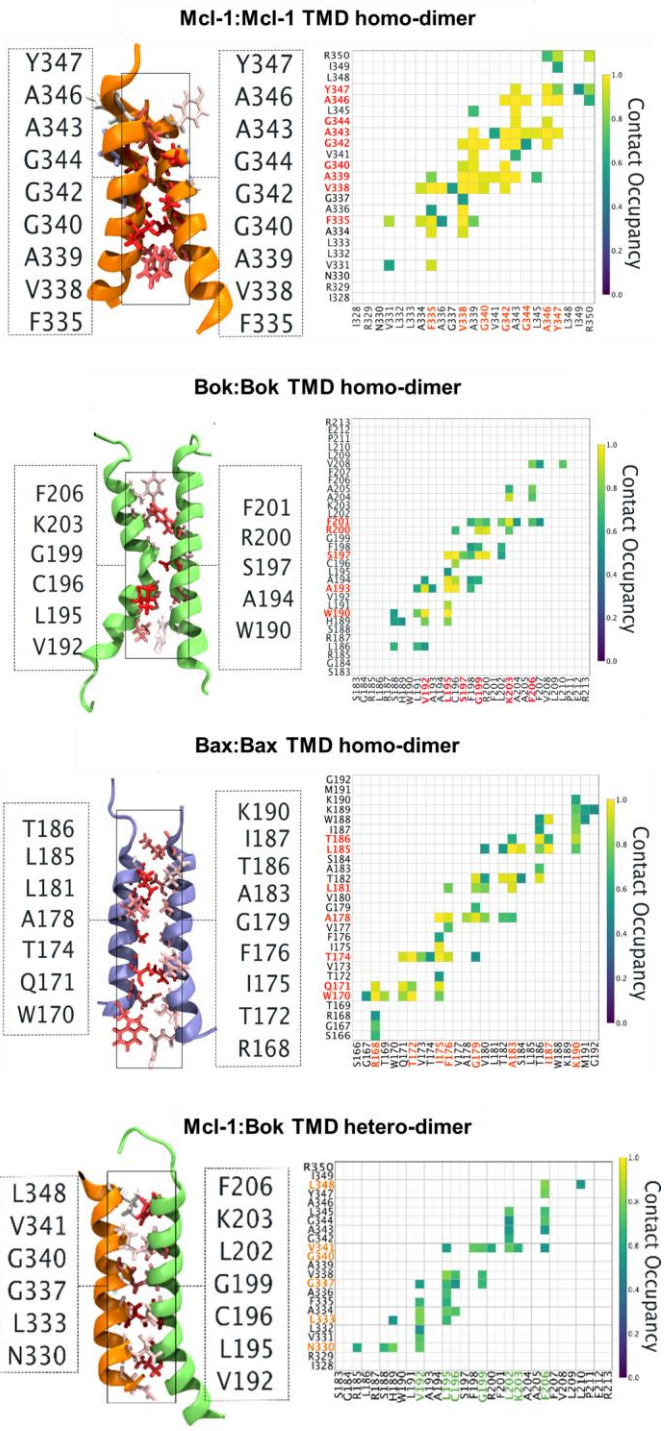
Mcl-1:Mcl-1 TMD homo-dimer
Y347
A346
A343
G344
G342
G340
A339
V338
F335
Y347
A346
A343
G344
G342
G340
A339
V338
F335
Contact Occupancy
Bok:Bok TMD homo-dimer
F206
K203
G199
C196
L195
V192
F201
R200
S197
A194
W190
Contact Occupancy
Bax:Bax TMD homo-dimer
T186
L185
L181
A178
T174
Q171
W170
K190
I187
T186
A183
G179
F176
I175
T172
R168
Contact Occupancy
Mcl-1:Bok TMD hetero-dimer
L348
V341
G340
G337
L333
N330
F206
K203
L202
G199
C196
L195
V192
Contact Occupancy

Figure 17. Dimer atomistic molecular dynamics simulations. Dimer cartoons represent the average structure of Mcl-1, Bok, and Bax TMD homo-dimers and the hetero-dimer between Mcl-1 and Bok TMDs, based on the binding mode Cluster2. Binding interfaces illustrate the contribution of each residue to the interaction, with a contribution > 0.5. Contact residues of the binding surface are colored using the blue-white-red color scale, where red indicates larger values of contribution to the contact site. Contact occupancy panels show the corresponding average residue-residue contact occupancy. Values equal to 1.0 correspond to residues that are in constant binding. Two residues were considered in contact when any of their atoms were closer than 0.6 nm.

We also performed MD simulations of the Mcl-1 G340P and Mcl-1 G344I TMDs to further validate the prediction model described above. In the Cluster2 binding mode, the mutation G340P resulted in less stable homo-dimer interactions (Figure 18, left panel). On the contrary, the G344I mutation retained a stable dimerization interface as the Mcl-1 WT TMD homo-dimer (Figure 18, right panel).

Altogether, these results agree with data from cellular experiments, suggesting that MD simulation can accurately predict molecular interactions of Bcl TMDs dimers.

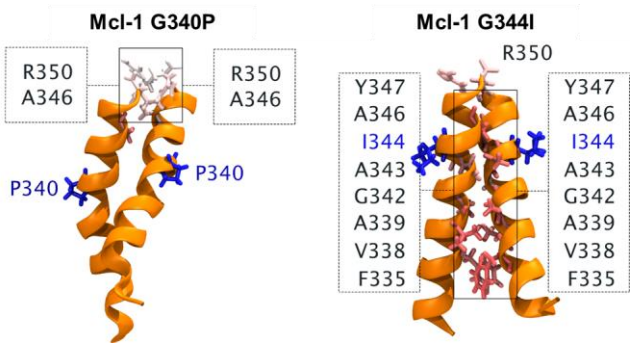

Figure 18. Molecular dynamics simulations of mutated Mcl-1 TMD homo-dimers. Graphs represent homo-dimer average structure from Cluster2. Contact residues of the binding surface are colored using the blue-white-red color scale, where red indicates larger values of contribution to the contact site.

3.3.5. The Mcl-1 TMD facilitates the Bok TMD mitochondrial localization.

Recently, the role of Bok as MOMP executioner has been definitively accepted[76,227]. However, Bok mainly localizes to the ER[74,76], thereby it seems probable that Bok requires translocating and/or accumulating into the mitochondrial membrane to exert its proapoptotic function. Based on the Mcl-1 and Bok TMDs interaction demonstrated above, and the functional relevance of this hetero-oligomerization in the modulation of apoptosis, we aimed to analyze whether this interaction might facilitate the presence of Bok in the mitochondria. To this end, we performed confocal microscopy studies finding that Mcl-1 TMD homo-oligomerized in both the mitochondria and the ER, while Bok TMD homo-oligomers formed and co-localized preferentially with the ER (Figure 19A). Interestingly, the co-expression of the VC Bok TMD and the VN Mcl-1 TMD showed that they interacted in both the ER and the mitochondria (Figure 19A and B). These results suggest a putative role for the Mcl-1 TMD in the transference of Bok from the ER to the mitochondria to trigger MOMP and apoptosis.

Thus, we reasoned that an increase in the number of contact sites between both organelles could be a possible mechanism to facilitate the Bok TMD translocation from the ER to the mitochondria. To test this notion, we

analyzed the number of ER-mitochondria contact sites or mitochondrial associated membranes (MAMs) by in situ proximity ligation assays (PLA)[210]. This technique allows the detection of two proteins that are in close proximity (distance < 40 nm). We identified and quantified interactions between VDAC1 and IP3R1 proteins, from the outer mitochondrial membrane and ER membranes, respectively, which form a multiprotein complex to transfer Ca^{2+} into the mitochondrial matrix[228,229]. This methodology confirmed our hypothesis since the expression of Mcl-1/Bok TMDs significantly increased the number of MAMs when compared to the VN/VC Mock TMD transfected cells (from 152 ± 65 to 232 ± 64) (Figure 19C). Therefore, this result suggests that Mcl-1 and Bok TMDs could promote the formation or stabilization of MAMs, which may explain the translocation of the Bok TMD from the ER to the mitochondria to trigger apoptosis.

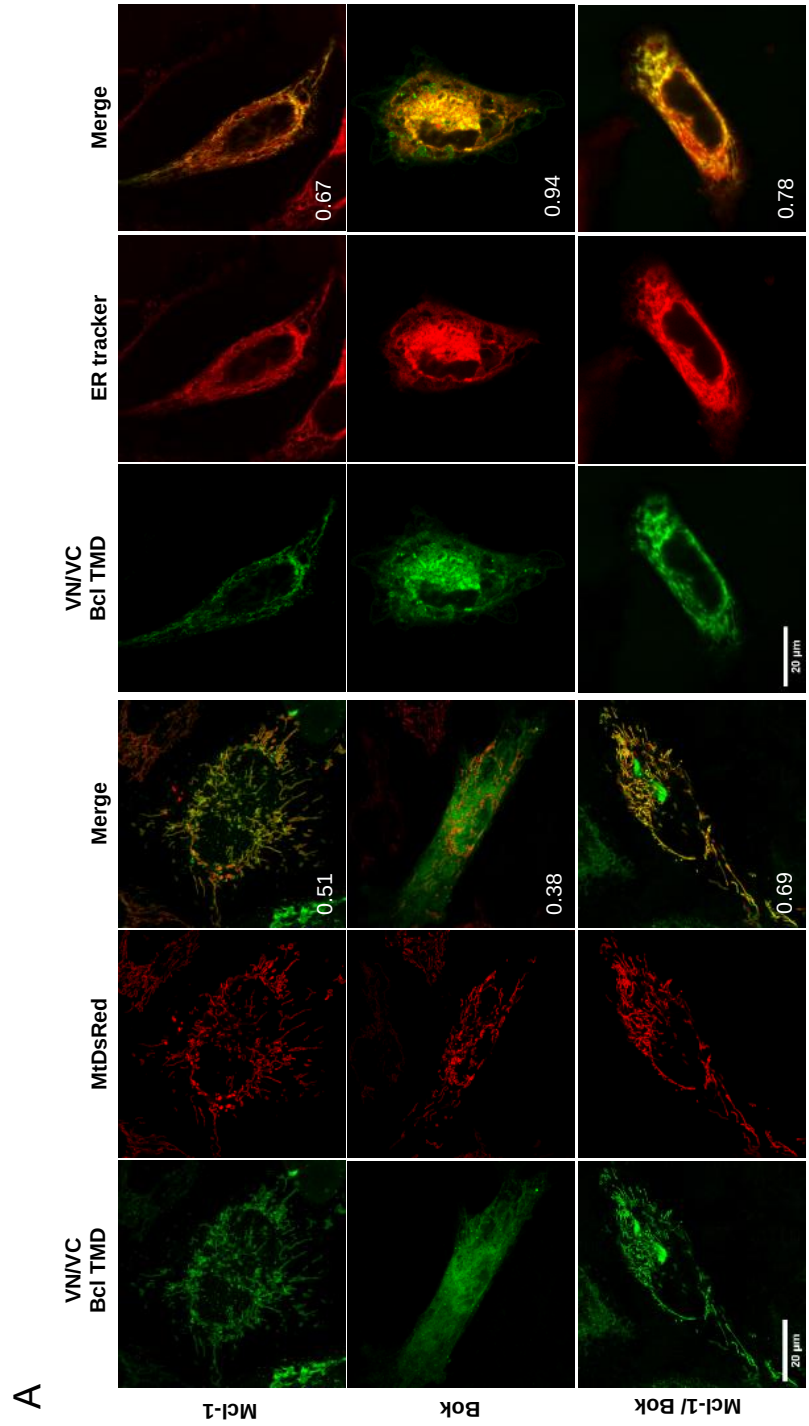
A
VN/VC Bcl TMD
MtDsRed
Merge
VN/VC Bcl TMD
ER tracker
Merge
Mcl-1
Bok
Mcl-1/ Bok
0.51
0.38
0.69
0.67
0.94
0.78
20 µm
20 µm

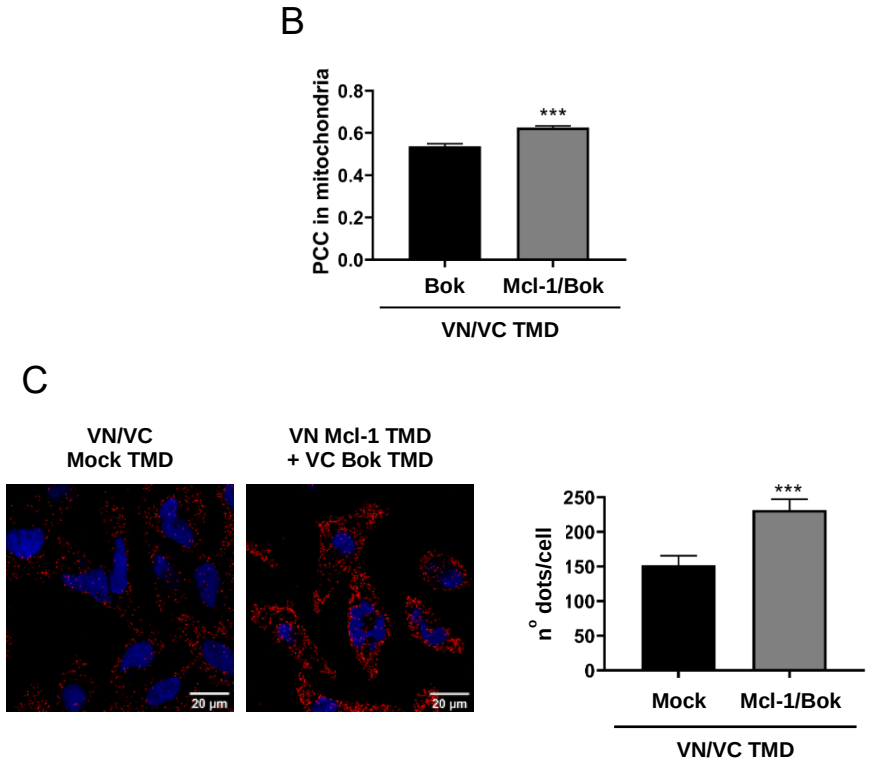

Figure 19. The Mcl-1 TMD facilitates Bok TMD mitochondrial localization. A) Representative confocal images of HeLa cells expressing a red mitochondrial matrix marker (MtDsRed) (left panel) or stained with ER tracker (right panel**)** and transfected with VN/VC Mcl-1 TMD, Bok TMD, and VN Mcl-1/VC Bok TMDs. Oligomer formation was detected in the green channel (scale bar, 20 µm). The mitochondrial and the ER markers were detected in the red channel. Merge images represent the co-localization of both channels and include Pearson's correlation coefficient (PCC). **B)** The graph shows PCC in the mitochondria from A images. Bars represent mean ± SEM (n = 86 cells per condition); *P*-value, according to Student t-test, displayed ***P < 0.001. **C)** Representative confocal images (left panel) of MAMs (red channel) in HeLa cells transfected with VN/VC Mock TMD constructs or VN Mcl-1 TMD / VC Bok TMD as indicated. The right panel shows

dots (MAMs) quantification (20 transfected cells per condition). Bars represent the mean ± SEM, n = 3; ***P < 0.001.

3.3.6. The relevance of Mcl-1 TMD somatic mutations.

To study real the contribution of the Mcl-1 TMD to pathological situations, we investigated the appearance of mutations in cancer patients. Analysis of COSMIC[230] data revealed the existence of somatic mutations within the Mcl-1 transmembrane region[231,232], with a high pathological score (Table 4). The pathogenic score refers to how cancerous or damaging a mutation is and it has been predicted by the Functional Analysis Through Hidden Markov Models - Math Kernel Library (FATHMM-MKL) algorithm[233]. These functional scores are indicated as a p-value, considering somatic mutations with a p-value > 0.7 as pathogenic variants.

Table 4. Somatic mutations of the Mcl-1 TMD from the COSMIC database.

Protein	Mutation	Pathogenic score	Tissue	Primary histology	PMID
Mcl-1	A339T	0.93	-	Malignant melanoma	24265153
	L348V	0.79	Lung	Adenocarcinoma	22980975

We introduced these mutations by using site-directed mutagenesis in the Mcl-1 TMD BiFC system and analyzed the self-interacting capacity of these constructs. Both patient mutants significantly disrupted the formation of Mcl-1 TMD homo-oligomers (Figure 20A), while they properly localized with and inserted into the mitochondrial membrane, as shown by confocal

imaging and subcellular fractionation experiments, respectively (Figure 20B and C).

Next, we evaluated the hetero-interaction capability of the Mcl-1 A339T and the Mcl-1 L348V TMDs with the Bok TMD, concluding that both mutants hetero-oligomerized with it (Figure 20D). To explore the relevance of these interactions in the context of apoptosis modulation, we introduced the A339T and the L348V mutations in the full-length protein (Mcl-1 A339T FL and Mcl-1 L348V FL) and analyzed their antiapoptotic activity (Figure 20E). Upon Bok-induced cell death, both cancer mutants displayed a greater protective activity than the wild type protein, which may provide a survival advantage to tumor cells.

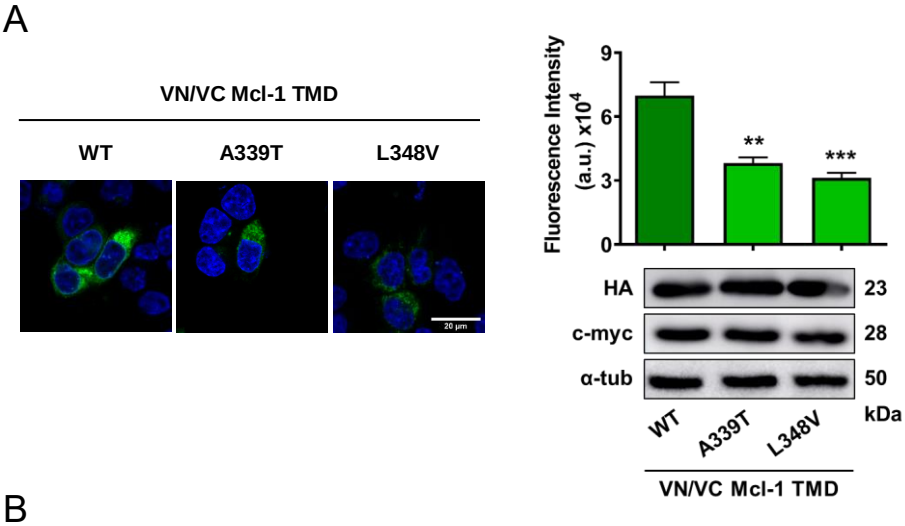
A
VN/VC Mcl-1 TMD
WT
A339T
L348V
20 µm
Fluorescence Intensity (a.u.) x10^4
9
6
3
0
**
***
HA
c-myc
α-tub
23
28
50
kDa
WT
A339T
L348V
VN/VC Mcl-1 TMD

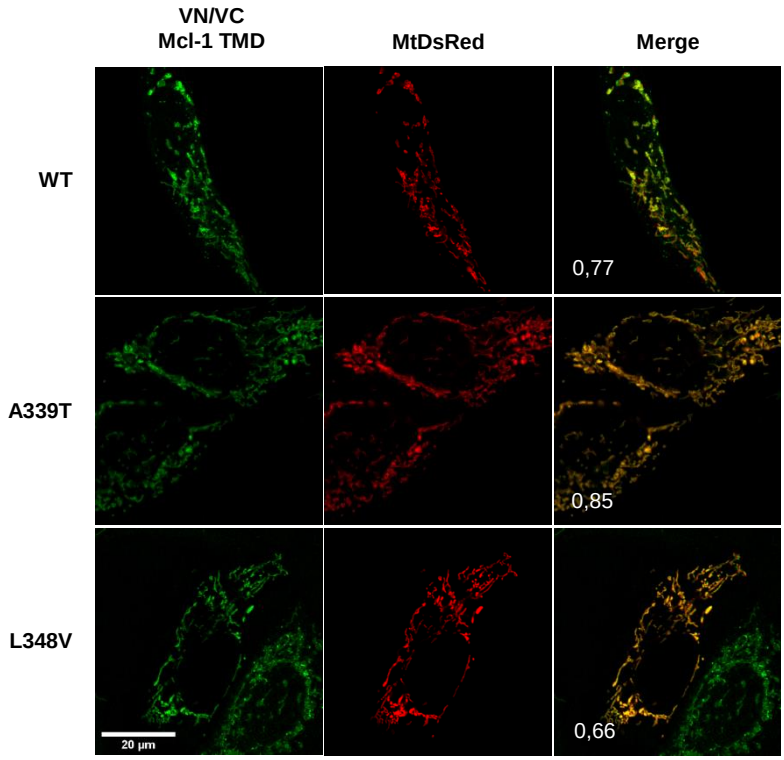
B
VN/VC Mcl-1 TMD
MtDsRed
Merge
WT
A339T
L348V
0,77
0,85
0,66
20 µm

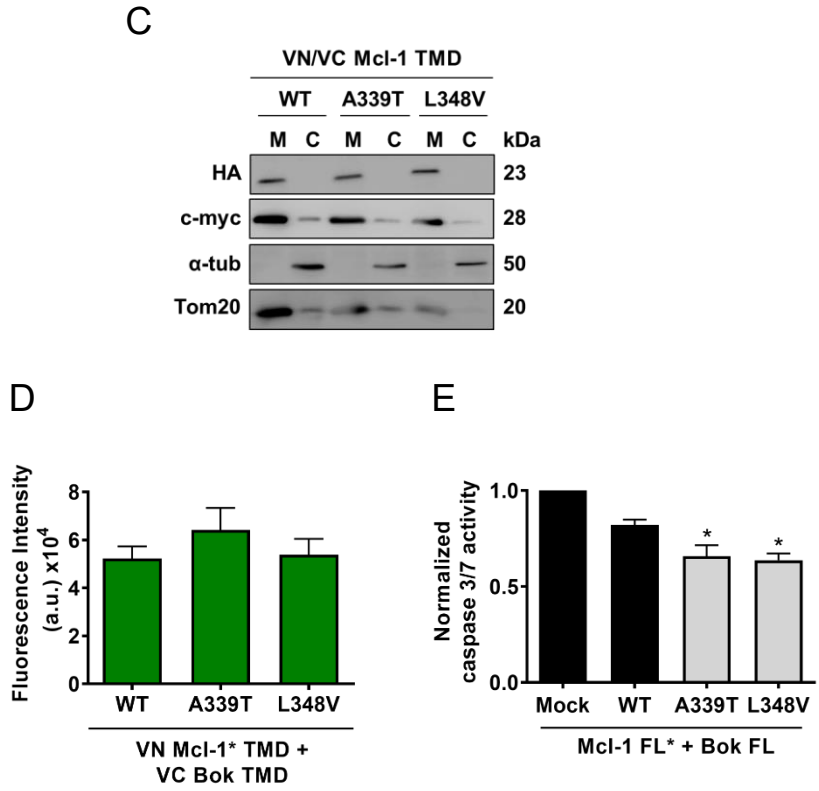

Figure 20. Cancer-related mutations of the Mcl-1 TMD affect the functionality of the protein. A) Self-association analysis of the Mcl-1 TMD somatic mutants measured by the BiFC assay in HCT116 cells. Representative confocal images (left panel, scale bar 20 µm) and Venus fluorescence quantification (right panel) of Mcl-1 TMD oligomers formation. Error bars represent the mean ± SEM, n = 4. Significant differences were compared to the WT Mcl-1 TMD. **P < 0.01; ***P < 0.001. VN and VC chimeric protein expression is included. **B)** Representative confocal images of HeLa cells expressing VN and VC Mcl-1 TMD somatic mutants. Mcl-1 homo-oligomers (green channel, first column, scale bar 20 µm) and mitochondria (mtDsRed marker, second column) co-localized (merge, third column showing the Pearson's correlation coefficient). **C)** Subcellular fractionation of HCT116 cells transfected with mutated VN (c-myc) and VC (HA) Mcl-1 TMD constructs

and controlled with Tom20 (mitochondrial fraction, M) and α-tubulin (cytosol, C). **D)** Hetero-oligomer formation of the Mcl-1 TMD mutants with the Bok TMD analyzed by the BiFC system in HCT116 cells. **E)** Caspase 3/7 activity induced by Bok FL and measured in cytosolic extracts of HCT116 cells previously transfected with the Mock plasmid or the Mcl-1 FL constructs (WT and somatic mutants). Error bars represent the mean ± SEM, n = 4. Significant differences were compared to the WT Mcl-1 FL / Bok FL sample. *P < 0.05.

3.4.DISCUSSION

Recent studies have revealed that Bcl TMDs fulfill crucial functions in cells; they regulate steady-state dynamics and shuttling rates of Bcl-2 family members[91,98,129], mitochondrial fission[234], Ca^{2+} signaling, and bioenergetics[235]. Indeed, in our previous work, we uncovered that Bcl TMDs homo- and hetero-oligomerizations contribute to control mitochondrial apoptosis[58]. In the present study, we corroborated such apoptosis modulation with the Mcl-1 TMD. We also confirmed the role of Bcl TMDs in the interplay between prosurvival and proapoptotic members, since the Mcl-1 TMD associates with the Bok TMD and regulates its cytotoxic effect (Figures 14A and B).

Bok is a bona fide MOMP effector and appears to be constitutively active, being independent of BH3-only proteins for activation[76,227]. The proapoptotic function of Bok seems to be controlled by protein degradation since proteasome inhibition leads to Bok accumulation and apoptosis induction. Moreover, Bok only co-precipitates with Mcl-1, although the Bok BH3 domain has a low affinity to bind Mcl-1[76]. In agreement with this, Stehle et al.[117] reported that a mutation in the Bok BH3 domain (Bok L70E)

does not affect its killing activity, while the combined deletion of the TMD (Bok L70E ΔTMD) significantly increases Bok-mediated apoptosis, which is not prevented by Mcl-1. The authors also showed that TMDs of both Bok and Mcl-1 are essential for their efficient interaction. We corroborated the association of both Bok and Mcl-1 TMDs (Figure 14A) and the inhibitory role of the Mcl-1 TMD under Bok TMD-induced cell death (Figure 14B).

Bcl TMDs actively regulate the concentration and distribution of Bcl-2 proteins in intracellular compartments. For example, the Bcl-xL TMD is essential for Bax retrotranslocation and Bcl-xL shuttling and thus, regulates the content of both proteins in the cytosol and mitochondria[98]. Here, we investigated the localization of Mcl-1 and Bok TMDs oligomers by the BiFC assay, finding that Bok TMD oligomers partially colocalized with mitochondria, while they strongly associated with the ER (Figure 19A). Since the BiFC methodology only allows Bok TMD dimers visualization, it does not exclude that Bok TMD locates at mitochondria in a monomeric conformation (Figure 19A). However, Echeverry and colleagues[74] did not detect a clear co-localization of EGFP-tagged Bok TMD with mitochondrial markers, while it efficiently localized on the ER, supporting our results.

Mcl-1 TMD and Bok TMD co-expression resulted in Venus fluorescence colocalization with both the ER and mitochondria (Figure 19A). Two possible scenarios could explain such Venus reconstitution. First, ER and mitochondria localization of both Mcl-1 TMD and Bok TMD could lead to their lateral interaction and thus, to BiFC signal. Second, ER-resident Bok TMD and mitochondria-located Mcl-1 TMD could face to each other, especially when associated with MAMs where both membranes are in close

proximity, hence allowing Venus reconstitution. However, the correlation between the BiFC signal (Figure 14A) and Bok TMD-mediated cell death inhibited by Mcl-1 TMD (Figure 14B) suggests a direct TMD-TMD interaction, which supports our hypothesis that Mcl-1TMD possibly mediates Bok TMD translocation from the ER to mitochondria and potentially modulates the cell death threshold.

Additionally, MAMs quantification indicates that co-expression of both Mcl-1 and Bok TMDs stabilize and/or increase the number of mitochondria and ER junctions (Figure 19C), which could serve as membrane platform for Bok translocation between both organelles.

It is also well-established that Mcl-1 is cleaved upon caspase activation and apoptosis commitment[114,236]. This cleavage produces the Mcl-1$^{128\text{-}350}$ fragment, which contains BH1, BH2, BH3 domains, and the TMD and can activate cell death[113]. It has been reported that the Mcl-1$^{128\text{-}350}$ product requires an intact BH3 domain to interact with Bax and promote apoptosis, while interaction with Bak but not its activation was detected[113]. In contrast to these data, we have described that the Mcl-1 TMD is sufficient to induce cell death and it does in a Bax/Bak-independent and Bok-dependent manner (Figure 15). Since the cleavage of Mcl-1 and the accumulation of the Mcl-1$^{128\text{-}350}$ fragment occurs physiologically during apoptosis, it would be of interest to study the role of Bok in the process. Moreover, the contribution to apoptosis amplification of both the Mcl-1 BH3 and the Mcl-1 TMD should be tested.

Although our work sheds light on the functional role of Mcl-1 TMD as a relevant domain for apoptosis modulation, additional efforts will be needed to fully characterize its interaction with Bok under both physiological and tumoral circumstances.

3.5. CONCLUSIONS

Our data demonstrate that the Mcl-1 TMD forms homo-oligomers by a sequence-specific packing interface. We also highlight the role of the Mcl-1 TMD in apoptosis modulation by altering the Mcl-1 interaction equilibria. It binds to the full-length protein, sequestering it and competing with its antiapoptotic activity, thereby promoting Bok-dependent cell death.

We demonstrate for the first time the interaction between TMDs of Mcl-1 and Bok and suggest a putative role of the Mcl-1 TMD facilitating the translocation of Bok from the ER to the mitochondria to trigger cell death.

In the present work, we also characterize patient-derived mutations within the Mcl-1 TMD. We conclude that side-by-side Bcl TMD interactions are relevant for apoptosis regulation since Mcl-1 TMD variants showed different levels of antiapoptotic activity under cell death induced by Bok overexpression, even when they had the same intact BH3 binding groove. And finally, that the enhanced antiapoptotic activity of Mcl-1 A339T FL and Mcl-1 L348V FL proteins may provide a survival advantage to tumor cells expressing these mutations in the Mcl-1 TMD, contributing to cancer maintenance and progression.

Chapter II

High Throughput Screening to Discover Inhibitors of Mcl-1/Bok Transmembrane Interactions

Graphical abstract

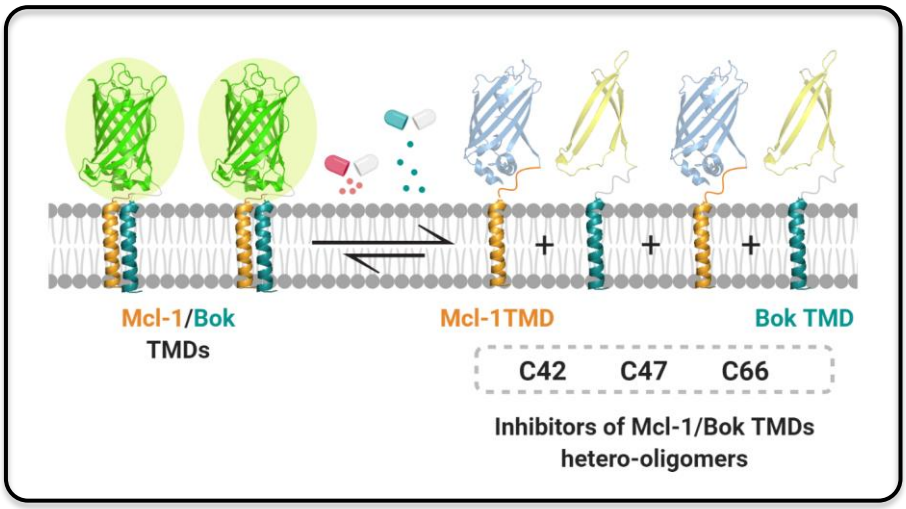

4.1. INTRODUCTION

Mcl-1 is highly expressed in a variety of human cancers and is associated with high tumor grade, poor survival, and resistance to chemotherapy[237]. Particularly, the role of Mcl-1 as a driver of adaptive cancer cell survival has been largely studied[140,238-240], in both tumor cell lines and patient samples. This large body of evidence highlights the potential of Mcl-1 inhibitors for tumor treatment.

To date, there are seven specific and direct inhibitors of Mcl-1 designed to disrupt the PPI between Mcl-1 and the BH3 motif of proapoptotic proteins (Figure 21). The development of Mcl-1 inhibitors is challenging due to its rigid hydrophobic BH3-binding groove and large molecular interfaces. The

nature of its BH3-binding site results in large, lipophilic, and acidic ligands, features often related to poor drug-like properties[195]. Four of the seven Mcl-1 inhibitors, AZD5991, AMG-176, AMG-397, and S64315/MIK665 are being evaluated in phase 1 clinical trials (NCT03218683, NCT02675452, NCT03797261, NCT03465540, NCT02979366, NCT02992483, and NCT03672695) for the treatment of acute myeloid leukemia, multiple myeloma, non-Hodgkin lymphoma, and CLL patients. These drugs are being tested as monotherapy and in some cases, in combination with the Bcl-2 inhibitor venetoclax. Despite the lack of data about their clinical toxicity in humans, two humanized Mcl-1 mouse models have been developed to predict their possible on-target side effects. Caenepeel, S. et al.[241] tested AMG-176 alone and in combination with venetoclax in human Mcl-1 knock-in mice, showing that both treatments resulted in reduced numbers of B cells, monocytes, and neutrophils in the blood, although without overt systemic toxicity. Similar results were obtained by Brennan, MS. and colleagues[242], who evaluated the tolerability of S63845 (predecessor molecule of S64315/MIK665) in a humanized Mcl-1 mouse model. The treatment with S63845 correlated with a transient reduction of B cells and red blood cells, and changes in the spleen (loss of normal architecture and increased size). However, overall their results indicated that S63845 treatment can be tolerated in these mice and promote Eμ-Myc lymphoma regression alone or in combination with cyclophosphamide.

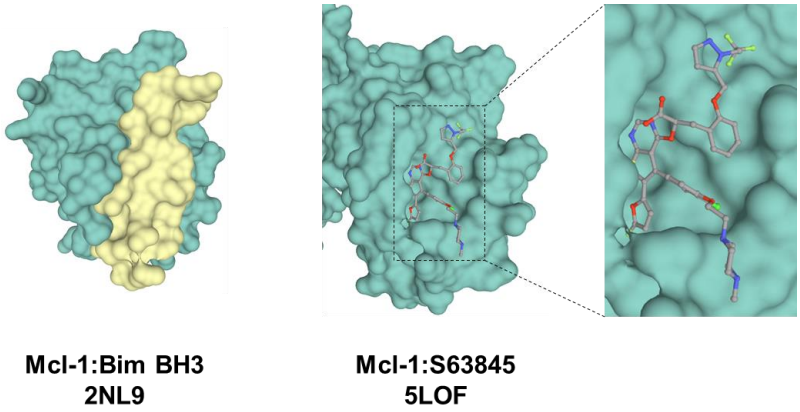

Figure 21. Crystal structures for Mcl-1 in complex with the Bim BH3 peptide and the BH3-mimetic S63845. In the left panel, Mcl-1 (green) binds the Bim BH3 peptide (yellow) into the BC groove (PDB 2NL9). The right panel depicts the BH3-mimetic S63845 into the BC groove of Mcl-1 (PDB 5LOF). Crystal structures were published in[243,244]. Images were created with Mol* (D. Sehnal, A.S. Rose, J. Kovca, S.K. Burley, S. Velankar (2018) Mol*: Towards a common library and tools for web molecular graphics MolVA/EuroVis Proceedings. doi:10.2312/molva.20181103); provided by RCSB PDB (https://www.rcsb.org/).

Mcl-1 overexpression also leads to acquired resistance to anticancer therapies in solid tumor malignancies, although they are predominantly refractory to Mcl-1–BH3 mimetics. To exploit Mcl-1 dependency in these tumors, some authors have proposed a potential effect of selective Mcl-1 inhibitors by enhancing the cancer-killing activity of other chemotherapy agents and targeted therapies[140,245,246]. Moreover, a deeper understanding of Mcl-1 biology can enable the evaluation of new molecules targeting alternative Mcl-1 binding surfaces, which may result in a more efficient pharmacological inhibition of Mcl-1 for the treatment of those tumors.

Mcl-1–BH3 mimetics disrupt the formation of Mcl-1:Bim and Mcl-1:Bak complexes, releasing both proapoptotic proteins and thus, promoting cell death. This mechanism provides the rationale for exploiting other interacting interfaces between Mcl-1 and proapoptotic Bcl-2 members as new drug targets for anticancer therapy. Our results, along with the work of others[117], have described that the interaction between Mcl-1 and Bok transmembrane regions modulates mitochondrial apoptosis. Specifically, Stehle and colleagues[117] suggest that Mcl-1 may inhibit Bok-induced apoptosis by the direct interaction of their TMDs. This strongly supports the idea of drugging Mcl-1 and Bok TMDs interaction as an alternative molecular interface for the modulation of Mcl-1 antiapoptotic activity.

From a pharmaceutical perspective, the development of Mcl-1:Bok TMDs hetero-oligomer inhibitors is crucial because small molecules that bind within TMDs can be used as both potential clinical drugs and basic research tools relevant in the membrane protein field. They can be useful in determining TMD binding partners, to solve protein structures or in the designing of drugs targeting similar binding sites.

To mention two examples, in a brilliant work, Levitz's group[247] employed the positive allosteric drug LY483739, which modulates the activity of metabotropic glutamate receptor 2 (mGluR2), to describe the role of inter-TMD interactions in mGluR2 modulation and activation. Specifically, using LY483739, they revealed the conformational rearrangements between TMD dimers that occur during receptor modulation. In another excellent study, two negative allosteric modulators, PF-06372222 and NNC0640, proved useful as molecular probes for solving the TMD

structures of the human glucagon-like peptide-1 receptor (hGLPR-1) that allowed mapping their binding sites to develop new therapeutic agents[248].

Therefore, this evidence motivated us to exploit the first-time-demonstrated transmembrane interaction of Mcl-1 and Bok as a novel target for anticancer therapy. We hypothesized that a compound able to disrupt the interaction of Mcl-1 and Bok TMDs would release Bok, decreasing the antiapoptotic capability of Mcl-1 and thus, enabling Bok-mediated cell death.

4.2. MATERIALS AND METHODS

4.2.1. Cell culture.

HCT116 cells were grown as described in CHAPTER I, 3.2. MATERIALS AND METHODS, 3.2.1. Cell culture.

4.2.2. Primary and secondary high-throughput screening.

A high-throughput screening (HTS) assay was developed to identify inhibitors of Mcl-1/Bok TMDs hetero-oligomerization, based on the BiFC TMD assay. The HTS was performed in a 96-well format, where HCT116 cells (25,000) were seeded and transfected after 24 h with 100 µl serum free McCoy's 5A medium, 0.6 µl TurboFect, and 0.1 µg VN Mcl-1 TMD plus 0.1 µg VC Bok TMD plasmids, per well. As a negative control, VN Bid / VC Bok TMDs co-transfection was used. Four hours after transfection, 5 µl of compounds from the MyriaScreen library (Sigma-Aldrich) or DMSO (to

the positive and negative controls) were added to the assay plate. Compound treatments were performed at 50 µM final concentration and 2% DMSO. In the primary HTS assay, two compounds were mixed per well. Fluorescence images were acquired after 20 h, using a Leica SP8 confocal microscope. Venus and Hoechst mean fluorescence intensities (MFIs) were quantified and the ratio Venus MFI/Hoechst MFI was calculated to get the normalized MFI per well.

For the deconvolution assay, the same transfection conditions were performed although only one compound was added per well, at 50 µM final concentration and 2% DMSO.

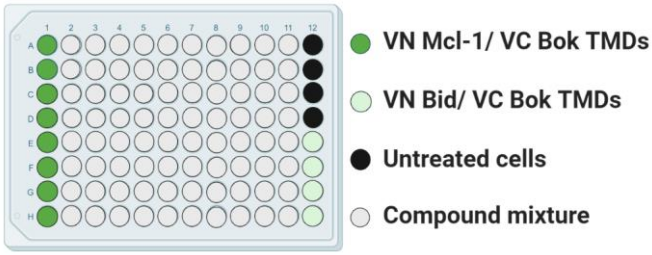

Figure 22. Representation of an HTS assay plate. It is indicated the position of the positive control (VN Mcl-1/VC Bok TMDs), the negative control (VN Bid/VC Bok TMDs), the untreated wells, and the compound-treated wells.

4.2.3. Bcl TMD specificity.

To confirm the specific inhibition of Mcl-1 and Bok TMDs interaction, lead compounds were tested under overexpression of other VN and VC Bcl TMDs (same conditions as mentioned above). HCT116 cells were transfected with VN and VC of Bcl-xL, Bcl-2, Mcl-1, and Bok TMDs. Four

hours after transfection, cells were treated with 2% DMSO (100% Bcl TMD oligomerization) or lead compounds at 50 µM, 2% DMSO, and confocal imaging was performed after 16 h treatment. For nuclei detection, cells were stained with Hoechst. Venus and Hoechst fluorescence were acquired with solid-state diode-pumped lasers at excitation wavelengths of 405 nm (for blue emission) and 488 nm (for green emission). Venus and Hoechst MFI quantification was assessed with the Leica Application Suite X software.

4.2.4. Statistical analysis.

All the values represent the mean ± S.E.M. of at least three independent experiments. Statistical significance was determined by one-way ANOVA, applying the Dunnet´s post-test, or the Student t-test. $P < 0.05$ was considered statistically significant.

4.2.5. Software.

Schematic figures were ‘Created with Biorender.com’ and the PyMOL software. Statistical analysis was performed using Graph Pad 8 software. Confocal image analysis was performed using the Leica Application Suite X software. Drug-likeness was analyzed with the online tool OSIRIS Property Explorer https://www.organic-chemistry.org/prog/peo/.

4.3. RESULTS

4.3.1. Development of high-throughput screening to identify inhibitors of Mcl-1 and Bok TMDs hetero-oligomerization.

To address this aim, we performed an HTS assay based on the BiFC system. We screened the MyriaScreen small molecule library (Figure 23A and B) that is composed of high-purity drug-like compounds obtained to maximize chemical diversity. First, we established the HTS assay and optimized several parameters to a 96-well plate format including the number of cells (25,000 cells/well), amount of plasmids co-transfected (0.1 µg VN Mcl-1 TMD and 0.1 µg VC Bok TMD) and incubation time (16 h).

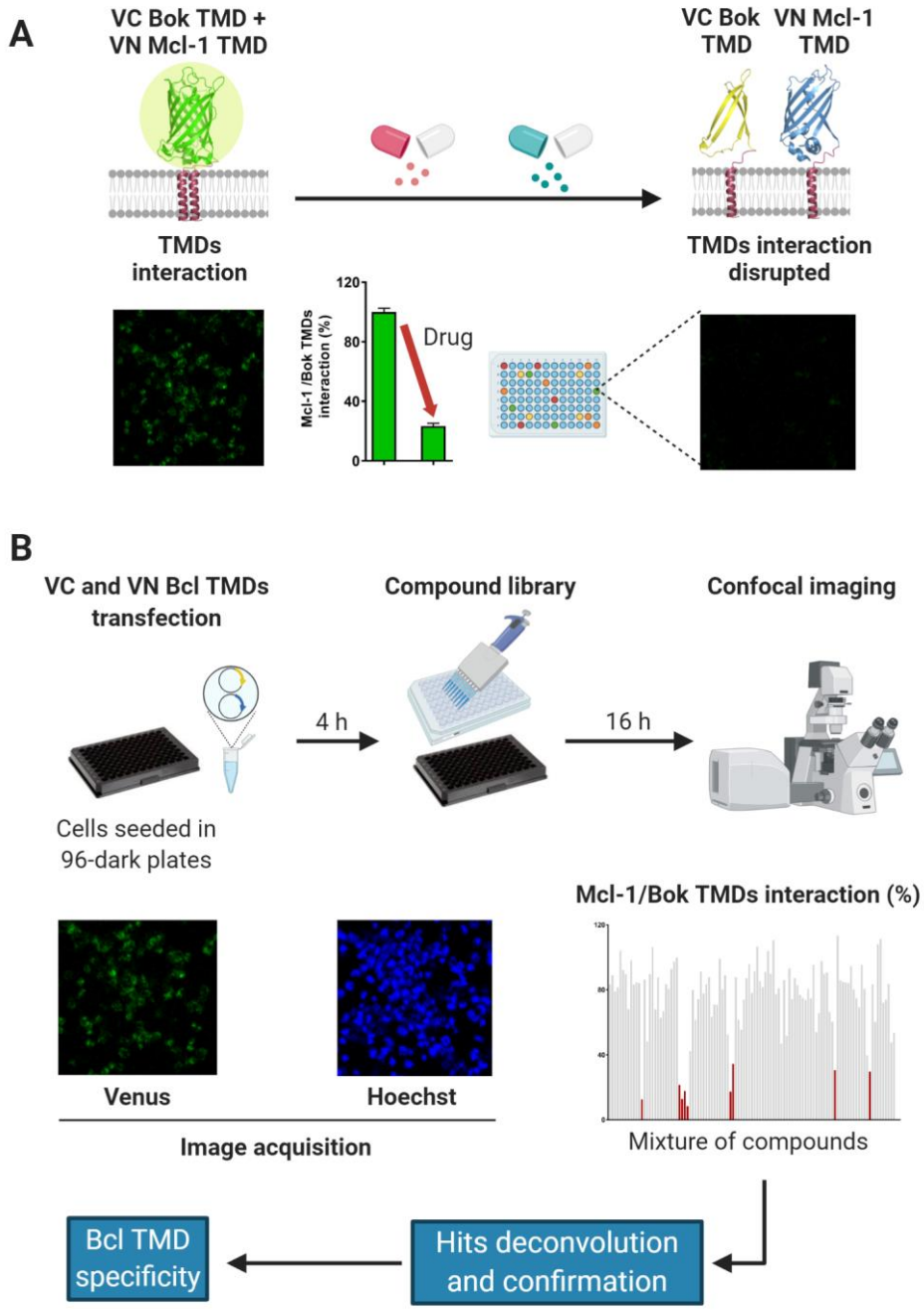
A
VC Bok TMD +
VN Mcl-1 TMD
VC Bok TMD
VN Mcl-1 TMD
TMDs interaction
TMDs interaction disrupted
Mcl-1 /Bok TMDs interaction (%)
120
80
40
0
Drug
B
VC and VN Bcl TMDs transfection
Compound library
Confocal imaging
4 h
16 h
Cells seeded in 96-dark plates
Mcl-1/Bok TMDs interaction (%)
Venus
Hoechst
Image acquisition
Mixture of compounds
Hits deconvolution and confirmation
Bcl TMD specificity

Figure 23. Identification of Mcl-1 and Bok TMDs inhibitors by HTS assay. A) Schematic representation of the BiFC assay used for screening the Mcl-1 and Bok TMDs disruptors**.** Active TMD-interaction inhibitors prevent Venus complementation, resulting in a lower fluorescence signal. **B)** Workflow of the BiFC-based HTS assay. HCT116 cells plated in 96 well-dark plates were transfected with VN Mcl-1 TMD/VC Bok TMD and the negative control of interaction VN Bid TMD/VC Bok TMD. Four hours post-transfection, chemical treatment was performed and 16 h later, Venus and Hoechst fluorescences were acquired by confocal imaging. Venus mean fluorescence intensity (MIF) was divided by Hoechst MFI to get the normalized MFI per well. The percentage of Mcl-1 and Bok TMDs interaction relative to the positive control was calculated based on the normalized Venus MFI of each well. The mixture of compounds that disrupted Mcl-1 and Bok TMDs interaction by at least 70 % were selected out and further tested for activity confirmation, deconvolution, and target specificity.

A necessary parameter to optimize any HTS assay is the Z' factor value, which represents the suitability and quality of the assay[249]. It is calculated as follows:

$$Z' = 1 - \frac{3SD\ positive\ + 3SD\ negative}{(|mean\ positive - mean\ negative|)}$$

where SD represents the standard deviation of positive and negative controls (here, interacting and non-interacting VN/VC Bcl TMDs, respectively). As indicated in the formula, the Z' factor considers the dynamic range and the variability of the assay's data. A Z' factor greater than 0.5 represents an excellent assay.

To evaluate the suitability of our assay, we tested two Bcl TMDs combinations as inhibition and non-interacting (negative) controls: the VN Mcl-1 G340P TMD with the VC Bok TMD, and the VN Bid TMD with the

VC Bok TMD (hereafter Mcl-1 G340P / Bok TMDs and Bid / Bok TMDs, respectively) (Figure 24A). The fluorescence signal of both combinations was significantly lower compared with the positive control Mcl-1 WT / Bok TMDs (Figure 24B), although Bid / Bok TMDs showed a greater inhibition of the TMD interaction allowing an appropriate screening window to identify inhibitory compounds (Z' factor = 0.7). For that reason, we selected it as standard negative control of the assay.

The MyriaScreen small molecule library presents compounds dissolved in dimethyl sulfoxide (DMSO), which made necessary to test the stability of the VN Mcl-1 / VC Bok TMDs hetero-dimer in presence of 2% DMSO (final concentration used in the current HTS), showing that DMSO did not interfere with Venus reconstitution upon Mcl-1 and Bok TMDs interaction (Figure 24C).

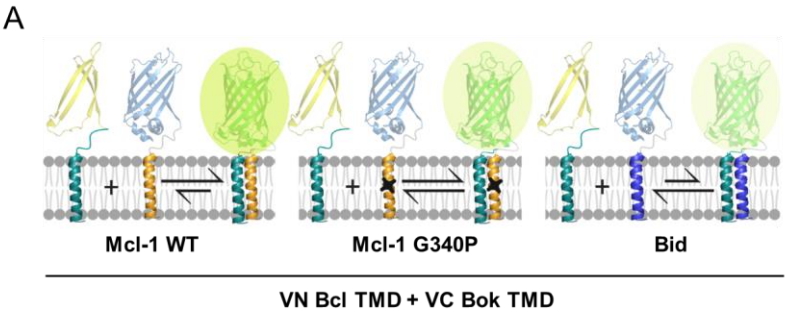
A
Mcl-1 WT
Mcl-1 G340P
Bid
VN Bcl TMD + VC Bok TMD

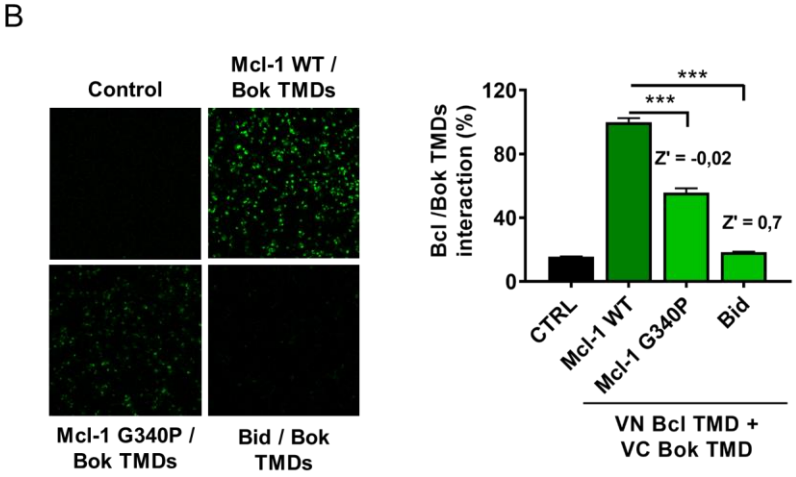
B
Control
Mcl-1 WT / Bok TMDs
Mcl-1 G340P / Bok TMDs
Bid / Bok TMDs
Bcl /Bok TMDs interaction (%)
120
80
40
0
***
***
Z' = -0,02
Z' = 0,7
CTRL
Mcl-1 WT
Mcl-1 G340P
Bid
VN Bcl TMD + VC Bok TMD

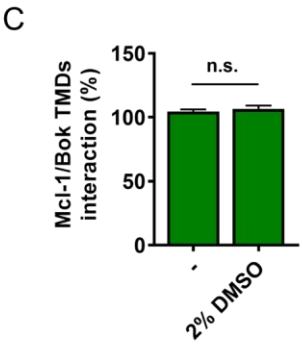
C
Mcl-1/Bok TMDs interaction (%)
150
100
50
0
n.s.
-
2% DMSO

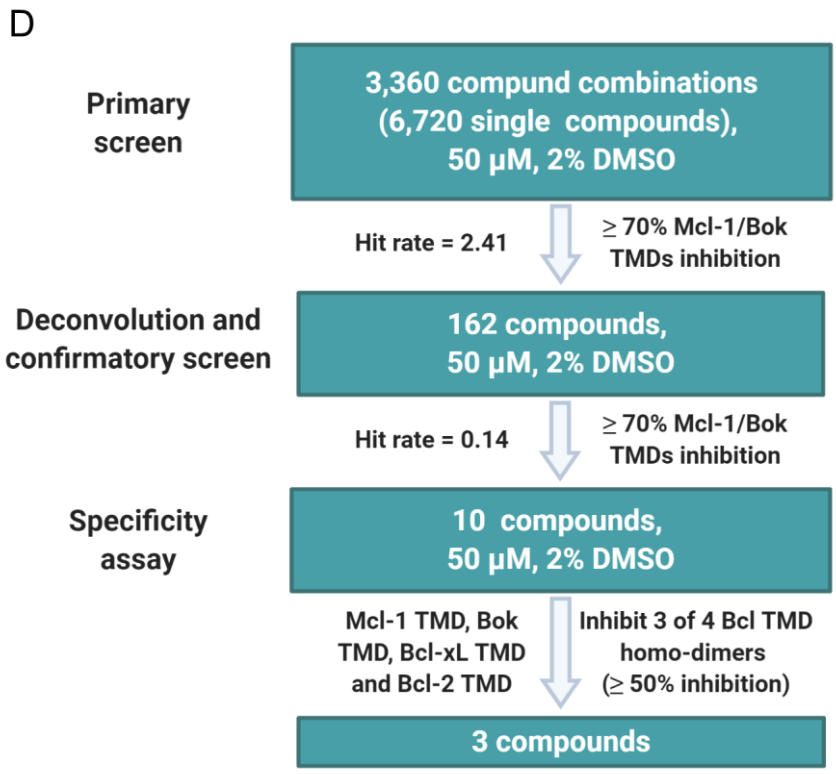

Figure 24. Establishment of the BiFC assay for screening inhibitors of Mcl-1 and Bok TMDs interaction. A) Schematic representation of the VN Bcl / VC Bok TMDs combinations evaluated as controls for the HTS assay. Helices represent the TMDs of Bok (purple), Mcl-1 (orange), Mcl-1 G340P mutant (orange with a black star), and Bid (blue). **B)** Interaction percentage of each VN/VC TMD co-transfection relative to the positive control VN Mcl-1 WT / VC Bok TMDs. Bars represent mean ± SEM, n = 3. *P*-value according to Dunnett's test is displayed. ***P < 0.001. **C)** Comparison of the Mcl-1/Bok TMDs interaction (%) with and w/o DMSO. Bars represent mean ± SEM, n = 3. **D)** Flow chart for Mcl-1/Bok TMDs BiFC-based HTS screening platform including the primary, deconvolution and confirmatory, and specificity assays. The criteria for compound selection and the number of compounds at each step are listed.

4.3.2. Preliminary identification of three inhibitors of Mcl-1 and Bok TMDs hetero-oligomerization.

In a primary HTS, we screened 6,720 small molecules of the MyriaScreen library, provided by the Screening facility at the Príncipe Felipe Research Center. HCT116 cells were transiently co-transfected with the VN Mcl-1 TMD and the VC Bok TMD, and mixtures of two chemical compounds per well were transferred into assay plates. The final concentration of each compound was 50 µM at 2% DMSO. Sixteen hours post-treatment, we performed fluorescence detection using a TCS SP8 confocal microscope (Leica). The Z' factor for most assay plates was greater than 0.5, indicating a robust assay performance. From the primary screening, we selected 81 mixture compound hits (hit rate = 2.41%) that inhibited Mcl-1 and Bok TMDs hetero-interaction by at least 70% (Figure 25).

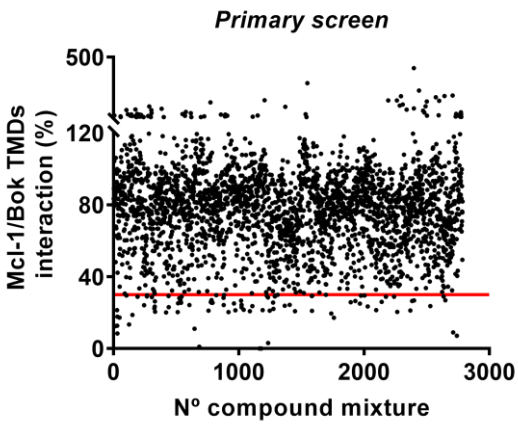

Figure 25. Overview of the primary screening data. Each spot represents a combination of two compounds at 50 µM each. Data are relative to DMSO-positive control (VN Mcl-1

TMD / VC Bok TMD). Compound combinations with at least 70% interaction inhibition were selected out as primary hits.

Because each hit was a combination of two compounds, we performed a secondary screening to achieve mixture deconvolution and hits validation. We screened 162 individual compounds in the same conditions, confirming 10 single compounds (hit rate = 0.14) that interfered with the molecular interaction of Mcl-1 and Bok TMDs (Figure 26).

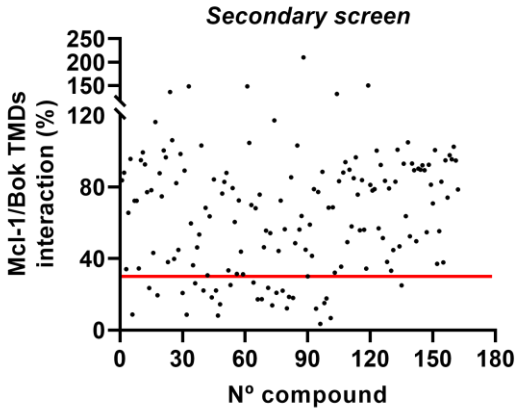

Figure 26. Hits validation and compound deconvolution in a secondary screening assay. Single compounds with 70% inhibitory activity of Mcl-1 and Bok TMDs interaction were selected out.

Small molecules that disrupt Mcl-1 and Bok TMDs hetero-dimer formation should target intracellular membranes, where this and additional Bcl transmembrane interactions take place. This scenario motivated us to analyze the target specificity of selected compounds since the aim of the HTS was to discover specific inhibitors of Mcl-1 and Bok TMDs packing interaction. For that reason, we tested the capacity of the selected

compounds to impede the formation of other Bcl TMD oligomers, using the same BiFC-based screen assay. HCT116 cells overexpressing the homo-oligomers Mcl-1, Bok, Bcl-xL, and Bcl-2 TMDs were treated with compounds at 50 µM or 2% DMSO (positive control). For each tested homo-dimer, the ratio Venus MFI/Hoechst MFI of the positive control was considered as 100% Bcl TMD interaction and the percentage of interaction, for each compound, was calculated as follows:

$$\text{Bcl TMD homo-dimer interaction (\%)} = \frac{\left(\frac{Venus\ MFI}{Hoechst\ MFI}\right) Sample}{Positive\ control} x\ 100$$

where sample refers to cells treated with hit compounds.

Results from the specificity assay revealed that compounds C42, C47, and C66 showed greater inhibition of the Mcl-1/Bok TMDs hetero-oligomerization surface than that observed for homo-dimers of Mcl-1, Bok, Bcl-xL or Bcl-2 TMDs. The rest of the compounds had increased target promiscuity since they also affected the oligomerization of Mcl-1, Bok, Bcl-xL, or Bcl-2 TMDs (Figure 27).

.

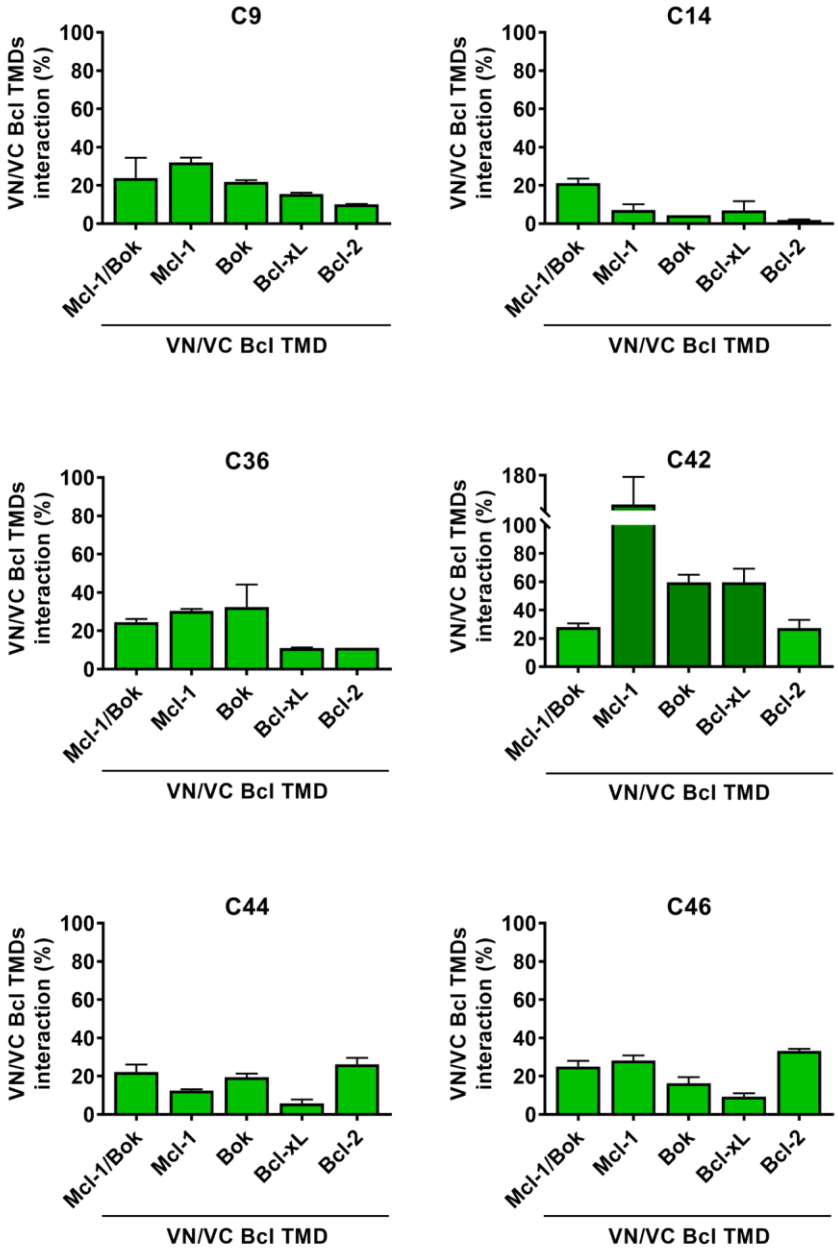
C9
C14
C36
C42
C44
C46
VN/VC Bcl TMDs interaction (%)
0
20
40
60
80
100
180
Mcl-1/Bok
Mcl-1
Bok
Bcl-xL
Bcl-2
VN/VC Bcl TMD

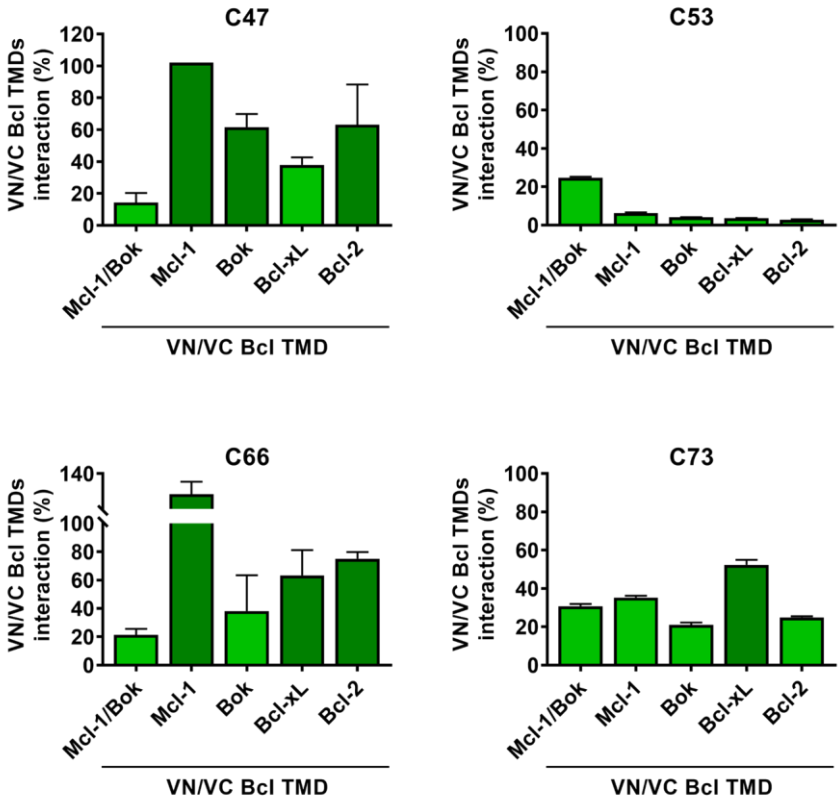

Figure 27. Transmembrane domain specificity of active inhibitors. Inhibitory activity of selected compounds was analyzed for Bcl TMD interface specificity. Venus and Hoechst MFI were acquired 16 h after the treatment of co-expressed VN and VC Bcl TMDs. Cells expressing VN/VC Bcl TMDs with no treatment represented 100% Bcl TMDs interaction and served as a positive control to calculate the percentage of inhibition for each treated Bcl TMD interaction.

Drug discovery is a time-consuming and expensive process and hence, an early description of physicochemical properties reduces both cost and time consumption and increases the success in finding drug-like compounds[250,251]. The Lipinski's rule-of-five[252] defines that those molecules with more than 5 H-bond donors, 10 H-bond acceptors, a molecular weight

greater than 500 Da, and a partition coefficient (log P) greater than 5 may present low oral bioavailability and should not be considered for drug development. Based on these values, we analyzed such descriptors provided by the MyriaScreen library confirming that C42, C47, and C66 exhibit optimal physicochemical properties for oral activity (Table 5).

Table 5. Inhibitors of Mcl-1/Bok TMDs interaction.

N° hit	Log P	Molecular weight	Acceptors	Donors
42	1.22916	438,52825	5	1
47	-1.0509	289,29905	2	3
66	3.8437	295,79018	2	1

Data provided by the MyriaScreen library.

As Mcl-1 and Bok TMDs interaction takes place within intracellular membranes, it is expected that active inhibitors would penetrate lipid bilayers to reach the binding site and disrupt the hetero-dimer. The most commonly used parameter to describe the permeability and lipophilicity of drug-like compounds is log P, which is defined as follows:

$$Log\ P = log10\ (Partition\ Coefficient)$$

$$Partition\ Coefficient, P = \frac{[organic]}{[aqueous]}$$

where [ ] indicates the concentration of a compound in the organic and aqueous partition (N-octanol and water, respectively). Positive values indicate a higher concentration in the lipid phase (i.e. lipophilic compounds).

Considering log P values of selected molecules, compound 66 presents greater lipophilicity than C42 and C47, which suggests that it has apparently better drug-likeness, and it could be a lead candidate to perform drug development.

To analyze better the physicochemical descriptors of our hits, we employed the OSIRIS Property Explorer, a bioinformatic tool that predicts some drug-relevant properties, such as the mentioned log P but also the aqueous solubility (log S), the toxicity risk, and the fragment based drug-likeness. Furthermore, this tool combines these physicochemical parameters to calculate the drug score that evaluates the compound's overall potential to be considered a drug candidate. Considering OSIRIS results (Table 6), C47 shows the best pharmacological profile due to it presents the greatest aqueous solubility and drug-likeness, it is the smallest molecule and the only compound that does not present any toxicity risk.

Table 6. OSIRIS predictions of Mcl-1/Bok TMDs inhibitors.

Hit	Drug score	Log P (Score)	Log S (Score)	MW (Score)	Fragmented based drug-likeness (Score)	Toxicity risk			
						Mutagenicity	Tumorigenicity	Irritating	Reproductive
42	0.187	Log P = 2.702 (0.908)	Log S = -4.831 (0.542)	MW = 438 (0.677)	-4.361 (0.012)	1	1	0.6	1
47	0.946	Log P = -0.813 (0.997)	Log S = -1.883 (0.957)	MW = 275 (0.937)	6.743 (0.998)	1	1	1	1
66	0.575	Log P = 3.324 (0.842)	Log S = -4.187 (0.692)	MW = 295 (0.921)	2.476 (0.922)	0.8	1	1	1

Risk of mutagenecity, tumorigenicity, irritating effect or reporductive effect: no risk, score 1; medium risk, score 0.8; high risk, score 0.6.

Althoug lipophilicity can compromise the oral bioavailability of a drug, compounds targeting TMDs should reach membrane-embedded sites; therefore, we reasoned they may present a delicate balance between aqueous solubility and membrane permeability. Indeed, analysis of some molecules targeting transmembrane segments shows log P > 3 for the majority of them (Table 7). This supports that compounds acting within the membrane should present a certain level of lipophilicity to permeate the lipid bilayer.

Table 7. Transmembrane domain modulators.

Compound	Target	Log P	Source
BTPU	P2Y1 Receptor	6.1	PubChem (predicted)[1]
Vorapaxar	Protease-activated receptor-1 (PAR-1)	5.39	ChEMBL
ZINC19797057	Glucagon-like peptide 1 receptor (GLP-1R)	3.897	PMID: 31758355
m-MPEP	Metabotropic glutamate receptor 5 (mGluR5)	3.3	PubChem (predicted)[1]
NSC49652	TMD of the p75 neurotrophin receptor (p75NTR)	1.96	OSIRIS (predicted)[1]

[1]Predicted indicates log P values computationally calculated.

Altogether, these results suggest that physicochemical descriptors should be specifically considered when analyzing drug candidates for TMD targeting. Besides, further identification and investigation of TMD modulators will allow discriminating which parameters are more adequate

to evaluate these compounds and identify specific drug-descriptors for this type of targets.

4.4.DISCUSSION

In this work, we have established a TMD BiFC-based system for high-throughput screening to discover inhibitors of the Mcl-1/Bok TMDs interaction. Our approach represents a relatively simple, fast, and economic procedure, which has high quality and suitability (Z' factor values) for drug identification. It also presents several advantages that complement drug discovery strategies based on soluble protein structures. First, active inhibitors target TMD interactions that are actually taking place within the membrane. Second, hits are selected with a proven ability to penetrate the lipid bilayer. Third, the cellular system includes relevant features that also influence the Mcl-1/Bok TMDs association: interactions with membrane lipids and other anchored Bcl-2 proteins, membrane lipid composition, or molecular crowding in the membrane. Finally, other studies have also applied the BiFC system to drug discovery[253] demonstrating, together with our data that it is a powerful approach for drug discovery in live cells.

Mcl-1 overexpression is frequent in human primary and drug-resistant tumors, which claims the use of Mcl-1 inhibitors for cancer treatment[254]. Currently, several clinical trials are testing the efficacy of four Mcl-1–BH3 mimetics[195], although there are still little data about their toxicity profile in humans. Based on conditional *Mcl-1* knockout mouse models and preclinical studies, their on-target side effects have been predicted,

including toxicity towards hematopoietic stem cells and cardiomyocytes, among others[255]. Indeed, a recent study has uncovered that *in vitro* S63845-mediated Mcl-1 inhibition causes severe defects in cardiomyocytes functionality[256]. This is due to non-apoptotic functions of Mcl-1, such us regulation of mitochondrial morphology and dynamics. Based on these data, we propose Mcl-1 TMD modulators as an alternative strategy to inhibit Mcl-1. Such inhibitors will allow elucidating what functions the transmembrane segment is involved in. Dissecting the functions that specifically control each Mcl-1 domain will get a deep insight into the protein biology, which will permit the optimization of Mcl-1 inhibition as tumor therapy. It may be possible to modulate selectively specific functions of the protein, preventing potential toxicities associated with Mcl-1's non-apoptotic activities.

The toxicity profile of our three drug candidates (C42, C66, and C47), in the presence and absence of overexpressed Mcl-1/Bok TMDs, are needed to further characterize their molecular mechanism. Additionally, the hetero-dimer structure predicted in the *Chapter I* of this Thesis will be useful for the identification of potential ligand-binding sites (SiteFinder analysis) and the *in silico* analysis of C42, C66, and C47 binding capacity to Mcl-1/Bok TMDs. Finally, once the binding site will be determined, site-specific mutagenesis studies will be performed to confirm the proposed binding site[257].

The ideal compound for anti-cancer therapy would inhibit Mcl-1 TMD-mediated antiapoptotic activity but not affect the membrane perturbation capacity of Bok. Analysis of TMD specificity revealed that C66

disrupted both Mcl-1/Bok TMDs hetero-dimer and Bok TMD homo-dimer (Figure 27). We reasoned that C66 binding site might be present in the Bok TMD, thereby affecting its interactome. The TMD has been described dispensable for membrane permeabilization by Bok[221]; however, its deletion reduced Bok-induced cell death[117]. For that reason, we suggest further studies to test Bok proapoptotic activity in the presence of C66, which could shed light on the contribution of the Bok TMD to the protein functionality.

Since TMD interactions became consider druggable surfaces, most research efforts have been focused on targeting TMDs of plasma membrane proteins, leading to the development of a few molecules capable of interfering TMD-TMD association and clustering[176,258-260]. To the best of our knowledge, this is the first work aimed to modulate intracellular TMD interactions of human proteins, which represents the next step into the TMD druggability.

Inhibitors of the yet-poorly-explored Mcl-1/Bok TMDs association are themselves a scientific achievement. The negative allosteric modulators PF-06372222 and NNC0640 have allowed the GLP-1R TMD structure solution and the identification of drug binding pockets[248]. Based on this solved structure, compound C-1 has been recently identified as an allosteric modulator of GLP-1R binding a TMD pocket[257]. Likewise, C42, C66, or C47 could serve as potential molecular probes for the structural characterization of the Mcl-1 and Bok TMDs hetero-dimer, making more feasible rational and computational drug design.

Our results also provide promiscuous compounds that target other Bcl TMDs interactions, such as homo-dimers of Mcl-1, Bok, Bcl-xL, and Bcl-2 TMDs (Figure 27). Structure comparisons of specific and promiscuous small molecules may be useful to identify the inhibitory binding site of Mcl-1/ Bok TMDs dimer and discriminate effective physicochemical descriptors of drug candidates.

4.5. CONCLUSIONS

Herein, we propose the first-time-described Mcl-1 and Bok TMDs interaction as a new drug target for Mcl-1 inhibition in cancer therapy. Using Mcl-1/Bok TMDs inhibitors to trigger Bok-induced apoptosis in cancer cells can be an effective therapy to treat tumors expressing high levels of both Mcl-1 and Bok proteins.

Encouraged from promising drug discoveries performed in the laboratory, we have developed an HTS assay to identify Mcl-1/Bok TMDs inhibitors employing membrane-anchored proteins. Our results reveal three modulators with preferential targeting for Mcl-1/Bok TMDs hetero-dimer and promiscuous compounds that also disrupt other Bcl TMDs associations. Overall, these molecules emerge as potential TMD modulators and pave the way for the structural understanding of Bcl TMDs interactions and their chemical modulation. Moreover, the discovery of small molecules able to target TMDs represents a scientific advantage in the challenging field of membrane proteins.

In conclusion, we propose three small molecules as candidates for drug development to target Mcl-1 and Bok TMDs interaction as a new drugging site for anti-cancer therapy.

Chapter III

Somatic Mutations of Bcl-2 and Bcl-xL Transmembrane Domains: Molecular and Functional Analysis

Graphical abstract

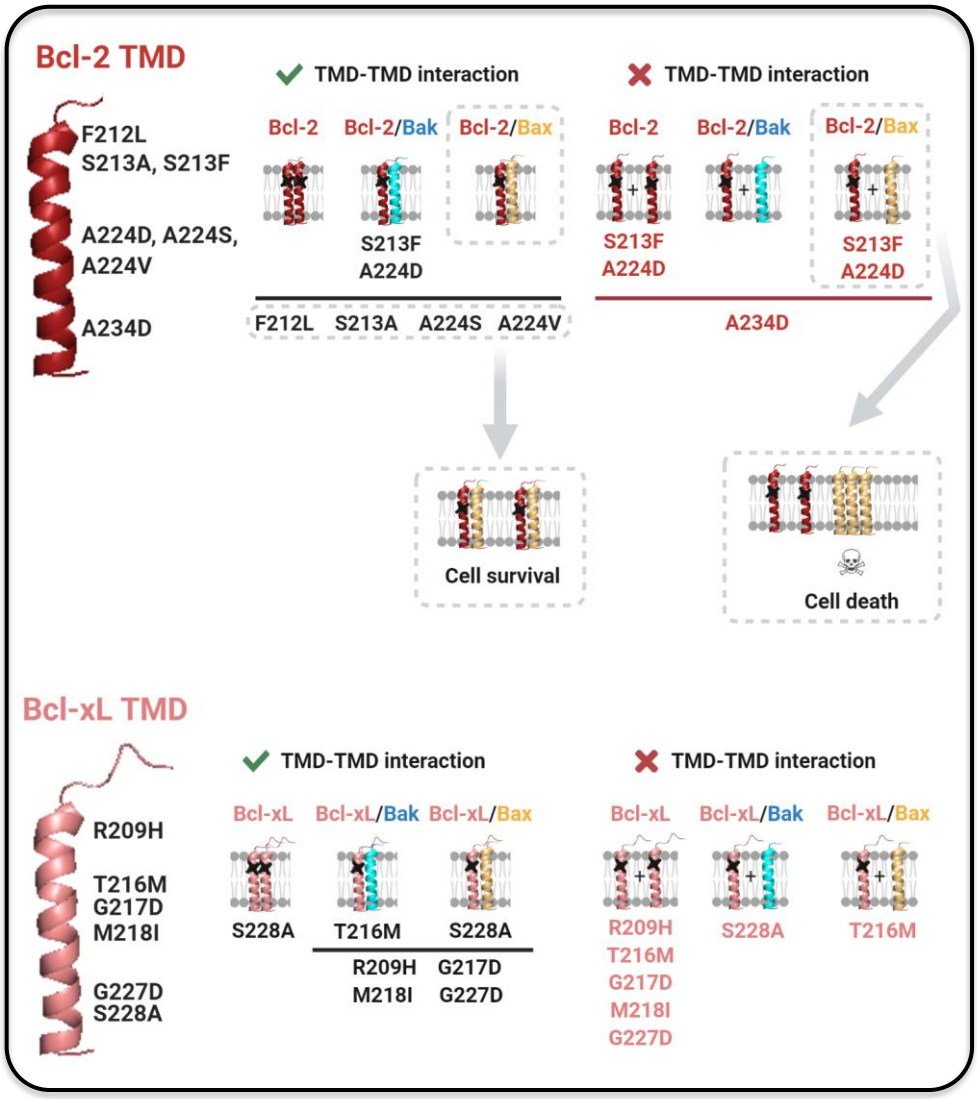

5.1. INTRODUCTION

Next-generation sequencing of DNA from tumor samples has enabled a comprehensive characterization of somatic mutations in cancer patients[261,262]. Considering the relevant role of proteins from the Bcl-2 family in tumor maintenance, several studies have explored their cancer-related mutations. To date, Bcl-2 has been the most analyzed protein, appearing highly mutated in hematological malignancies. It has been observed that some Bcl-2 mutants exhibit enhanced prosurvival activity in lymphoma cells[263], while in follicular lymphoma patients Bcl-2 mutations correlate with an increased risk of transformation and shortened survival[264]. Somatic mutations that inactivate the proapoptotic gene *Bad* have been identified in human colon cancers[265]. In the case of Mcl-1, mutations D155G, D155H, and L174S have been described in glioblastoma multiforme patients and their overexpression in glioma cells significantly accelerated cellular growth. Regarding the proapoptotic protein Bax, mutational studies performed in cell lines found no detectable Bax expression due to frameshift mutations[266,267]. Furthermore, a bioinformatic study has recapitulated somatic mutations of Bfl-1 present in breast cancer samples. Mutations M75R and L99R are predicted to alter protein stability while the Y120C mutant could destabilize interactions between the BH3 binding site of Bfl-1 and other Bcl-2 proteins[268].

Based on these data, a recent mathematical model has been developed to investigate the functional role of somatic mutations identified in this family of proteins[269]. Using molecular dynamics simulation, the authors

have established that functional domains with high influence in apoptosis modulation, such as Bax and Bid TMDs, tend to carry a relatively greater number of mutations. In other words, the mutation enrichment of these domains correlates with the sensitivity of altering the apoptotic pathway.

It is expected that mutations within the TMD of Bcl-2 proteins may modify relevant PPIs between members of this family. Moreover, Bcl TMDs mutations can affect interactions between members of the Bcl-2 family and proteins or lipids in the mitochondrial membrane. Any of these changes can ultimately alter the interactome of Bcl-2 proteins in the membrane, leading to a dysregulation of the apoptotic pathway and affecting other non-apoptotic functions executed by this family of proteins.

The lack of studies analyzing cancer mutations present within the transmembrane segments of Bcl-2 proteins encouraged us to explore their functional consequences in cell death modulation.

5.2. MATERIALS AND METHODS

5.2.1. Cell culture.

HCT116 cells were grown as described in CHAPTER I, 3.2. MATERIALS AND METHODS, 3.2.1. Cell culture.

5.2.2. Bcl-2 and Bcl-xL somatic mutants.

Somatic mutations within the TMD of the antiapoptotic proteins Bcl-2 and Bcl-xL were identified in the Catalogue Of Somatic Mutations In Cancer (COSMIC). All the selected mutations had a high pathological score.

Bcl-2 and Bcl-xL somatic mutations were introduced in the BiFC system (VN and VC Bcl TMD plasmids) to analyze the oligomeric state and the subcellular localization of the TMD mutants, as well as a possible effect in apoptosis modulation.

BiFC-TMD point mutations were obtained using standard site-directed mutagenesis with the Stratagene Quickchange II kit (Agilent), according to the manufacturer's instructions. Primers were designed using the web-based QuikChange Primer Design Program available online at www.agilent.com/genomics/qcpd (Table 8). All constructs were verified by sequencing.

Table 8. Primers for Bcl-2 and Bcl-xL TMD mutagenesis.

Protein	TMD Mutation	Forward (5' - 3')	Reverse (5' - 3')
Bcl-2	F212L (pBiFC-VN)	gagtagcggccgctttgatctgtcctggctgtct	agacagccaggacagatcaaagcggccgctactc
	F212L (pBiFC-VC)	gaagagcggccgctttgatctgtcctggctgtc	gacagccaggacagatcaaagcggccgctcttc
	S213A	gcggccgctttgatttcgcgtggctgtctctgaa	ttcagagacagccacgcgaaatcaaagcggccgc
	VC S213F	gaagagcggccgctttgatttcttttggctgtctctg	cagagacagccaaaagaaatcaaagcggccgctcttc
	VN S213F	gagtagcggccgctttgatttcttttggctgtctctg	cagagacagccaaaagaaatcaaagcggccgctactc
	A224D	gactctgctcagtttggatctggtgggagcttgcat	atgcaagctcccaccagatccaaactgagcagagtc
	A224S	gactctgctcagtttgtctctggtgggagcttgca	tgcaagctcccaccagagacaaactgagcagagtc
	A224V	ctctgctcagtttggtgctggtgggagcttgc	gcaagctcccaccagcaccaaactgagcagag
	A234D	ttgcatcaccctgggtgattatctgggccacaagtg	cacttgtggcccagataatcacccagggtgatgcaa

Protein	TMD Mutation	Forward (5' - 3')	Reverse (5' - 3')
Bcl-xL	R209H	cgaaagggccaggaacatttcaaccgctggttcc	ggaaccagcggttgaaatgttcctggccctttcg
	T216M	gcttcaaccgctggttcctgatgggcatgactg	cagtcatgcccatcaggaaccagcggttgaagc
	G217D	gctggttcctgacggatatgactgtggccggc	gccggccacagtcatatccgtcaggaaccagc
	M218I	ttcctgacgggcattactgtggccggc	gccggccacagtaatgcccgtcaggaa
	G227C	ggcgtggttctgctgtgctcactcttcagtc	gactgaagagtgagcacagcagaaccacgcc
	S228A	cgtggttctgctgggcgcgctcttcagtcggaaat	atttccgactgaagagcgcgcccagcagaaccacg

5.2.3. BiFC-based screen of Bcl-2 and Bcl-xL TMD somatic mutants oligomerization.

To analyze the influence of Bcl-2 and Bcl-xL TMD somatic mutations in their oligomeric capability, a BiFC screening assay was performed. Twenty-five thousand HCT116 cells per well were seeded in dark 96-well plates (Santa Cruz, 204468) and transfected the following day. Transfection solution contained 100 µl serum-free McCoy's 5A medium, 0.6 µl TurboFect, and 0.1 µg VN Bcl TMD plus 0.1 µg VC Bcl TMD plasmids, per well. Twenty hours after VN/VC Bcl TMDs expression, fluorescence images were acquired with a Leica SP8 confocal microscope and Venus MFI was measured using the Leica Application Suite X software.

The hetero-oligomeric state of Bcl TMD somatic mutants with Bax or Bak TMDs was also analyzed by a BiFC-based screening, under the same experimental conditions. The transfected plasmids corresponded with the VN Bax TMD (or the VN Bak TMD) plus the VC Bcl TMDs.

5.2.4. Caspase 3/7 activity of the Bcl-2 and Bcl-xL TMD somatic mutations.

To evaluate the functional impact of Bcl-2 and Bcl-xL transmembrane somatic mutations, apoptosis induction was determined by measuring caspase 3/7 activation. HCT116 cells were seeded in dark 96-well plates (Santa Cruz, 204468) at 20,000 cells/well confluence. The next day, cells were transfected with 0.2 µg VN Bcl TMD plasmids per well, in 100 µl serum-free McCoy's 5A medium with 0.6 µl TurboFect. Apoptosis

induction was analyzed 20 h after VN Bcl TMD expression using the Apo-ONE® Homogeneous Caspase-3/7 Assay (Promega) and following manufacturer's instructions. Fluorescence of the cleaved product was measured using a Wallac 1420 Workstation (λexcitation 485 nm and λemission 535 nm). Caspase 3/7 activity was expressed as arbitrary units (a.u.).

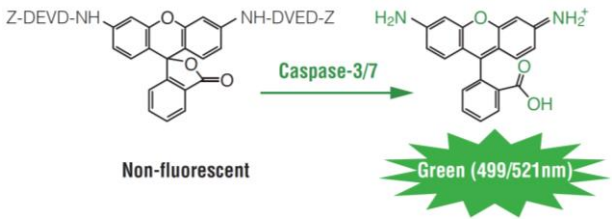

Figure 28. Caspase 3/7 cleaves the non-fluorescent Caspase Substrate Z-DEVD-R110 and creates the fluorescent Rhodamine 110. The amount of caspase 3/7 activity contained in the sample is proportional to the amount of fluorescent product generated (www.promega.com/protocols/).

To analyze the protective effect of Bcl TMD somatic mutants in Bax-mediated cell death, the same experimental procedure was performed. Although, in this case, HCT116 cells were transfected with 0.1 µg VN Bcl TMD plus 0.1 µg VN Bax TMD plasmids. It is worth noting that to measure caspase 3/7 activity, the transfected plasmids were both VN Bcl TMDs to prevent Venus reconstitution and therefore, avoid Venus fluorescence emission.

5.2.5. Immunoblotting.

VN and VC Bcl TMDs protein expression was analyzed by western blotting, as described in CHAPTER I, 3.2. MATERIALS AND METHODS, 3.2.3. Immunoblotting.

5.2.6. Subcellular fractionation.

VN and VC Bcl TMDs membrane localization was by subcellular fractionation and subsequent western blotting, as described in CHAPTER I, 3.2. MATERIALS AND METHODS, 3.2.4. Subcellular fractionation.

5.2.7. Statistical analysis.

All the values represent the mean ± S.E.M. of at least three independent experiments. Statistical significance was determined by one-way ANOVA, applying the Dunnet´s test. $P < 0.05$ was considered statistically significant.

5.2.8. Software.

Somatic mutations of Bcl-2 and Bcl-xL TMDs were identified in the Catalogue Of Somatic Mutations In Cancer (COSMIC, https://cancer.sanger.ac.uk/cosmic). Confocal image analysis was performed using the Leica Application Suite X software. Statistical analysis was performed using Graph Pad 8 software. Helical wheel projections were obtained with the web tool HeliQuest https://heliquest.ipmc.cnrs.fr/cgi-bin/ComputParams.py.

5.3. RESULTS AND DISCUSSION

5.3.1. Analysis of cancer mutations within the Bcl-xL TMD.

To evaluate the clinical significance of the Bcl-xL TMD, we searched the COSMIC[230] database and identified six cancer-related mutations within it (Table 9). We studied their effect in the Bcl-xL functionality and analyzed several parameters that influence it, such as Bcl-xL TMD self-interaction, subcellular localization, or antiapoptotic ability under Bax TMD-induced cell death.

Table 9. Somatic mutations of Bcl-xL TMD (data obtained from the COSMIC database).

Bcl-xL TMD: $_{203}$SRKGQERFNRWFLTGMTVAGVVLLGSLFSRK$_{233}$

Protein	Mutation	Pathogenic score	Tissue	Primary histology	PMID
Bcl-xL	R209H	0.76	Skin	Malignant melanoma	26286987
	T216M	0.84	Large intestine/ Oesophagus	Adenocarcinoma	27149842/ 28481359
	G217D	0.92	Pancreas	Adenoma	22158988
	M218I	0.84	-	Carcinoma	28481359
	G227C	0.97	Lung	Squamous cell carcinoma	-
	S228A	0.91	Pancreas	Ductal carcinoma	28481359

First, we introduced these mutations in the Bcl-xL TMD BiFC system and evaluated their homo-oligomerization capacity. Fluorescence quantification demonstrated that all mutants interfered with Bcl-xL TMD

self-association to a greater or lesser extent, except the Bcl-xL S228A TMD that homo-dimerized at the same level as the Bcl-xL WT TMD (Figure 29A). Protein expression analyses corroborated these results, except for the mutant G217D which showed lower protein levels (Figure 29A, bottom panel).

It has been proposed that membrane-anchored Bcl-xL has an enhanced antiapoptotic activity than the soluble form[100]. This is based on the observation that the BH3 mimetic WEHI-539 has a limited ability to inhibit Bcl-xL in cellular systems. The authors also demonstrated that modifications in the Bcl-xL TMD restore cellular sensitivity to the anticancer drug due to an altered subcellular distribution of the protein. For that reason, we investigated whether cancer-related Bcl-xL TMD mutants impact its mitochondrial localization. To this end, we performed subcellular fractionation experiments and we observed that mitochondrial membrane targeting of all mutants was similar to that of the Bcl-xL WT (Figure 29B).

Of note, the G217D mutant showed a slower SDS-PAGE migration compared to the WT protein. Sodium dodecyl sulfate micelles have been shown to recapitulate protein:lipid interactions due to its membrane mimicking capability[270], which suggests that the G217D mutant modifies the interaction of the Bcl-xL TMD with membranes.

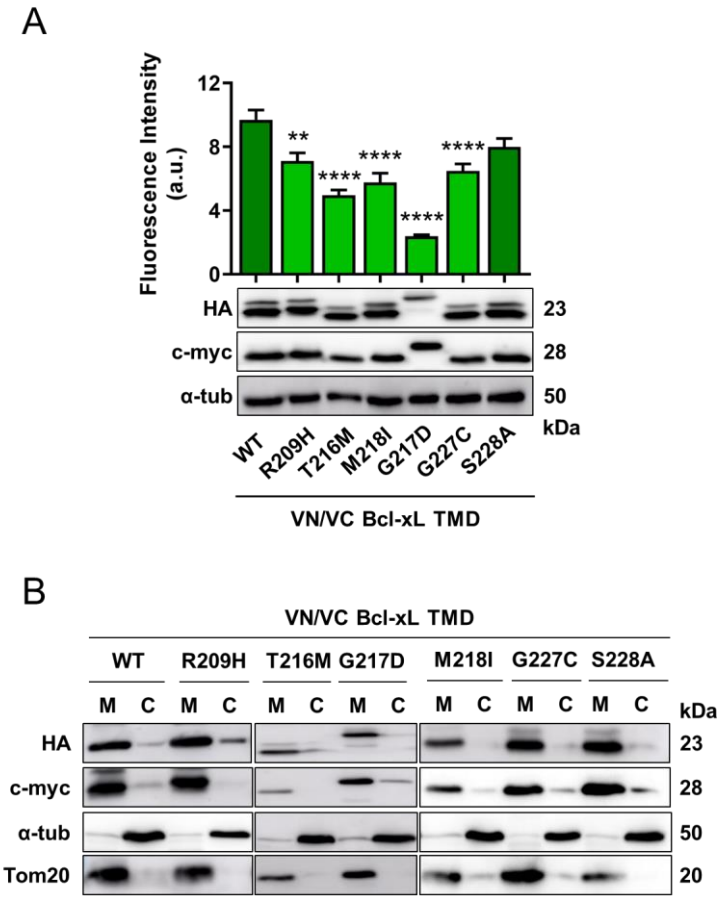

Figure 29. Somatic mutations of the Bcl-xL TMD have different patterns of oligomerization. A) Homo-oligomer formation of the wild-type Bcl-xL TMD and single amino acid mutants measured by BiFC assay in HCT116 cells. The graph shows the Venus fluorescence quantification by confocal imaging. Error bars represent the mean ± SEM, n = 4. Significant differences to the Bcl-xL WT TMD were analyzed using Dunnett's Multiple Comparison Test (95% CI). *P*-value according to Dunnett's test is displayed. **P < 0.01, ****P < 0.0001. VC (HA) and VN (c-myc) protein expression was compared in the bottom panel with α-tubulin as a loading control. **B)** Subcellular fractionation of HCT116 cells transfected with VN (c-myc) and VC (HA) Bcl-xL TMD constructs was controlled using Tom20 (mitochondrial fraction, M) and α-tubulin (cytosol, C).

The transmembrane segment of Bcl-xL is involved in homo-dimer formation but also in hetero-oligomerization with Bax. These interactions influence Bcl-xL shuttling off the mitochondria[91] and mediate Bax retrotranslocation from the mitochondria to the cytosol[98], respectively. These localization dynamics determine protein accumulation on the mitochondria, modifying their interaction equilibrium and thus, regulating apoptosis. Therefore, we tested the hetero-oligomer formation capacity of Bcl-xL TMD mutants with the Bak and Bax TMDs. The hetero-dimer Bcl-xL TMD / Bak TMD was slightly affected by the S228A mutation (Figura 30A, left panel), while the association between Bcl-xL and Bax TMDs was partially disrupted by the T216M mutant (Figura 30A, right panel).

Regarding the functional implications of Bcl-xL TMD homo- and hetero-interactions in apoptosis modulation, we wondered whether interferences on the Bcl-xL TMD oligomerization capability could alter its antiapoptotic activity. We analyzed caspase 3/7 activation in VN Bcl-xL TMD-expressing cells under both non-stress conditions and VN Bax TMD-induced apoptosis. In normal conditions (Figure 30B, left panel), caspase 3/7 activity measured in transfected cells was similar to the basal activity of non-transfected cells for all mutants, indicating the disruption of Bcl-xL TMD homo-dimers do not change the harmless effect of the Bcl-xL WT TMD protein. Similar results were obtained under cell death mediated by the Bax TMD (Figure 30B, right panel), where the majority of the somatic mutants maintained their antiapoptotic function, although the Bcl-xL G217D TMD mutant failed to protect cells from death. It seems that

interaction with the Bax TMD is not sufficient to inhibit its proapoptotic activity. We propose that the G217D mutation could impair the retrotranslocation activity of Bcl-xL, thereby leading to Bax accumulation and oligomerization into the mitochondria. These results also tempt us to hypothesize that the Bcl-xL TMD might require a certain level of homo-oligomerization to block Bax TMD-mediated cell death since the G217D mutation dramatically decreased its self-association.

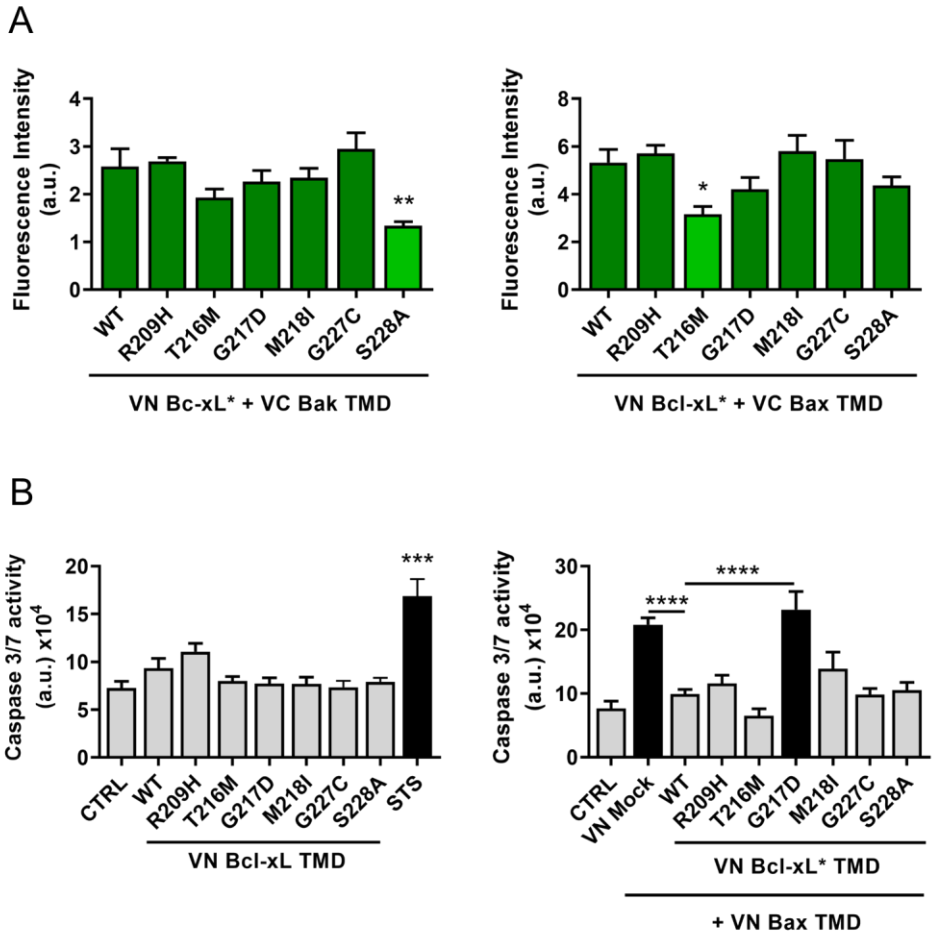

Figure 30. Bcl-xL TMD cancer-related mutations share hetero-oligomerization and antiapoptotic activities with the WT protein. A) Hetero-interaction of Bcl-xL TMD somatic mutants with the Bak TMD (left panel) and the Bax TMD (right panel), analyzed by the BiFC system in HCT116 cells. Error bars represent the mean ± SEM, n = 3. Significant differences compared to the WT Bcl-xL TMD were analyzed. *P*-value according to Dunnett's test is displayed. *P < 0.05, **P < 0.01. Antiapoptotic activity of VN Bcl-xL TMD somatic mutations under normal conditions **(B)** or Bax TMD-induced cell death **(C)**, measured by caspase 3/7 activity in HCT116 cells. Error bars represent the mean ± SEM, n = 3. Significant differences were compared to the Bcl-xL WT TMD. ***P < 0.001, ****P < 0.0001. Control (Ctrl) refers to non-transfected cells. Cells treated with 100 nM staurosporine (STS) were used as a positive control of apoptosis.

Overall, these results suggest that the G217D is the somatic mutant that influences the most on Bcl-xL TMD membrane interactome (Table 10) since it disrupts its homo-dimerization; slightly, although not significantly, decreases hetero-dimerization with the Bax TMD, and impairs its prosurvival function. Moreover, this mutation may influence Bcl-xL TMD interaction with the lipid bilayer. The global effect of the G217D mutation will depend on the contribution of each altered equilibria (homo- and hetero-associations as well as interactions with the intracellular membranes). Further experiments should be performed in parallel with mutated Bcl-xL TMD and full-length protein to decipher whether this mutation would represent an advantage for tumor cells.

Furthermore, Bcl-xL has been associated with non-apoptotic functions. For example, its expression has been correlated with an enhanced metastatic potential in breast cancer cells[271,272]. Specifically, it has been recently proposed that Bcl-xL controls breast cancer cell migration by acting on

VDAC1 permeabilization and enhancing mitochondrial-dependent ROS production[273]. Moreover, Bcl-xL has been reported to promote cell migration in pancreatic cancer[274,275]. Based on our results and the above mentioned Bcl-xL functions in the tumor context, we propose to transfer cancer-related mutations to the Bcl-xL full-length protein and study their effect in the context of the whole protein. Evaluation of their cell-protective effect as well as their influence on Bcl-xL's non-apoptotic roles, such as cell migration and tumor metastasis, will help us to elucidate whether somatic mutations within the Bcl-xL TMD provide an advantage to tumor cells and if so, in which mechanisms they are involved.

Table 10. Interaction pattern and protein activity of Bcl-xL TMD somatic mutants.

Bcl-xL TMD	Interaction with Bcl TMD[a]			Apoptosis induction[b]	Antiapoptotic[c]
	Bcl-xL	Bak	Bax		
WT				X	✓
R209H				X	✓
T216M				X	✓
G217D				X	X
M218I				X	✓
G217C				X	✓
S228A				X	✓

[a]Heatmap of Bcl-2 TMDs homo- and hetero-interactions. Dark blue, strong interaction; medium blue; light blue, weak interaction.

[b and c]Ticks and cross mean the Bcl-2 TMD exerts or not the indicated function, respectively.

5.3.2. Cancer mutations in the Bcl-2 TMD alter the oligomerization state and the antiapoptotic function.

We were also interested in the study of somatic mutations present within the Bcl-2 TMD. Analysis of the COSMIC database[230] revealed the existence of seven cancer-related mutations (Table 11). As we did for the Bcl-xL TMD, we generated VN and VC Bcl-2 TMD constructs containing the somatic mutants to perform BiFC assays.

Table 11. Somatic mutations of Bcl-2 TMD (data obtained from the COSMIC database).

Bcl-2 TMD: $_{212}$FSWLSLKTLLSLALVGACITLGAYLGHK$_{239}$

Protein	Mutation	Pathogenic score	Tissue	Primary histology	PMID
Bcl-2	F212L	0.94	Large intestine	Colon carcinoma	28481359
	S213A	0.88	Hematopoietic and lymphoid	Lymphoid neoplasm	28481359
	S213F	0.9	Skin	Malignant melanoma	28481359
	A224D	0.83	Liver	-	-
	A224S	0.95	Lung	Adenocarcinoma	22980975
	A224V	0.72	Skin	Malignant melanoma	-
	A234D	0.96	Ovary	Carcinoma	28481359

We first analyzed their self-association capacity and observed that mutations S213F, A224D, and A234D apparently disrupted the formation of Bcl-2 TMD oligomers (Figure 31A). Protein expression experiments corroborated this effect for the Bcl-2 S213F TMD, but not for Bcl-2 A224D

and Bcl-2 A234D TMDs since those mutants showed a lower protein expression or stability than the WT constructs (Figure 31A, bottom panel). Hence, whether the decrease in Venus fluorescence for A224D and A234D mutants is due to an impaired self-interacting capacity should be further tested.

Of note, serine 213 mutants had different oligomer behaviors depending on the added amino acid: the Bcl-2 S213A TMD oligomerized at the same level as the Bcl-2 WT TMD, while the S213F mutant significantly reduced homo-oligomerization. Probably, the introduction of a bulky amino acid such as Phenylalanine interferes with the packing interface.

Helical wheel projections showed residues S213, A224 and A234 orientated to the same α-helix interface supporting this region as the packing interface of Bcl-2 TMD homo-interaction (Figure 31D). Indeed, we have previously reported that a mutation of the G227 residue, which locates in the same interface, disrupted homo-oligomer formation[58]. Altogether, these results confirm that the Bcl-2 TMD self-associates by a sequence-specific packing interface that is mutated in some cancer patients.

Next, we analyzed the subcellular distribution of Bcl-2 TMD homo-oligomers. Subcellular fractionation assays confirmed that all Bcl-2 TMD cancer-related mutants were found in the same fraction as the Tom20 outer mitochondrial membrane protein (Figure 31B). However, lower protein levels of A224D and A234D mutants were detected compared to the Bcl-2 WT TMD. Again, this could be a consequence of the lower protein expression/stability showed by these constructs. But it also could be due to

an altered mitochondrial membrane anchoring since negatively charged residues are rare in transmembrane segments and they are especially suppressed in the TMD core[276,277].

In our previous work[58] and *Chapter I* of this Thesis, we have demonstrated that Bcl TMDs play an active role in modulating apoptosis. Based on these findings, we explored the activation of caspase 3/7 after exogenous expression of the VN Bcl-2 TMD somatic mutants. Interestingly, mutants that had a lower protein level and apparently interfered homo-oligomer formation, Bcl-2 A224D and Bcl-2 A234D TMDs, induced cytotoxicity (Figure 31C). The addition of a negatively charged residue in the α-helix lowers its hydrophobicity that could affect its residency in the membrane. Additionally, the introduction of Aspartic acid in the core of the Bcl-2 TMD could promote mitochondrial membrane destabilization, which might contribute to the cytotoxic activity of the A224D mutant[273]. We suggest a similar mechanism for the A2234D mutant, which also has a lower hydrophobicity compared to the Bcl-2 WT TMD. However, mutation A234D could be better tolerated by the lipid bilayer since it locates on the flanking region of the α-helix[276]. Moreover, both TMD mutants might also impair the interactome of Bcl-2 with other mitochondrial proteins leading to apoptosis induction. Therefore, we further investigated this possibility.

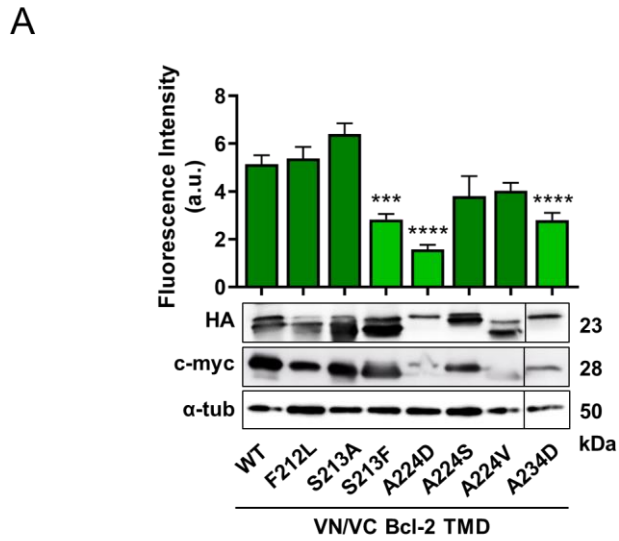
A
Fluorescence Intensity (a.u.)
8
6
4
2
0
***
****
****
HA
c-myc
α-tub
23
28
50
kDa
WT
F212L
S213A
S213F
A224D
A224S
A224V
A234D
VN/VC Bcl-2 TMD

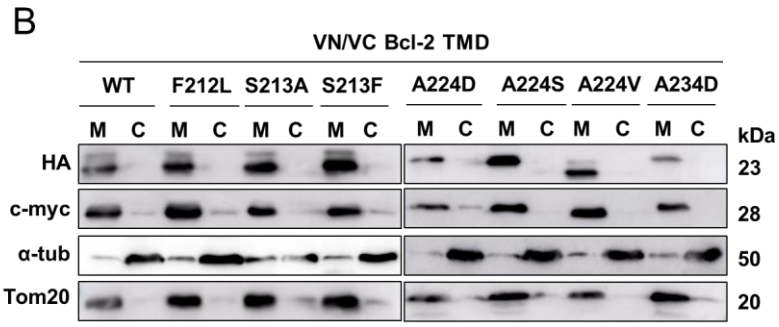
B
VN/VC Bcl-2 TMD
WT
F212L
S213A
S213F
A224D
A224S
A224V
A234D
M C M C M C M C M C M C M C M C
kDa
HA
c-myc
α-tub
Tom20
23
28
50
20

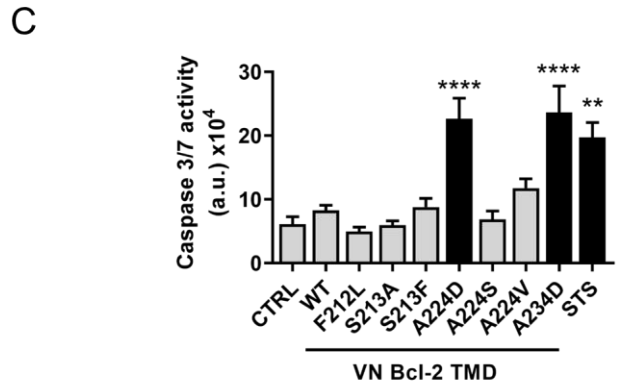
C
Caspase 3/7 activity (a.u.) x10^4
30
20
10
0
****
****
**
CTRL
WT
F212L
S213A
S213F
A224D
A224S
A224V
A234D
STS
VN Bcl-2 TMD

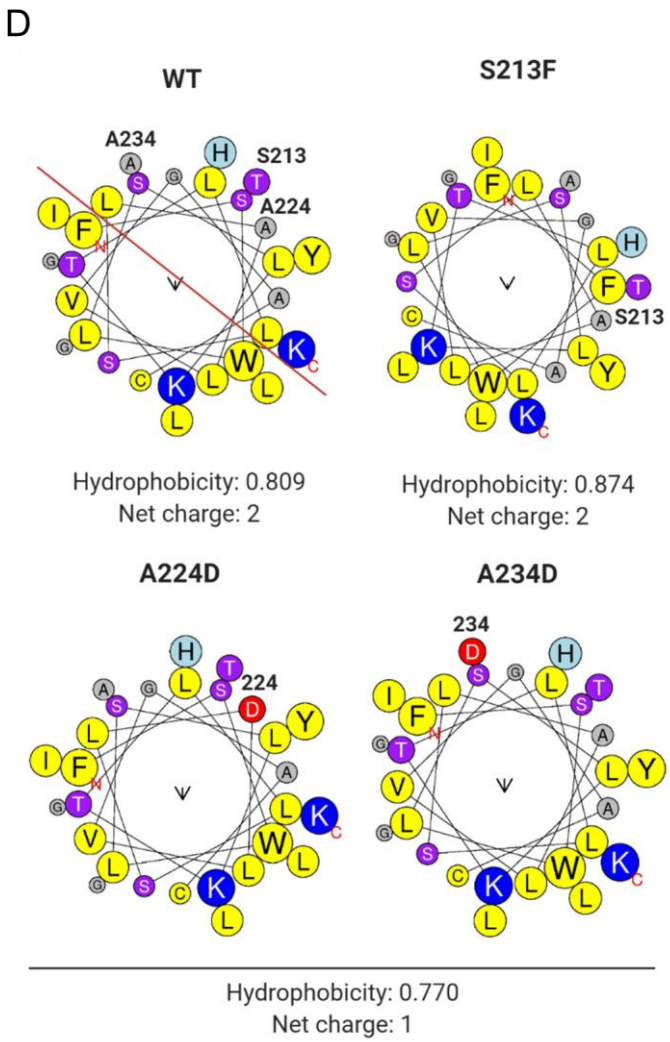

Figure 31. Somatic mutations of the Bcl-2 TMD affect the oligomerization state and functionality. A) Self-association of wild-type Bcl-2 TMD and single amino acid mutants measured by BiFC in HCT116 cells. The graph shows the Venus fluorescence quantification. Error bars represent the mean ± SEM, n = 4. Significant differences compared to the WT Bcl-2 TMD were analyzed using Dunnett's Multiple Comparison Test (***P < 0.001, ****P < 0.0001). The bottom panel compares chimeric protein expression

of VC (HA) and VN (c-myc) constructs, using α-tubulin as loading control. All samples were analyzed in the same membrane. A non-related sample has been removed. **B)** Subcellular fractionation of HCT116 cells transfected with VN (c-myc) and VC (HA) Bcl-2 TMD constructs was analyzed using Tom20 (mitochondrial fraction, M) and α-tubulin (cytosol, C). **C)** Caspase 3/7 activity induced by the VN Bcl-2 TMD somatic mutants. As a positive control, cells were treated with 100 nM staurosporine (STS). Control (Ctrl) refers to non-transfected cells. Error bars represent the mean ± SEM, n = 3. Significant differences were compared to the WT Bcl-2 TMD. *P*-value according to Dunnett's test (**P < 0.01, ****P < 0.0001). **D)** Helical wheel projections of Bcl-2 TMDs. Graphics were obtained and adapted from HeliQuest. The arrow depicts the hydrophobic moment.

The binding equilibria of the Bcl-2 family proteins are governed by protein affinities and concentrations at intracellular locations, which ultimately results in the activation or inhibition of the apoptotic pathway[34]. For that reason, we asked whether cell death promoted by some Bcl-2 TMD mutants might be explained by their hetero-oligomerization with the proapoptotic members Bak and Bax. We co-expressed the VN Bcl-2 TMDs with the VC Bak (or Bax) TMD and we observed that only the Bcl-2 A234D TMD slightly attenuated the hetero-interaction with the Bak TMD (Figure 32A, left panel). However, Bcl-2:Bax TMDs complexes were disrupted by three mutants: S213F, A224D, and A234D (Figure 32A, right panel), which could suggest that the Bcl-2 TMD utilizes the same interface (or part of it) for homo- and hetero-dimerization with the Bax TMD. These results should be carefully considered since A224D and A234D TMD mutants previously showed low protein levels, supporting further investigation to corroborate their disruptive effect.

To gain more insight into the functional implication of these interactions, we evaluated the protective activity of Bcl-2 TMD cancer mutants. To do that, caspase 3/7 activity was measured after co-expression of VN Bcl-2 TMDs and the apoptosis inducer VN Bax TMD. As shown in figure 32B, the cellular toxicity of the VN Bax TMD was blocked by the hetero-oligomerizing VN Bcl-2 TMD mutants, at the same level as the Bcl-2 WT TMD. It seems that these somatic mutations (F212L, S213A, A224S, and A224V) did not enhance the Bcl-2 antiapoptotic activity. Thus, if mutated Bcl-2 versions represent an advantage for cancer cells it must be by playing non-apoptotic functions.

In the case of the non-interacting Bcl-2 TMD mutants, we observed three different scenarios. First, the Bcl-2 S213F TMD did not show cell death protection under VN Bax-mediated apoptosis, which is in agreement with the oligomerization assay. Second, the Bcl-2 A224D TMD also failed to decrease the caspase 3/7 activation; however, it remains to be investigated whether it was due to an impaired hetero-interaction capability with the Bax TMD or its reduced protein expression/stability (Figure 32A and 31A). Finally, the Bcl-2 A234D TMD displayed similar antiapoptotic activity to the Bcl-2 WT TMD (Figure 32B), despite it showed a possible interfering effect regarding oligomer formation (Figure 32A, right panel). This suggests that TMDs of Bcl-2 A234D and Bax probably can interact; thereby, the decreased in fluorescence intensity might be explained by its lower protein level.

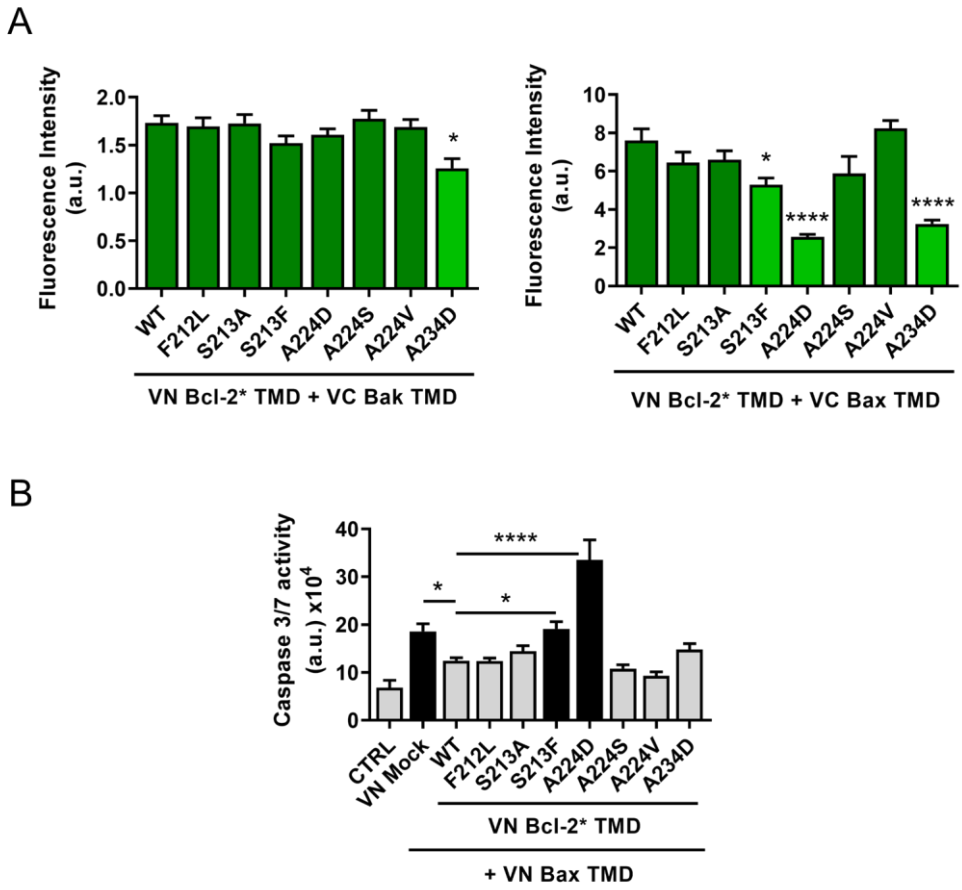

Figure 32. Somatic mutations of the Bcl-2 TMD impair the oligomerization with the Bax TMD and the antiapoptotic function. A) Transmembrane domain interactions between Bcl-2 TMD mutants and TMDs from Bak (left panel) and Bax (right panel), analyzed by the BiFC system in HCT116 cells. Error bars represent the mean ± SEM, n = 3. Significant differences were compared to the WT Bcl-2 TMD. *P*-value according to Dunnett's test is displayed. *P < 0.05, ****P < 0.0001. **B)** Antiapoptotic activity of Bcl-2 TMD somatic mutants under Bax TMD-induced cell death, measured by caspase 3/7 activity in HCT116 cells co-transfected with VN Bcl TMD constructs. Error bars represent the mean ± SEM, n = 3. Significant differences were compared to the WT Bcl-2 TMD. *P < 0.05, ****P < 0.0001. Control (Ctrl) refers to non-transfected cells.

Taken together, these results demonstrate that the analyzed cancer-related mutations affect the Bcl-2 TMD functionality in different manners (Table 13):

- Four mutants, F212L, S213A, A224S, and A224V, behave similarly to the WT protein suggesting that if they are an advantage for tumor cells, it might be regarding non-apoptotic functions.

- The S213F mutant slightly impairs the homo-association packing interface. It also has a lower antiapoptotic activity under Bax TMD-mediated apoptosis due to reduced hetero-oligomerization capacity.

- Amino acid substitution A224D has a major impact on protein functionality. It interferes with homo-oligomerization and shows lower protein expression and/or stability compared to the WT. Aspartic acid is not frequent in membrane penetrating segments; therefore, we reason that the presence of a hydrophilic residue in the core of the TMD might result in mitochondrial membrane destabilization and cell death induction. The A224D mutation also affects interaction with the Bax TMD, which explains why it fails in blocking apoptosis.

- Mutation A234D apparently disrupts homo- and hetero-interactions. However, its low protein level makes necessary to analyze further its interaction profile to elucidate if this mutation actually modifies the Bcl-2 TMD packing interface. This mutant also shows a cytotoxic

effect that might be partially promoted by the destabilization of the mitochondrial membrane. Intriguingly, it seems that its low protein level is enough to prevent apoptosis induced by the Bax TMD, reflecting an increased antiapoptotic potential of tumor cells expressing the A234D mutation.

Table 13. Interaction pattern and protein activity of Bcl-2 TMD somatic mutants.

Bcl-2 TMD	Interaction with Bcl TMD[a]			Protein expression/ stability[b]	Apoptosis induction[c]	Antiapoptotic[d]
	Bcl-2	Bak	Bax			
WT					X	✓
F212L					X	✓
S213A					X	✓
S213F					X	X
A224D				↓	✓	XX
A224S					X	✓
A224V					X	✓
A234D				↓	✓	✓

[a]Heatmap of Bcl-2 TMDs homo- and hetero-interactions. Dark blue, strong interaction; medium blue, medium interaction; light blue, weak interaction. [b]Down arrows indicate lower protein expression/stability level compared to the WT. [c and d]Ticks and cross mean the Bcl-2 TMD exerts or not the indicated function, respectively.

Finally, further experiments will be performed to confirm definitively the role of Bcl-2 A224D and A234D mutations in the homo- and hetero-oligomerization pattern of the protein and elucidate how they affect its expression or stability. Moreover, introducing these single amino acid

variants into the full-length Bcl-2 protein will allow us to analyze several functions in the context of the whole protein. For example, the antiapoptotic activity or the implication in cancer cell migration, but also features such as protein turnover or subcellular localization.

5.4. CONCLUSIONS

In the present study, we have characterized mutations within transmembrane segments of Bcl-2 and Bcl-xL with a high pathological score identified in cancer patients. Our results demonstrate that some of these mutations alter their homotypic interaction as well as that with Bax and Bak, which translates into an altered antiapoptotic activity. These findings again corroborate the specificity of Bcl TMD packing interactions and reinforce their role in apoptosis modulation.

Although this research remains unfinished, the results reported here support further analysis of Bcl transmembrane mutations to understand better both their influence into the Bcl-2 proteins' functionality (apoptotic and non-apoptotic functions) and their contribution to cancer progression.

CONCLUSIONS

The objectives achieved during the development of this Thesis reinforce the knowledge of the Bcl-2 proteins interactome in the modulation of apoptosis. The main conclusions are:

1. We demonstrated for the first time that the Mcl-1 TMD forms homo-oligomers, sequesters Mcl-1 full-length protein, and competes with its antiapoptotic function. The Mcl-1 TMD also induces cell death in a Bok-dependent manner and may drive the Bok TMD movement between the ER and the mitochondria, facilitating Bok mitochondrial localization and potentially modulating the cell death threshold.

   Furthermore, co-expression of Mcl-1 and Bok TMDs increases MAMs formation and/or stability, which might be the platform for Bok translocation.
2. Somatic mutations detected in cancer patients and affecting the Mcl-1 TMD alter its interactome and enhance Mcl-1 antiapoptotic activity of Bok-mediated killing, highlighting the clinical relevance of Mcl-1 TMD lateral interactions.
3. We developed a BiFC-based high-throughput screening to identify inhibitors of Mcl-1 and Bok TMDs hetero-oligomerization.
4. We identified three possible Mcl-1/Bok TMDs inhibitors with promising applications in the fields of antitumoral drug discovery and membrane proteins.
5. Single point mutants of Bcl-2 and Bcl-xL TMDs identified in cancer patients affected both the membrane protein interactome and the cell death modulation capability. These results pave the way to

understand the clinical relevance of Bcl TMD somatic mutations in cancer progression.

BIBLIOGRAPHY

1. Galluzzi L, Bravo-San Pedro JM, Vitale I, Aaronson SA, Abrams JM, Adam D, Alnemri ES, Altucci L, Andrews D, Annicchiarico-Petruzzelli M and others. Essential versus accessory aspects of cell death: recommendations of the NCCD 2015. Cell Death Differ 2015;22(1):58-73.
2. Galluzzi L, Vitale I, Aaronson SA, Abrams JM, Adam D, Agostinis P, Alnemri ES, Altucci L, Amelio I, Andrews DW and others. Molecular mechanisms of cell death: recommendations of the Nomenclature Committee on Cell Death 2018. Cell Death Differ 2018;25(3):486-541.
3. Lockshin RA, Williams CM. PROGRAMMED CELL DEATH--I. CYTOLOGY OF DEGENERATION IN THE INTERSEGMENTAL MUSCLES OF THE PERNYI SILKMOTH. J Insect Physiol 1965;11:123-33.
4. Kerr JF, Wyllie AH, Currie AR. Apoptosis: a basic biological phenomenon with wide-ranging implications in tissue kinetics. Br J Cancer 1972;26(4):239-57.
5. Kroemer G, Galluzzi L, Vandenabeele P, Abrams J, Alnemri ES, Baehrecke EH, Blagosklonny MV, El-Deiry WS, Golstein P, Green DR and others. Classification of cell death: recommendations of the Nomenclature Committee on Cell Death 2009. Cell Death Differ 2009;16(1):3-11.
6. Elliott MR, Ravichandran KS. Clearance of apoptotic cells: implications in health and disease. J Cell Biol 2010;189(7):1059-70.
7. Kalkavan H, Green DR. MOMP, cell suicide as a BCL-2 family business. Cell Death & Differentiation 2017;25(1):46-55.
8. Giorgi C, Baldassari F, Bononi A, Bonora M, De Marchi E, Marchi S, Missiroli S, Patergnani S, Rimessi A, Suski JM and others. Mitochondrial Ca(2+) and apoptosis. Cell Calcium 2012;52(1):36-43.
9. Li J, Yuan J. Caspases in apoptosis and beyond. Oncogene 2008;27(48):6194-206.
10. Shalini S, Dorstyn L, Dawar S, Kumar S. Old, new and emerging functions of caspases. Cell Death Differ 2015;22(4):526-39.
11. Shi Y. Caspase activation, inhibition, and reactivation: a mechanistic view. Protein Sci 2004;13(8):1979-87.
12. Green DR, Llambi F. Cell Death Signaling. Cold Spring Harb Perspect Biol. 2015;7(12):a006080.
13. Dickens LS, Powley IR, Hughes MA, MacFarlane M. The 'complexities' of life and death: death receptor signalling platforms. Exp Cell Res 2012;318(11):1269-77.
14. Fulda S, Debatin K-M. Extrinsic versus intrinsic apoptosis pathways in anticancer chemotherapy. Oncogene 2006;25(34):4798-4811.
15. Goldschneider D, Mehlen P. Dependence receptors: a new paradigm in cell signaling and cancer therapy. Oncogene 2010;29(13):1865-82.
16. Fulda S, Debatin KM. Exploiting death receptor signaling pathways for tumor therapy. Biochim Biophys Acta 2004;1705(1):27-41.
17. Mandal R, Barron JC, Kostova I, Becker S, Strebhardt K. Caspase-8: The double-edged sword. Biochim Biophys Acta Rev Cancer 2020;1873(2):188357.
18. Gibert B, Mehlen P. Dependence Receptors and Cancer: Addiction to Trophic Ligands. Cancer Res 2015;75(24):5171-5.
19. Negulescu AM, Mehlen P. Dependence receptors - the dark side awakens. The FEBS J 2018;285(21):3909-3924.
20. Blank M, Shiloh Y. Programs for cell death: apoptosis is only one way to go. Cell Cycle 2007;6(6):686-95.
21. Tait SW, Green DR. Mitochondria and cell death: outer membrane permeabilization and beyond. Nat Rev Mol Cell Biol 2010;11(9):621-32.
22. Li P, Nijhawan D, Budihardjo I, Srinivasula SM, Ahmad M, Alnemri ES, Wang X. Cytochrome c and dATP-dependent formation of Apaf-1/caspase-9 complex initiates an apoptotic protease cascade. Cell 1997;91(4):479-89.

23. Orzaez M, Sancho M, Marchan S, Mondragon L, Montava R, Valero JG, Landeta O, Basanez G, Carbajo RJ, Pineda-Lucena A and others. Apaf-1 inhibitors protect from unwanted cell death in in vivo models of kidney ischemia and chemotherapy induced ototoxicity. PLoS One 2014;9(10):e110979.
24. Yang S, Zhao X, Xu H, Chen F, Xu Y, Li Z, Sanchis D, Jin L, Zhang Y, Ye J. AKT2 Blocks Nucleus Translocation of Apoptosis-Inducing Factor (AIF) and Endonuclease G (EndoG) While Promoting Caspase Activation during Cardiac Ischemia. Int J Mol Sci 2017;18(3):565.
25. Li LY, Luo X, Wang X. Endonuclease G is an apoptotic DNase when released from mitochondria. Nature 2001;412(6842):95-9.
26. Ugarte-Uribe B, García-Sáez AJ. Apoptotic foci at mitochondria: in and around Bax pores. Philos Trans R Soc Lond B Biol Sci 2017;372(1726):20160217.
27. Webster KA. Mitochondrial membrane permeabilization and cell death during myocardial infarction: roles of calcium and reactive oxygen species. Future Cardiol 2012;8(6):863-84.
28. Hu L, Su C, Song X, Shi Q, Fu J, Xia X, Xu D, Song E, Song Y. Tetrachlorobenzoquinone triggers the cleavage of Bid and promotes the cross-talk of extrinsic and intrinsic apoptotic signalings in pheochromocytoma (PC) 12 cells. Neurotoxicology 2015;49:149-57.
29. Wang S, Xu Y, Li C, Tao H, Wang A, Sun C, Zhong Z, Wu X, Li P, Wang Y. Gambogic acid sensitizes breast cancer cells to TRAIL-induced apoptosis by promoting the crosstalk of extrinsic and intrinsic apoptotic signalings. Food Chem Toxicol 2018;119:334-341.
30. Luo X, Budihardjo I, Zou H, Slaughter C, Wang X. Bid, a Bcl2 interacting protein, mediates cytochrome c release from mitochondria in response to activation of cell surface death receptors. Cell 1998;94(4):481-90.
31. Li H, Zhu H, Xu CJ, Yuan J. Cleavage of BID by caspase 8 mediates the mitochondrial damage in the Fas pathway of apoptosis. Cell 1998;94(4):491-501.
32. Kaufmann T, Strasser A, Jost PJ. Fas death receptor signalling: roles of Bid and XIAP. Cell Death Differ 2012;19(1):42-50.
33. Hardwick JM, Soane L. Multiple functions of BCL-2 family proteins. Cold Spring Harb Perspect Biol 2013;5(2).
34. Kale J, Osterlund EJ, Andrews DW. BCL-2 family proteins: changing partners in the dance towards death. Cell Death Differ 2018;25(1):65-80.
35. Tsujimoto Y, Cossman J, Jaffe E, Croce CM. Involvement of the bcl-2 gene in human follicular lymphoma. Science 1985;228(4706):1440-3.
36. Chipuk JE, Moldoveanu T, Llambi F, Parsons MJ, Green DR. The BCL-2 family reunion. Mol Cell 2010;37(3):299-310.
37. Kaufmann T, Schlipf S, Sanz J, Neubert K, Stein R, Borner C. Characterization of the signal that directs Bcl-x(L), but not Bcl-2, to the mitochondrial outer membrane. J Cell Biol 2003;160(1):53-64.
38. Youle RJ, Strasser A. The BCL-2 protein family: opposing activities that mediate cell death. Nat Rev Mol Cell Biol 2008;9(1):47-59.
39. Chen HC, Kanai M, Inoue-Yamauchi A, Tu HC, Huang Y, Ren D, Kim H, Takeda S, Reyna DE, Chan PM and others. An interconnected hierarchical model of cell death regulation by the BCL-2 family. Nat Cell Biol 2015;17(10):1270-81.
40. Gross A, Katz SG. Non-apoptotic functions of BCL-2 family proteins. Cell Death & Differentiation 2017;24(8):1348-1358.
41. Hinds MG, Lackmann M, Skea GL, Harrison PJ, Huang DC, Day CL. The structure of Bcl-w reveals a role for the C-terminal residues in modulating biological activity. EMBO J 2003;22(7):1497-1507.
42. Yao Y, Fujimoto LM, Hirshman N, Bobkov AA, Antignani A, Youle RJ, Marassi FM. Conformation of BCL-XL upon Membrane Integration. J Mol Biol 2015;427(13):2262-70.
43. Suzuki M, Youle RJ, Tjandra N. Structure of Bax: coregulation of dimer formation and intracellular localization. Cell 2000;103(4):645-54.

44. Day CL, Chen L, Richardson SJ, Harrison PJ, Huang DC, Hinds MG. Solution structure of prosurvival Mcl-1 and characterization of its binding by proapoptotic BH3-only ligands. J Biol Chem 2005;280(6):4738-44.
45. Moldoveanu T, Follis AV, Kriwacki RW, Green DR. Many players in BCL-2 family affairs. Trends Biochem Sci 2014;39(3):101-11.
46. Dutta S, Gulla S, Chen TS, Fire E, Grant RA, Keating AE. Determinants of BH3 binding specificity for Mcl-1 versus Bcl-xL. J Mol Biol 2010;398(5):747-62.
47. Chen L, Willis SN, Wei A, Smith BJ, Fletcher JI, Hinds MG, Colman PM, Day CL, Adams JM, Huang DC. Differential targeting of prosurvival Bcl-2 proteins by their BH3-only ligands allows complementary apoptotic function. Mol Cell 2005;17(3):393-403.
48. Petros AM, Olejniczak ET, Fesik SW. Structural biology of the Bcl-2 family of proteins. Biochim Biophys Acta 2004;1644(2-3):83-94.
49. Czabotar PE, Lee EF, Thompson GV, Wardak AZ, Fairlie WD, Colman PM. Mutation to Bax beyond the BH3 domain disrupts interactions with pro-survival proteins and promotes apoptosis. J Biol Chem 2011;286(9):7123-31.
50. Letai A, Bassik MC, Walensky LD, Sorcinelli MD, Weiler S, Korsmeyer SJ. Distinct BH3 domains either sensitize or activate mitochondrial apoptosis, serving as prototype cancer therapeutics. Cancer Cell 2002;2(3):183-92.
51. Kuwana T, Bouchier-Hayes L, Chipuk JE, Bonzon C, Sullivan BA, Green DR, Newmeyer DD. BH3 domains of BH3-only proteins differentially regulate Bax-mediated mitochondrial membrane permeabilization both directly and indirectly. Mol Cell 2005;17(4):525-35.
52. Garcia-Saez AJ, Ries J, Orzaez M, Perez-Paya E, Schwille P. Membrane promotes tBID interaction with BCL(XL). Nat Struct Mol Biol 2009;16(11):1178-85.
53. Leber B, Lin J, Andrews DW. Embedded together: the life and death consequences of interaction of the Bcl-2 family with membranes. Apoptosis 2007;12(5):897-911.
54. Shamas-Din A, Kale J, Leber B, Andrews DW. Mechanisms of action of Bcl-2 family proteins. Cold Spring Harb Perspect Biol 2013;5(4):a008714.
55. Llambi F, Moldoveanu T, Tait SW, Bouchier-Hayes L, Temirov J, McCormick LL, Dillon CP, Green DR. A unified model of mammalian BCL-2 protein family interactions at the mitochondria. Mol Cell 2011;44(4):517-31.
56. Chipuk JE, McStay GP, Bharti A, Kuwana T, Clarke CJ, Siskind LJ, Obeid LM, Green DR. Sphingolipid metabolism cooperates with BAK and BAX to promote the mitochondrial pathway of apoptosis. Cell 2012;148(5):988-1000.
57. Basanez G, Soane L, Hardwick JM. A new view of the lethal apoptotic pore. PLoS Biol 2012;10(9):e1001399.
58. Andreu-Fernández V, Sancho M, Genovés A, Lucendo E, Todt F, Lauterwasser J, Funk K, Jahreis G, Pérez-Payá E, Mingarro I and others. Bax transmembrane domain interacts with prosurvival Bcl-2 proteins in biological membranes. Proc Natl Acad Sci U S A 2017;114(2):310-315.
59. Popgeorgiev N, Jabbour L, Gillet G. Subcellular Localization and Dynamics of the Bcl-2 Family of Proteins. Front Cell Dev Biol 2018;6:13.
60. Hausmann G, O'Reilly LA, van Driel R, Beaumont JG, Strasser A, Adams JM, Huang DC. Pro-Apoptotic Apoptosis Protease–Activating Factor 1 (Apaf-1) Has a Cytoplasmic Localization Distinct from Bcl-2 or Bcl-XL. J Cell Biol 2000; 149(3): 623-634.
61. Akao Y, Otsuki Y, Kataoka S, Ito Y, Tsujimoto Y. Multiple subcellular localization of bcl-2: detection in nuclear outer membrane, endoplasmic reticulum membrane, and mitochondrial membranes. Cancer Res 1994;54(9):2468-71.
62. Nijhawan D, Fang M, Traer E, Zhong Q, Gao W, Du F, Wang X. Elimination of Mcl-1 is required for the initiation of apoptosis following ultraviolet irradiation. Genes Dev 2003;17(12):1475-86.

63. Hsu YT, Wolter KG, Youle RJ. Cytosol-to-membrane redistribution of Bax and Bcl-XL during apoptosis. Proc Natl Acad Sci U S A 1997;94(8):3668-3672.
64. Wilson-Annan J, O'Reilly LA, Crawford SA, Hausmann G, Beaumont JG, Parma LP, Chen L, Lackmann M, Lithgow T, Hinds MG and others. Proapoptotic BH3-only proteins trigger membrane integration of prosurvival Bcl-w and neutralize its activity. J Cell Biol 2003;162(5):877-87.
65. Yang T, Kozopas KM, Craig RW. The intracellular distribution and pattern of expression of Mcl-1 overlap with, but are not identical to, those of Bcl-2. J Cell Biol 1995;128(6):1173-1184.
66. Huang CR, Yang-Yen HF. The fast-mobility isoform of mouse Mcl-1 is a mitochondrial matrix-localized protein with attenuated anti-apoptotic activity. FEBS Lett 2010;584(15):3323-30.
67. Perciavalle RM, Stewart DP, Koss B, Lynch J, Milasta S, Bathina M, Temirov J, Cleland MM, Pelletier S, Schuetz JD and others. Anti-apoptotic MCL-1 localizes to the mitochondrial matrix and couples mitochondrial fusion to respiration. Nat Cell Biol 2012;14(6):575-83.
68. Nakajima W, Hicks MA, Tanaka N, Krystal GW, Harada H. Noxa determines localization and stability of MCL-1 and consequently ABT-737 sensitivity in small cell lung cancer. Cell Death Dis 2014;5:e1052.
69. Liu H, Peng HW, Cheng YS, Yuan HS, Yang-Yen HF. Stabilization and enhancement of the antiapoptotic activity of mcl-1 by TCTP. Mol Cell Biol 2005;25(8):3117-26.
70. Kuwana T, King LE, Cosentino K, Suess J, Garcia-Saez AJ, Gilmore AP, Newmeyer DD. Mitochondrial residence of the apoptosis inducer BAX is more important than BAX oligomerization in promoting membrane permeabilization. J Biol Chem 2020;295(6):1623-1636.
71. Wolter KG, Hsu YT, Smith CL, Nechushtan A, Xi XG, Youle RJ. Movement of Bax from the cytosol to mitochondria during apoptosis. J Cell Biol 1997;139(5):1281-92.
72. Griffiths GJ, Dubrez L, Morgan CP, Jones NA, Whitehouse J, Corfe BM, Dive C, Hickman JA. Cell damage-induced conformational changes of the pro-apoptotic protein Bak in vivo precede the onset of apoptosis. J Cell Biol 1999;144(5):903-14.
73. Zong WX, Li C, Hatzivassiliou G, Lindsten T, Yu QC, Yuan J, Thompson CB. Bax and Bak can localize to the endoplasmic reticulum to initiate apoptosis. J Cell Biol 2003;162(1):59-69.
74. Echeverry N, Bachmann D, Ke F, Strasser A, Simon HU, Kaufmann T. Intracellular localization of the BCL-2 family member BOK and functional implications. Cell Death Differ 2013;20(6):785-99.
75. Schulman JJ, Wright FA, Han X, Zluhan EJ, Szczesniak LM, Wojcikiewicz RJ. The Stability and Expression Level of Bok Are Governed by Binding to Inositol 1,4,5-Trisphosphate Receptors. J Biol Chem 2016;291(22):11820-8.
76. Llambi F, Wang YM, Victor B, Yang M, Schneider DM, Gingras S, Parsons MJ, Zheng JH, Brown SA, Pelletier S and others. BOK Is a Non-canonical BCL-2 Family Effector of Apoptosis Regulated by ER-Associated Degradation. Cell 2016;165(2):421-33.
77. Lei K, Davis RJ. JNK phosphorylation of Bim-related members of the Bcl2 family induces Bax-dependent apoptosis. Proc Natl Acad Sci U S A 2003;100(5):2432-7.
78. Shibata M, Hattori H, Sasaki T, Gotoh J, Hamada J, Fukuuchi Y. Temporal profiles of the subcellular localization of Bim, a BH3-only protein, during middle cerebral artery occlusion in mice. J Cereb Blood Flow Metab 2002;22(7):810-20.
79. Day CL, Puthalakath H, Skea G, Strasser A, Barsukov I, Lian LY, Huang DC, Hinds MG. Localization of dynein light chains 1 and 2 and their pro-apoptotic ligands. Biochem J 2004;377(Pt 3):597-605.
80. Kim JY, So KJ, Lee S, Park JH. Bcl-rambo induces apoptosis via interaction with the adenine nucleotide translocator. FEBS Lett 2012;586(19):3142-9.

81. Nakano K, Vousden KH. PUMA, a novel proapoptotic gene, is induced by p53. Mol Cell 2001;7(3):683-94.
82. Ambroise G, Portier A, Roders N, Arnoult D, Vazquez A. Subcellular localization of PUMA regulates its pro-apoptotic activity in Burkitt's lymphoma B cells. Oncotarget 2015;6(35):38181-94.
83. Oda E, Ohki R, Murasawa H, Nemoto J, Shibue T, Yamashita T, Tokino T, Taniguchi T, Tanaka N. Noxa, a BH3-only member of the Bcl-2 family and candidate mediator of p53-induced apoptosis. Science 2000;288(5468):1053-8.
84. Lowman XH, McDonnell MA, Kosloske A, Odumade OA, Jenness C, Karim CB, Jemmerson R, Kelekar A. The proapoptotic function of Noxa in human leukemia cells is regulated by the kinase Cdk5 and by glucose. Mol Cell 2010;40(5):823-33.
85. Hekman M, Albert S, Galmiche A, Rennefahrt UE, Fueller J, Fischer A, Puehringer D, Wiese S, Rapp UR. Reversible membrane interaction of BAD requires two C-terminal lipid binding domains in conjunction with 14-3-3 protein binding. J Biol Chem 2006;281(25):17321-36.
86. Harada H, Becknell B, Wilm M, Mann M, Huang LJ, Taylor SS, Scott JD, Korsmeyer SJ. Phosphorylation and inactivation of BAD by mitochondria-anchored protein kinase A. Mol Cell 1999;3(4):413-22.
87. Lutter M, Perkins GA, Wang X. The pro-apoptotic Bcl-2 family member tBid localizes to mitochondrial contact sites. BMC Cell Biol 2001;2:22.
88. Germain M, Mathai JP, Shore GC. BH-3-only BIK functions at the endoplasmic reticulum to stimulate cytochrome c release from mitochondria. J Biol Chem 2002;277(20):18053-60.
89. Pattingre S, Tassa A, Qu X, Garuti R, Liang XH, Mizushima N, Packer M, Schneider MD, Levine B. Bcl-2 antiapoptotic proteins inhibit Beclin 1-dependent autophagy. Cell 2005;122(6):927-39.
90. Janiak F, Leber B, Andrews DW. Assembly of Bcl-2 into microsomal and outer mitochondrial membranes. J Biol Chem 1994;269(13):9842-9.
91. Todt F, Cakir Z, Reichenbach F, Youle RJ, Edlich F. The C-terminal helix of Bcl-x(L) mediates Bax retrotranslocation from the mitochondria. Cell Death Differ 2013;20(2):333-42.
92. Kim H, Tu HC, Ren D, Takeuchi O, Jeffers JR, Zambetti GP, Hsieh JJ, Cheng EH. Stepwise activation of BAX and BAK by tBID, BIM, and PUMA initiates mitochondrial apoptosis. Mol Cell 2009;36(3):487-99.
93. Motz C, Martin H, Krimmer T, Rassow J. Bcl-2 and porin follow different pathways of TOM-dependent insertion into the mitochondrial outer membrane. J Mol Biol 2002;323(4):729-38.
94. Kuwana T, Mackey MR, Perkins G, Ellisman MH, Latterich M, Schneiter R, Green DR, Newmeyer DD. Bid, Bax, and lipids cooperate to form supramolecular openings in the outer mitochondrial membrane. Cell 2002;111(3):331-42.
95. Lucken-Ardjomande S, Montessuit S, Martinou JC. Bax activation and stress-induced apoptosis delayed by the accumulation of cholesterol in mitochondrial membranes. Cell Death Differ 2008;15(3):484-93.
96. Horie C, Suzuki H, Sakaguchi M, Mihara K. Characterization of signal that directs C-tail-anchored proteins to mammalian mitochondrial outer membrane. Mol Biol Cell 2002;13(5):1615-25.
97. Lindsay J, Esposti MD, Gilmore AP. Bcl-2 proteins and mitochondria--specificity in membrane targeting for death. Biochim Biophys Acta 2011;1813(4):532-9.
98. Jeong SY, Gaume B, Lee YJ, Hsu YT, Ryu SW, Yoon SH, Youle RJ. Bcl-xL sequesters its C-terminal membrane anchor in soluble, cytosolic homodimers. EMBO J 2004;23(10):2146-2155.
99. Zheng JY, Tsai YC, Kadimcherla P, Zhang R, Shi J, Oyler GA, Boustany NN. The C-Terminal Transmembrane Domain of Bcl-xL Mediates Changes in Mitochondrial Morphology. Biophys J 2008; 94(1):286-297.

100. Pecot J, Maillet L, Le Pen J, Vuillier C, Trecesson SC, Fetiveau A, Sarosiek KA, Bock FJ, Braun F, Letai A and others. Tight Sequestration of BH3 Proteins by BCL-xL at Subcellular Membranes Contributes to Apoptotic Resistance. Cell Rep 2016;17(12):3347-3358.
101. Mérino D, Khaw SL, Glaser SP, Anderson DJ, Belmont LD, Wong C, Yue P, Robati M, Phipson B, Fairlie WD and others. Bcl-2, Bcl-xL, and Bcl-w are not equivalent targets of ABT-737 and navitoclax (ABT-263) in lymphoid and leukemic cells. Blood 2012;119(24): 5807–5816.
102. Dixon EP, Stephenson DT, Clemens JA, Little SP. Bcl-Xshort is elevated following severe global ischemia in rat brains. Brain Res 1997;776(1-2):222-9.
103. Heermeier K, Benedict M, Li M, Furth P, Nunez G, Hennighausen L. Bax and Bcl-xs are induced at the onset of apoptosis in involuting mammary epithelial cells. Mech Dev 1996;56(1-2):197-207.
104. Wu L, Mao C, Ming X. Modulation of Bcl-x Alternative Splicing Induces Apoptosis of Human Hepatic Stellate Cells. Biomed Res Int 2016; 2016:7478650.
105. Hossini AM, Geilen CC, Fecker LF, Daniel PT, Eberle J. A novel Bcl-x splice product, Bcl-xAK, triggers apoptosis in human melanoma cells without BH3 domain. Oncogene 2006;25(15):2160-9.
106. Boise LH, Gonzalez-Garcia M, Postema CE, Ding L, Lindsten T, Turka LA, Mao X, Nunez G, Thompson CB. bcl-x, a bcl-2-related gene that functions as a dominant regulator of apoptotic cell death. Cell 1993;74(4):597-608.
107. Lindenboim L, Borner C, Stein R. Bcl-x(S) can form homodimers and heterodimers and its apoptotic activity requires localization of Bcl-x(S) to the mitochondria and its BH3 and loop domains. Cell Death Differ 2001;8(9):933-42.
108. Plötz M, Hossini AM, Gillissen B, Daniel PT, Stockfleth E, Eberle J. Mutual Regulation of Bcl-2 Proteins Independent of the BH3 Domain as Shown by the BH3-Lacking Protein Bcl-xAK. PLoS One 2012;7(4):e34549.
109. Brien G, Debaud AL, Robert X, Oliver L, Trescol-Biemont MC, Cauquil N, Geneste O, Aghajari N, Vallette FM, Haser R and others. C-terminal Residues Regulate Localization and Function of the Antiapoptotic Protein Bfl-1*. J Biol Chem 2009; 284(44):30257-30263.
110. Akgul C, Moulding DA, White MR, Edwards SW. In vivo localisation and stability of human Mcl-1 using green fluorescent protein (GFP) fusion proteins. FEBS Lett 2000;478(1-2):72-6.
111. Fujise K, Zhang D, Liu J, Yeh ET. Regulation of apoptosis and cell cycle progression by MCL1. Differential role of proliferating cell nuclear antigen. J Biol Chem 2000;275(50):39458-65.
112. Michels J, O'Neill JW, Dallman CL, Mouzakiti A, Habens F, Brimmell M, Zhang KY, Craig RW, Marcusson EG, Johnson PW and others. Mcl-1 is required for Akata6 B-lymphoma cell survival and is converted to a cell death molecule by efficient caspase-mediated cleavage. Oncogene 2004;23(28):4818-27.
113. Ménoret E, Gomez-Bougie P, Surget S, Trichet V, Oliver L, Pellat-Deceunynck C, Amiot M. Mcl-1(128-350) fragment induces apoptosis through direct interaction with Bax. FEBS Lett 2010;584(3):487-92.
114. Weng C, Li Y, Xu D, Shi Y, Tang H. Specific cleavage of Mcl-1 by caspase-3 in tumor necrosis factor-related apoptosis-inducing ligand (TRAIL)-induced apoptosis in Jurkat leukemia T cells. J Biol Chem 2005;280(11):10491-500.
115. Menoret E, Gomez-Bougie P, Geffroy-Luseau A, Daniels S, Moreau P, Le Gouill S, Harousseau JL, Bataille R, Amiot M, Pellat-Deceunynck C. Mcl-1L cleavage is involved in TRAIL-R1- and TRAIL-R2-mediated apoptosis induced by HGS-ETR1 and HGS-ETR2 human mAbs in myeloma cells. Blood 2006;108(4):1346-52.
116. Kim JH, Sim SH, Ha HJ, Ko JJ, Lee K, Bae J. MCL-1ES, a novel variant of MCL-1, associates with MCL-1L and induces mitochondrial cell death. FEBS Lett 2009;583(17):2758-64.

117. Stehle D, Grimm M, Einsele-Scholz S, Ladwig F, Johänning J, Fischer G, Gillissen B, Schulze-Osthoff K, Essmann F. Contribution of BH3-domain and Transmembrane-domain to the Activity and Interaction of the Pore-forming Bcl-2 Proteins Bok, Bak, and Bax. Sci Rep 2018;8(1):12434.
118. Denisov AY, Madiraju MS, Chen G, Khadir A, Beauparlant P, Attardo G, Shore GC, Gehring K. Solution structure of human BCL-w: modulation of ligand binding by the C-terminal helix. J Biol Chem 2003;278(23):21124-8.
119. Schinzel A, Kaufmann T, Schuler M, Martinalbo J, Grubb D, Borner C. Conformational control of Bax localization and apoptotic activity by Pro168. J Cell Biol 2004;164(7):1021-32.
120. Nechushtan A, Smith CL, Hsu YT, Youle RJ. Conformation of the Bax C-terminus regulates subcellular location and cell death. EMBO J 1999;18(9):2330-41.
121. Cartron PF, Arokium H, Oliver L, Meflah K, Manon S, Vallette FM. Distinct domains control the addressing and the insertion of Bax into mitochondria. J Biol Chem 2005;280(11):10587-98.
122. Simonyan L, Legiot A, Lascu I, Durand G, Giraud MF, Gonzalez C, Manon S. The substitution of Proline 168 favors Bax oligomerization and stimulates its interaction with LUVs and mitochondria. Biochim Biophys Acta Biomembr 2017;1859(6):1144-1155.
123. ABT-199 shows effectiveness in CLL. Cancer Discov 2014;4(9):OF7.
124. Bleicken S, Jeschke G, Stegmueller C, Salvador-Gallego R, Garcia-Saez AJ, Bordignon E. Structural model of active Bax at the membrane. Mol Cell 2014;56(4):496-505.
125. Zhang Z, Subramaniam S, Kale J, Liao C, Huang B, Brahmbhatt H, Condon SG, Lapolla SM, Hays FA, Ding J and others. BH3-in-groove dimerization initiates and helix 9 dimerization expands Bax pore assembly in membranes. EMBO J 2016;35(2):208-36.
126. Arokium H, Camougrand N, Vallette FM, Manon S. Studies of the interaction of substituted mutants of BAX with yeast mitochondria reveal that the C-terminal hydrophobic alpha-helix is a second ART sequence and plays a role in the interaction with anti-apoptotic BCL-xL. J Biol Chem 2004;279(50):52566-73.
127. Martinez-Senac Mdel M, Corbalan-Garcia S, Gomez-Fernandez JC. The structure of the C-terminal domain of the pro-apoptotic protein Bak and its interaction with model membranes. Biophys J 2002;82(1 Pt 1):233-243.
128. Iyer S, Bell F, Westphal D, Anwari K, Gulbis J, Smith BJ, Dewson G, Kluck RM. Bak apoptotic pores involve a flexible C-terminal region and juxtaposition of the C-terminal transmembrane domains. Cell Death Differ 2015;22(10):1665-75.
129. Todt F, Cakir Z, Reichenbach F, Emschermann F, Lauterwasser J, Kaiser A, Ichim G, Tait SW, Frank S, Langer HF and others. Differential retrotranslocation of mitochondrial Bax and Bak. EMBO J 2015;34(1):67-80.
130. Lazarou M, Stojanovski D, Frazier AE, Kotevski A, Dewson G, Craigen WJ, Kluck RM, Vaux DL, Ryan MT. Inhibition of Bak activation by VDAC2 is dependent on the Bak transmembrane anchor. J Biol Chem 2010;285(47):36876-83.
131. Hanahan D, Weinberg RA. The hallmarks of cancer. Cell 2000;100(1):57-70.
132. Vaux DL, Cory S, Adams JM. Bcl-2 gene promotes haemopoietic cell survival and cooperates with c-myc to immortalize pre-B cells. Nature 1988;335(6189):440-2.
133. Watanabe J, Kushihata F, Honda K, Mominoki K, Matsuda S, Kobayashi N. Bcl-xL overexpression in human hepatocellular carcinoma. Int J Oncol 2002;21(3):515-9.
134. Castilla C, Congregado B, Chinchon D, Torrubia FJ, Japon MA, Saez C. Bcl-xL is overexpressed in hormone-resistant prostate cancer and promotes survival of LNCaP cells via interaction with proapoptotic Bak. Endocrinology 2006;147(10):4960-7.
135. Schott AF, Apel IJ, Nunez G, Clarke MF. Bcl-XL protects cancer cells from p53-mediated apoptosis. Oncogene 1995;11(7):1389-94.

136. Del Bufalo D, Biroccio A, Leonetti C, Zupi G. Bcl-2 overexpression enhances the metastatic potential of a human breast cancer line. Faseb J 1997;11(12):947-53.
137. Raha P, Thomas S, Thurn KT, Park J, Munster PN. Combined histone deacetylase inhibition and tamoxifen induces apoptosis in tamoxifen-resistant breast cancer models, by reversing Bcl-2 overexpression. Breast Cancer Res 2015;17:26.
138. Olejniczak ET, Van Sant C, Anderson MG, Wang G, Tahir SK, Sauter G, Lesniewski R, Semizarov D. Integrative genomic analysis of small-cell lung carcinoma reveals correlates of sensitivity to bcl-2 antagonists and uncovers novel chromosomal gains. Mol Cancer Res 2007;5(4):331-9.
139. Del Gaizo Moore V, Brown JR, Certo M, Love TM, Novina CD, Letai A. Chronic lymphocytic leukemia requires BCL2 to sequester prodeath BIM, explaining sensitivity to BCL2 antagonist ABT-737. J Clin Invest 2007;117(1):112-21.
140. Montero J, Gstalder C, Kim DJ, Sadowicz D, Miles W, Manos M, Cidado JR, Paul Secrist J, Tron AE, Flaherty K and others. Destabilization of NOXA mRNA as a common resistance mechanism to targeted therapies. Nat Commun 2019;10(1):5157.
141. Gross A, Katz SG. Non-apoptotic functions of BCL-2 family proteins. Cell Death Differ 2017;24(8):1348-1358.
142. Um HD. Bcl-2 family proteins as regulators of cancer cell invasion and metastasis: a review focusing on mitochondrial respiration and reactive oxygen species. Oncotarget 2016;7(5):5193-203.
143. Singh L, Pushker N, Saini N, Sen S, Sharma A, Bakhshi S, Chawla B, Kashyap S. Expression of pro-apoptotic Bax and anti-apoptotic Bcl-2 proteins in human retinoblastoma. Clin Exp Ophthalmol 2015;43(3):259-67.
144. Fouqué A, Lepvrier E, Debure L, Gouriou Y, Malleter M, Delcroix V, Ovize M, Ducret T, Li C, Hammadi M and others. The apoptotic members CD95, BclxL, and Bcl-2 cooperate to promote cell migration by inducing Ca2+ flux from the endoplasmic reticulum to mitochondria. Cell Death Differ 2016; 23(10):1702-1716.
145. Lee HW, Lee SS, Lee SJ, Um HD. Bcl-w is expressed in a majority of infiltrative gastric adenocarcinomas and suppresses the cancer cell death by blocking stress-activated protein kinase/c-Jun NH2-terminal kinase activation. Cancer Res 2003;63(5):1093-100.
146. Lee WS, Woo EY, Kwon J, Park MJ, Lee JS, Han YH, Bae IH. Bcl-w Enhances Mesenchymal Changes and Invasiveness of Glioblastoma Cells by Inducing Nuclear Accumulation of beta-Catenin. PLoS One 2013;8(6):e68030.
147. Cheng EH, Wei MC, Weiler S, Flavell RA, Mak TW, Lindsten T, Korsmeyer SJ. BCL-2, BCL-X(L) sequester BH3 domain-only molecules preventing BAX- and BAK-mediated mitochondrial apoptosis. Mol Cell 2001;8(3):705-11.
148. Garner TP, Lopez A, Reyna DE, Spitz AZ, Gavathiotis E. Progress in targeting the BCL-2 family of proteins. Curr Opin Chem Biol 2017;39:133-142.
149. Oltersdorf T, Elmore SW, Shoemaker AR, Armstrong RC, Augeri DJ, Belli BA, Bruncko M, Deckwerth TL, Dinges J, Hajduk PJ and others. An inhibitor of Bcl-2 family proteins induces regression of solid tumours. Nature 2005;435(7042):677-81.
150. Tse C, Shoemaker AR, Adickes J, Anderson MG, Chen J, Jin S, Johnson EF, Marsh KC, Mitten MJ, Nimmer P and others. ABT-263: a potent and orally bioavailable Bcl-2 family inhibitor. Cancer Res 2008;68(9):3421-8.
151. Wilson WH, O'Connor OA, Czuczman MS, LaCasce AS, Gerecitano JF, Leonard JP, Tulpule A, Dunleavy K, Xiong H, Chiu YL and others. Navitoclax, a targeted high-affinity inhibitor of BCL-2, in lymphoid malignancies: a phase 1 dose-escalation study of safety, pharmacokinetics, pharmacodynamics, and antitumour activity. Lancet Oncol 2010;11(12):1149-59.
152. Gandhi L, Camidge DR, Ribeiro de Oliveira M, Bonomi P, Gandara D, Khaira D, Hann CL, McKeegan EM, Litvinovich E, Hemken PM and others. Phase I study of Navitoclax (ABT-

263), a novel Bcl-2 family inhibitor, in patients with small-cell lung cancer and other solid tumors. J Clin Oncol 2011;29(7):909-16.
153. Tolcher AW, LoRusso P, Arzt J, Busman TA, Lian G, Rudersdorf NS, Vanderwal CA, Waring JF, Yang J, Holen KD and others. Safety, efficacy, and pharmacokinetics of navitoclax (ABT-263) in combination with irinotecan: results of an open-label, phase 1 study. Cancer Chemother Pharmacol 2015;76(5):1041-9.
154. Tolcher AW, LoRusso P, Arzt J, Busman TA, Lian G, Rudersdorf NS, Vanderwal CA, Kirschbrown W, Holen KD, Rosen LS. Safety, efficacy, and pharmacokinetics of navitoclax (ABT-263) in combination with erlotinib in patients with advanced solid tumors. Cancer Chemother Pharmacol 2015;76(5):1025-32.
155. Roberts AW, Advani RH, Kahl BS, Persky D, Sweetenham JW, Carney DA, Yang J, Busman TB, Enschede SH, Humerickhouse RA and others. Phase 1 study of the safety, pharmacokinetics, and antitumour activity of the BCL2 inhibitor navitoclax in combination with rituximab in patients with relapsed or refractory CD20+ lymphoid malignancies. Br J Haematol 2015;170(5):669-78.
156. Kaefer A, Yang J, Noertersheuser P, Mensing S, Humerickhouse R, Awni W, Xiong H. Mechanism-based pharmacokinetic/pharmacodynamic meta-analysis of navitoclax (ABT-263) induced thrombocytopenia. Cancer Chemother Pharmacol 2014;74(3):593-602.
157. Schoenwaelder SM, Jarman KE, Gardiner EE, Hua M, Qiao J, White MJ, Josefsson EC, Alwis I, Ono A, Willcox A and others. Bcl-xL-inhibitory BH3 mimetics can induce a transient thrombocytopathy that undermines the hemostatic function of platelets. Blood 2011;118(6):1663-74.
158. Roberts AW, Davids MS, Pagel JM, Kahl BS, Puvvada SD, Gerecitano JF, Kipps TJ, Anderson MA, Brown JR, Gressick L and others. Targeting BCL2 with Venetoclax in Relapsed Chronic Lymphocytic Leukemia. N Engl J Med 2016;374(4):311-22.
159. DiNardo CD, Pratz K, Pullarkat V, Jonas BA, Arellano M, Becker PS, Frankfurt O, Konopleva M, Wei AH, Kantarjian HM and others. Venetoclax combined with decitabine or azacitidine in treatment-naive, elderly patients with acute myeloid leukemia. Blood 2019;133(1):7-17.
160. Vaillant F, Merino D, Lee L, Breslin K, Pal B, Ritchie ME, Smyth GK, Christie M, Phillipson LJ, Burns CJ and others. Targeting BCL-2 with the BH3 mimetic ABT-199 in estrogen receptor-positive breast cancer. Cancer Cell 2013;24(1):120-9.
161. Zelenetz AD, Salles G, Mason KD, Casulo C, Le Gouill S, Sehn LH, Tilly H, Cartron G, Chamuleau MED, Goy A and others. Venetoclax plus R- or G-CHOP in non-Hodgkin lymphoma: results from the CAVALLI phase 1b trial. Blood 2019;133(18):1964-1976.
162. Adams R, Worth CL, Guenther S, Dunkel M, Lehmann R, Preissner R. Binding sites in membrane proteins--diversity, druggability and prospects. Eur J Cell Biol 2012;91(4):326-39.
163. Yin H, Flynn AD. Drugging Membrane Protein Interactions. Annu Rev Biomed Eng 2016;18:51-76.
164. Venkatesan K, Rual JF, Vazquez A, Stelzl U, Lemmens I, Hirozane-Kishikawa T, Hao T, Zenkner M, Xin X, Goh KI and others. An empirical framework for binary interactome mapping. Nat Methods 2009;6(1):83-90.
165. Stumpf MP, Thorne T, de Silva E, Stewart R, An HJ, Lappe M, Wiuf C. Estimating the size of the human interactome. Proc Natl Acad Sci U S A 2008;105(19):6959-64.
166. Goncearenco A, Li M, Simonetti FL, Shoemaker BA, Panchenko AR. Exploring Protein-Protein Interactions as Drug Targets for Anti-cancer Therapy with In Silico Workflows. Methods Mol Biol 2017;1647:221-236.
167. Blundell TL, Burke DF, Chirgadze D, Dhanaraj V, Hyvonen M, Innis CA, Parisini E, Pellegrini L, Sayed M, Sibanda BL. Protein-protein interactions in receptor activation and intracellular signalling. Biol Chem 2000;381(9-10):955-9.

168. Sheng C, Dong G, Miao Z, Zhang W, Wang W. State-of-the-art strategies for targeting protein-protein interactions by small-molecule inhibitors. Chem Soc Rev 2015;44(22):8238-59.
169. Litvinov RI, Nagaswami C, Vilaire G, Shuman H, Bennett JS, Weisel JW. Functional and structural correlations of individual alphaIIbbeta3 molecules. Blood 2004;104(13):3979-85.
170. Kim M, Carman CV, Springer TA. Bidirectional transmembrane signaling by cytoplasmic domain separation in integrins. Science 2003;301(5640):1720-5.
171. Pahuja KB, Nguyen TT, Jaiswal BS, Prabhash K, Thaker TM, Senger K, Chaudhuri S, Kljavin NM, Antony A, Phalke S and others. Actionable Activating Oncogenic ERBB2/HER2 Transmembrane and Juxtamembrane Domain Mutations. Cancer Cell 2018;34(5):792-806.e5.
172. Stern HM. Improving treatment of HER2-positive cancers: opportunities and challenges. Sci Transl Med 2012;4(127):127rv2.
173. Freeman-Cook LL, Dimaio D. Modulation of cell function by small transmembrane proteins modeled on the bovine papillomavirus E5 protein. Oncogene 2005;24(52):7756-62.
174. Freeman-Cook LL, Dixon AM, Frank JB, Xia Y, Ely L, Gerstein M, Engelman DM, DiMaio D. Selection and characterization of small random transmembrane proteins that bind and activate the platelet-derived growth factor beta receptor. J Mol Biol 2004;338(5):907-20.
175. Wang X, Saludes JP, Zhao TX, Csakai A, Fiorini Z, Chavez SA, Li J, Lee GI, Varga K, Yin H. Targeting the lateral interactions of transmembrane domain 5 of Epstein-Barr virus latent membrane protein 1. Biochim Biophys Acta 2012;1818(9):2282-9.
176. Bokoch MP, Jo H, Valcourt JR, Srinivasan Y, Pan AC, Capponi S, Grabe M, Dror RO, Shaw DE, DeGrado WF and others. Entry from the Lipid Bilayer: A Possible Pathway for Inhibition of a Peptide G Protein-Coupled Receptor by a Lipophilic Small Molecule. Biochemistry 2018;57(39):5748-5758.
177. Hawes BE, Zhai Y, Hesk D, Wirth M, Wei H, Chintala M, Seiffert D. In vitro pharmacological characterization of vorapaxar, a novel platelet thrombin receptor antagonist. Eur J Pharmacol 2015;762:221-8.
178. Bai XC, McMullan G, Scheres SH. How cryo-EM is revolutionizing structural biology. Trends Biochem Sci 2015;40(1):49-57.
179. Cheng Y. Membrane protein structural biology in the era of single particle cryo-EM. Curr Opin Struct Biol 2018;52:58-63.
180. Kerppola TK. Bimolecular fluorescence complementation: visualization of molecular interactions in living cells. Methods Cell Biol 2008;85:431-70.
181. Langosch D, Brosig B, Kolmar H, Fritz HJ. Dimerisation of the glycophorin A transmembrane segment in membranes probed with the ToxR transcription activator. J Mol Biol 1996;263(4):525-30.
182. Armstrong CR, Senes A. Screening for transmembrane association in divisome proteins using TOXGREEN, a high-throughput variant of the TOXCAT assay. Biochim Biophys Acta 2016;1858(11):2573-2583.
183. Certo M, Del Gaizo Moore V, Nishino M, Wei G, Korsmeyer S, Armstrong SA, Letai A. Mitochondria primed by death signals determine cellular addiction to antiapoptotic BCL-2 family members. Cancer Cell 2006;9(5):351-65.
184. Oltvai ZN, Milliman CL, Korsmeyer SJ. Bcl-2 heterodimerizes in vivo with a conserved homolog, Bax, that accelerates programmed cell death. Cell 1993;74(4):609-19.
185. Cuconati A, Mukherjee C, Perez D, White E. DNA damage response and MCL-1 destruction initiate apoptosis in adenovirus-infected cells. Genes Dev 2003;17(23):2922-32.
186. Hsu SY, Kaipia A, McGee E, Lomeli M, Hsueh AJ. Bok is a pro-apoptotic Bcl-2 protein with restricted expression in reproductive tissues and heterodimerizes with selective anti-apoptotic Bcl-2 family members. Proc Natl Acad Sci U S A 1997;94(23):12401-6.
187. Yang T, Kozopas KM, Craig RW. The intracellular distribution and pattern of expression of Mcl-1 overlap with, but are not identical to, those of Bcl-2. J Cell Biol 1995;128(6):1173-84.

188. Chao JR, Wang JM, Lee SF, Peng HW, Lin YH, Chou CH, Li JC, Huang HM, Chou CK, Kuo ML and others. mcl-1 is an immediate-early gene activated by the granulocyte-macrophage colony-stimulating factor (GM-CSF) signaling pathway and is one component of the GM-CSF viability response. Mol Cell Biol 1998;18(8):4883-98.
189. Kozopas KM, Yang T, Buchan HL, Zhou P, Craig RW. MCL1, a gene expressed in programmed myeloid cell differentiation, has sequence similarity to BCL2. Proc Natl Acad Sci U S A 1993;90(8):3516-20.
190. Fernandez-Marrero Y, Spinner S, Kaufmann T, Jost PJ. Survival control of malignant lymphocytes by anti-apoptotic MCL-1. Leukemia 2016;30(11):2152-2159.
191. Sieghart W, Losert D, Strommer S, Cejka D, Schmid K, Rasoul-Rockenschaub S, Bodingbauer M, Crevenna R, Monia BP, Peck-Radosavljevic M and others. Mcl-1 overexpression in hepatocellular carcinoma: a potential target for antisense therapy. J Hepatol 2006;44(1):151-7.
192. Lin J, Fu D, Dai Y, Lin J, Xu T. Mcl-1 inhibitor suppresses tumor growth of esophageal squamous cell carcinoma in a mouse model. Oncotarget 2017;8(70):114457-114462.
193. Campbell KJ, Dhayade S, Ferrari N, Sims AH, Johnson E, Mason SM, Dickson A, Ryan KM, Kalna G, Edwards J and others. MCL-1 is a prognostic indicator and drug target in breast cancer. Cell Death Dis 2018;9(2):19.
194. Feng C, Yang F, Wang J. FBXO4 inhibits lung cancer cell survival by targeting Mcl-1 for degradation. Cancer Gene Ther 2017;24(8):342-347.
195. Hird AW, Tron AE. Recent advances in the development of Mcl-1 inhibitors for cancer therapy. Pharmacol Ther 2019;198:59-67.
196. Acoca S, Cui Q, Shore GC, Purisima EO. Molecular dynamics study of small molecule inhibitors of the Bcl-2 family. Proteins 2011;79(9):2624-36.
197. Lama D, Sankararamakrishnan R. Anti-apoptotic Bcl-XL protein in complex with BH3 peptides of pro-apoptotic Bak, Bad, and Bim proteins: comparative molecular dynamics simulations. Proteins 2008;73(2):492-514.
198. Grau B, Javanainen M, Garcia-Murria MJ, Kulig W, Vattulainen I, Mingarro I, Martinez-Gil L. The role of hydrophobic matching on transmembrane helix packing in cells. Cell Stress 2017;1(2):90-106.
199. Nishizawa M, Nishizawa K. Potential of mean force analysis of the self-association of leucine-rich transmembrane alpha-helices: difference between atomistic and coarse-grained simulations. J Chem Phys 2014;141(7):075101.
200. Li PC, Miyashita N, Im W, Ishido S, Sugita Y. Multidimensional umbrella sampling and replica-exchange molecular dynamics simulations for structure prediction of transmembrane helix dimers. J Comput Chem 2014;35(4):300-8.
201. Wassenaar TA, Pluhackova K, Moussatova A, Sengupta D, Marrink SJ, Tieleman DP, Böckmann RA. High-Throughput Simulations of Dimer and Trimer Assembly of Membrane Proteins. The DAFT Approach. J Chem Theory Comput 2015;11(5):2278-91.
202. Lelimousin M, Limongelli V, Sansom MS. Conformational Changes in the Epidermal Growth Factor Receptor: Role of the Transmembrane Domain Investigated by Coarse-Grained MetaDynamics Free Energy Calculations. J Am Chem Soc 2016;138(33):10611-22.
203. Kerppola TK. Bimolecular fluorescence complementation (BiFC) analysis as a probe of protein interactions in living cells. Annu Rev Biophys 2008;37:465-87.
204. Kodama Y, Hu CD. An improved bimolecular fluorescence complementation assay with a high signal-to-noise ratio. Biotechniques 2010;49(5):793-805.
205. Andreu-Fernández V. Characterizing BCL-2 family protein domains in membranes: Insertion, interaction and apoptotic modulation roles. Valencia: University of Valencia; 2015. 297 p.
206. Crowley LC, Christensen ME, Waterhouse NJ. Measuring Mitochondrial Transmembrane Potential by TMRE Staining. Cold Spring Harb Protoc 2016;2016(12).

207. Kabakov AE, Gabai VL. Cell Death and Survival Assays. Methods Mol Biol 2018;1709:107-127.
208. Javanainen M. Universal Method for Embedding Proteins into Complex Lipid Bilayers for Molecular Dynamics Simulations. J Chem Theory Comput 2014;10(6):2577-82.
209. Lee J, Cheng X, Swails JM, Yeom MS, Eastman PK, Lemkul JA, Wei S, Buckner J, Jeong JC, Qi Y and others. CHARMM-GUI Input Generator for NAMD, GROMACS, AMBER, OpenMM, and CHARMM/OpenMM Simulations Using the CHARMM36 Additive Force Field. J Chem Theory Comput 2016;12(1):405-13.
210. Alam MS. Proximity Ligation Assay (PLA). Curr Protoc Immunol 2018;123(1):e58.
211. Garcia-Saez AJ, Coraiola M, Dalla Serra M, Mingarro I, Menestrina G, Salgado J. Peptides derived from apoptotic Bax and Bid reproduce the poration activity of the parent full-length proteins. Biophys J 2005;88(6):3976-90.
212. Javadpour MM, Eilers M, Groesbeek M, Smith SO. Helix packing in polytopic membrane proteins: role of glycine in transmembrane helix association. Biophys J 1999;77(3):1609-18.
213. Teese MG, Langosch D. Role of GxxxG Motifs in Transmembrane Domain Interactions. Biochemistry 2015;54(33):5125-35.
214. Duarte JM, Biyani N, Baskaran K, Capitani G. An analysis of oligomerization interfaces in transmembrane proteins. BMC Struct Biol 2013;13:21.
215. Schinzel A, Kaufmann T, Borner C. Bcl-2 family members: intracellular targeting, membrane-insertion, and changes in subcellular localization. Biochimica et Biophysica Acta (BBA) - Molecular Cell Research 2004;1644(2-3):95-105.
216. Suhaili SH, Karimian H, Stellato M, Lee TH, Aguilar MI. Mitochondrial outer membrane permeabilization: a focus on the role of mitochondrial membrane structural organization. Biophys Rev 2017;9(4):443-457.
217. Gotoh T, Terada K, Oyadomari S, Mori M. hsp70-DnaJ chaperone pair prevents nitric oxide- and CHOP-induced apoptosis by inhibiting translocation of Bax to mitochondria. Cell Death Differ 2004;11(4):390-402.
218. Pan L, Fu TM, Zhao W, Zhao L, Chen W, Qiu C, Liu W, Liu Z, Piai A, Fu Q and others. Higher-Order Clustering of the Transmembrane Anchor of DR5 Drives Signaling. Cell 2019;176(6):1477-1489 e14.
219. Kwon B, Lee M, Waring AJ, Hong M. Oligomeric Structure and Three-Dimensional Fold of the HIV gp41 Membrane-Proximal External Region and Transmembrane Domain in Phospholipid Bilayers. J Am Chem Soc 2018;140(26):8246-8259.
220. Green DR. The Coming Decade of Cell Death Research: Five Riddles. Cell 2019;177(5):1094-1107.
221. Fernandez-Marrero Y, Bleicken S, Das KK, Bachmann D, Kaufmann T, Garcia-Saez AJ. The membrane activity of BOK involves formation of large, stable toroidal pores and is promoted by cBID. FEBS J 2017;284(5):711-724.
222. Westphal D, Dewson G, Czabotar PE, Kluck RM. Molecular biology of Bax and Bak activation and action. Biochim Biophys Acta 2011;1813(4):521-31.
223. Kazi A, Sun J, Doi K, Sung SS, Takahashi Y, Yin H, Rodriguez JM, Becerril J, Berndt N, Hamilton AD and others. The BH3 alpha-helical mimic BH3-M6 disrupts Bcl-X(L), Bcl-2, and MCL-1 protein-protein interactions with Bax, Bak, Bad, or Bim and induces apoptosis in a Bax- and Bim-dependent manner. J Biol Chem 2011;286(11):9382-92.
224. Ku B, Liang C, Jung JU, Oh BH. Evidence that inhibition of BAX activation by BCL-2 involves its tight and preferential interaction with the BH3 domain of BAX. Cell Res 2011;21(4):627-41.
225. Senichkin VV, Streletskaia AY, Zhivotovsky B, Kopeina GS. Molecular Comprehension of Mcl-1: From Gene Structure to Cancer Therapy. Trends Cell Biol 2019;29(7):549-562.

226. Hockings C, Alsop AE, Fennell SC, Lee EF, Fairlie WD, Dewson G, Kluck RM. Mcl-1 and Bcl-xL sequestration of Bak confers differential resistance to BH3-only proteins. Cell Death Differ 2018;25(4):721-734.
227. Zheng JH, Grace CR, Guibao CD, McNamara DE, Llambi F, Wang YM, Chen T, Moldoveanu T. Intrinsic Instability of BOK Enables Membrane Permeabilization in Apoptosis. Cell Rep 2018;23(7):2083-2094.e6.
228. Honrath B, Metz I, Bendridi N, Rieusset J, Culmsee C, Dolga AM. Glucose-regulated protein 75 determines ER–mitochondrial coupling and sensitivity to oxidative stress in neuronal cells. Cell Death Discov 2017;3:17076.
229. Xu L, Wang X, Tong C. Endoplasmic Reticulum-Mitochondria Contact Sites and Neurodegeneration. Front Cell Dev Biol. 2020;8:428.
230. Tate JG, Bamford S, Jubb HC, et al. COSMIC: the Catalogue Of Somatic Mutations In Cancer. Nucleic Acids Res 2019;47(D1):D941-D947.
231. Van Allen EM, Wagle N, Sucker A, Treacy DJ, Johannessen CM, Goetz EM, Place CS, Taylor-Weiner A, Whittaker S, Kryukov GV and others. The genetic landscape of clinical resistance to RAF inhibition in metastatic melanoma. Cancer Discov 2014;4(1):94-109.
232. Imielinski M, Berger AH, Hammerman PS, Hernandez B, Pugh TJ, Hodis E, Cho J, Suh J, Capelletti M, Sivachenko A and others. Mapping the hallmarks of lung adenocarcinoma with massively parallel sequencing. Cell 2012;150(6):1107-20.
233. Shihab HA, Rogers MF, Gough J, et al. An integrative approach to predicting the functional effects of non-coding and coding sequence variation. Bioinformatics 2015;31(10):1536-1543.
234. Ausman J, Abbade J, Ermini L, Farrell A, Tagliaferro A, Post M, Caniggia I. Ceramide-induced BOK promotes mitochondrial fission in preeclampsia. Cell Death Dis 2018;9(3):298.
235. Williams A, Hayashi T, Wolozny D, Yin B, Su TC, Betenbaugh MJ, Su TP. The non-apoptotic action of Bcl-xL: regulating Ca(2+) signaling and bioenergetics at the ER-mitochondrion interface. J Bioenerg Biomembr 2016;48(3):211-25.
236. Herrant M, Jacquel A, Marchetti S, Belhacene N, Colosetti P, Luciano F, Auberger P. Cleavage of Mcl-1 by caspases impaired its ability to counteract Bim-induced apoptosis. Oncogene 2004;23(47):7863-73.
237. Szlavik Z, Ondi L, Csekei M, Paczal A, Szabo ZB, Radics G, Murray J, Davidson J, Chen I, Davis B and others. Structure-Guided Discovery of a Selective Mcl-1 Inhibitor with Cellular Activity. J Med Chem 2019;62(15):6913-6924.
238. Shuang W, Hou L, Zhu Y, Li Q, Hu W. Mcl-1 stabilization confers resistance to taxol in human gastric cancer. Oncotarget 2017;8(47):82981-82990.
239. Lee KM, Giltnane JM, Balko JM, Schwarz LJ, Guerrero-Zotano AL, Hutchinson KE, Nixon MJ, Estrada MV, Sanchez V, Sanders ME and others. MYC and MCL1 Cooperatively Promote Chemotherapy-Resistant Breast Cancer Stem Cells via Regulation of Mitochondrial Oxidative Phosphorylation. Cell Metab 2017;26(4):633-647 e7.
240. Williams MM, Lee L, Hicks DJ, Joly MM, Elion D, Rahman B, McKernan C, Sanchez V, Balko JM, Stricker T and others. Key Survival Factor, Mcl-1, Correlates with Sensitivity to Combined Bcl-2/Bcl-xL Blockade. Mol Cancer Res 2017;15(3):259-268.
241. Caenepeel S, Brown SP, Belmontes B, et al. AMG 176, a Selective MCL1 Inhibitor, Is Effective in Hematologic Cancer Models Alone and in Combination with Established Therapies. Cancer Discov 2018;8(12):1582-1597.
242. Brennan MS, Chang C, Tai L, Lessene G, Strasser A, Dewson G, Kelly GL, Herold MJ. Humanized Mcl-1 Mice Enable Accurate Preclinical Evaluation of MCL-1 Inhibitors Destined for Clinical Use. Blood 2018;132(15):1573-1583.
243. Czabotar PE, Lee EF, van Delft MF, Day CL, Smith BJ, Huang DC, Fairlie WD, Hinds MG, Colman PM. Structural insights into the degradation of Mcl-1 induced by BH3 domains. Proc Natl Acad Sci U S A 2007;104(15):6217-22.

244. Kotschy A, Szlavik Z, Murray J, Davidson J, Maragno AL, Le Toumelin-Braizat G, Chanrion M, Kelly GL, Gong JN, Moujalled DM and others. The MCL1 inhibitor S63845 is tolerable and effective in diverse cancer models. Nature 2016;538(7626):477-482.
245. Merino D, Whittle JR, Vaillant F, Serrano A, Gong JN, Giner G, Maragno AL, Chanrion M, Schneider E, Pal B and others. Synergistic action of the MCL-1 inhibitor S63845 with current therapies in preclinical models of triple-negative and HER2-amplified breast cancer. Sci Transl Med 2017;9(401):eaam7049.
246. Nangia V, Siddiqui FM, Caenepeel S, Timonina D, Bilton SJ, Phan N, Gomez-Caraballo M, Archibald HL, Li C, Fraser C and others. Exploiting MCL1 Dependency with Combination MEK + MCL1 Inhibitors Leads to Induction of Apoptosis and Tumor Regression in KRAS-Mutant Non-Small Cell Lung Cancer. Cancer Discov 2018;8(12):1598-1613.
247. Gutzeit VA, Thibado J, Stor DS, Zhou Z, Blanchard SC, Andersen OS, Levitz J. Conformational dynamics between transmembrane domains and allosteric modulation of a metabotropic glutamate receptor. Elife 2019;8:e45116.
248. Song G, Yang D, Wang Y, de Graaf C, Zhou Q, Jiang S, Liu K, Cai X, Dai A, Lin G and others. Human GLP-1 receptor transmembrane domain structure in complex with allosteric modulators. Nature 2017;546(7657):312-315.
249. Zhang JH, Chung TD, Oldenburg KR. A Simple Statistical Parameter for Use in Evaluation and Validation of High Throughput Screening Assays. J Biomol Screen 1999;4(2):67-73.
250. Gorgulla C, Boeszoermenyi A, Wang ZF, Fischer PD, Coote PW, Padmanabha Das KM, Malets YS, Radchenko DS, Moroz YS, Scott DA and others. An open-source drug discovery platform enables ultra-large virtual screens. Nature 2020;580(7805):663-668.
251. Bharate SS, Kumar V, Vishwakarma RA. Determining Partition Coefficient (Log P), Distribution Coefficient (Log D) and Ionization Constant (pKa) in Early Drug Discovery. Comb Chem High Throughput Screen 2016;19(6):461-9.
252. Lipinski CA, Lombardo F, Dominy BW, Feeney PJ. Experimental and computational approaches to estimate solubility and permeability in drug discovery and development settings. Adv Drug Deliv Rev 2001;46(1-3):3-26.
253. Yue L, Li L, Li D, Yang Z, Han S, Chen M, Lan S, Xu X, Hui L. High-throughput screening for Survivin and Borealin interaction inhibitors in hepatocellular carcinoma. Biochem Biophys Res Commun 2017;484(3):642-647.
254. Xiang W, Yang CY, Bai L. MCL-1 inhibition in cancer treatment. Onco Targets Ther 2018;11:7301-7314.
255. Merino D, Kelly GL, Lessene G, Wei AH, Roberts AW, Strasser A. BH3-Mimetic Drugs: Blazing the Trail for New Cancer Medicines. Cancer Cell 2018;34(6):879-891.
256. Rasmussen ML, Taneja N, Neininger AC, Wang L, Robertson GL, Riffle SN, Shi L, Knollmann BC, Burnette DT, Gama V. MCL-1 Inhibition by Selective BH3 Mimetics Disrupts Mitochondrial Dynamics Causing Loss of Viability and Functionality of Human Cardiomyocytes. iScience 2020;23(4):101015.
257. Redij T, Ma J, Li Z, Hua X. Discovery of a potential positive allosteric modulator of glucagon-like peptide 1 receptor through virtual screening and experimental study. J Comput Aided Mol Des 2019;33(11):973-981.
258. Zhang X, Dong S, Xu F. Structural and Druggability Landscape of Frizzled G Protein-Coupled Receptors. Trends Biochem Sci 2018;43(12):1033-1046.
259. Goh ETH, Lin Z, Ahn BY, Lopes-Rodrigues V, Dang NH, Salim S, Berger B, Dymock B, Senger DL, Ibanez CF. A Small Molecule Targeting the Transmembrane Domain of Death Receptor p75(NTR) Induces Melanoma Cell Death and Reduces Tumor Growth. Cell Chem Biol 2018;25(12):1485-1494.e5.
260. Cong X, Cheron JB, Golebiowski J, Antonczak S, Fiorucci S. Allosteric Modulation Mechanism of the mGluR5 Transmembrane Domain. J Chem Inf Model 2019;59(6):2871-2878.

261. Hudson TJ, Anderson W, Artez A, Barker AD, Bell C, Bernabe RR, Bhan MK, Calvo F, Eerola I, Gerhard DS and others. International network of cancer genome projects. Nature 2010;464(7291):993-8.
262. Shen Q, Cheng F, Song H, Lu W, Zhao J, An X, Liu M, Chen G, Zhao Z, Zhang J. Proteome-Scale Investigation of Protein Allosteric Regulation Perturbed by Somatic Mutations in 7,000 Cancer Genomes. Am J Hum Genet 2017;100(1):5-20.
263. Smith AJ, Dai H, Correia C, Takahashi R, Lee SH, Schmitz I, Kaufmann SH. Noxa/Bcl-2 protein interactions contribute to bortezomib resistance in human lymphoid cells. J Biol Chem 2011;286(20):17682-92.
264. Correia C, Schneider PA, Dai H, Dogan A, Maurer MJ, Church AK, Novak AJ, Feldman AL, Wu X, Ding H and others. BCL2 mutations are associated with increased risk of transformation and shortened survival in follicular lymphoma. Blood 2015;125(4):658-67.
265. Lee JW, Soung YH, Kim SY, Nam SW, Kim CJ, Cho YG, Lee JH, Kim HS, Park WS, Kim SH and others. Inactivating mutations of proapoptotic Bad gene in human colon cancers. Carcinogenesis 2004;25(8):1371-6.
266. Brimmell M, Mendiola R, Mangion J, Packham G. BAX frameshift mutations in cell lines derived from human haemopoietic malignancies are associated with resistance to apoptosis and microsatellite instability. Oncogene 1998;16(14):1803-12.
267. Meijerink JP, Mensink EJ, Wang K, Sedlak TW, Sloetjes AW, de Witte T, Waksman G, Korsmeyer SJ. Hematopoietic malignancies demonstrate loss-of-function mutations of BAX. Blood 1998;91(8):2991-7.
268. Konig SM, Rissler V, Terkelsen T, Lambrughi M, Papaleo E. Alterations of the interactome of Bcl-2 proteins in breast cancer at the transcriptional, mutational and structural level. PLoS Comput Biol 2019;15(12):e1007485.
269. Zhao L, Sun T, Pei J, Ouyang Q. Mutation-induced protein interaction kinetics changes affect apoptotic network dynamic properties and facilitate oncogenesis. Proc Natl Acad Sci U S A 2015;112(30):E4046-54.
270. Tulumello DV, Deber CM. SDS micelles as a membrane-mimetic environment for transmembrane segments. Biochemistry 2009;48(51):12096-103.
271. Martin SS, Ridgeway AG, Pinkas J, Lu Y, Reginato MJ, Koh EY, Michelman M, Daley GQ, Brugge JS, Leder P. A cytoskeleton-based functional genetic screen identifies Bcl-xL as an enhancer of metastasis, but not primary tumor growth. Oncogene 2004;23(26):4641-5.
272. Fernandez Y, Espana L, Manas S, Fabra A, Sierra A. Bcl-xL promotes metastasis of breast cancer cells by induction of cytokines resistance. Cell Death Differ 2000;7(4):350-9.
273. Bessou M, Lopez J, Gadet R, Deygas M, Popgeorgiev N, Poncet D, Nougarede A, Billard P, Mikaelian I, Gonzalo P and others. The apoptosis inhibitor Bcl-xL controls breast cancer cell migration through mitochondria-dependent reactive oxygen species production. Oncogene 2020;39(15):3056-3074.
274. Du YCN, Lewis BC, Hanahan D, Varmus H. Assessing Tumor Progression Factors by Somatic Gene Transfer into a Mouse Model: Bcl-xL Promotes Islet Tumor Cell Invasion. PLoS Biol 2007;5(10):e276.
275. Hager JH, Ulanet DB, Hennighausen L, Hanahan D. Genetic ablation of Bcl-x attenuates invasiveness without affecting apoptosis or tumor growth in a mouse model of pancreatic neuroendocrine cancer. PLoS One 2009;4(2):e4455.
276. Baker JA, Wong WC, Eisenhaber B, Warwicker J, Eisenhaber F. Charged residues next to transmembrane regions revisited: "Positive-inside rule" is complemented by the "negative inside depletion/outside enrichment rule". BMC Biol 2017;15(1):66.
277. Mayol E, Campillo M, Cordomi A, Olivella M. Inter-residue interactions in alpha-helical transmembrane proteins. Bioinformatics 2019;35(15):2578-2584.